

TECHNIQUES FOR CLIMATE MODELING

by

David B Burkhard

A thesis submitted to the faculty of
The University of Utah
in partial fulfillment of the requirements for the degree of

Master of Science

Department of Mathematics

The University of Utah

December 2014

Copyright © David B Burkhard 2014

All Rights Reserved

The University of Utah Graduate School

STATEMENT OF THESIS APPROVAL

The thesis of _____ **David B Burkhard** _____

has been approved by the following supervisory committee members:

_____ **Peter Alfeld** _____, Chair _____ **09/26/2014** _____
Date Approved

_____ **Elena Cherkaev** _____, Member _____ **09/26/2014** _____
Date Approved

_____ **Jingyi Zhu** _____, Member _____ **10/03/2014** _____
Date Approved

and by _____ **Peter Trapa** _____, Chair/Dean of

the Department/College/School of _____ **Mathematics** _____

and by David B. Kieda, Dean of The Graduate School.

ABSTRACT

This thesis reviews the techniques used to model the circulation of the atmosphere and oceans. Models of the atmospheric and oceanic circulation can be used to evaluate future and past conditions of the climate of the Earth. They can also be used to evaluate what affect any changes to the parameters for the Earth's environment might have on the climate of the Earth.

For models of the atmosphere, physical properties of the air and of the rotating Earth are used to develop equations for the state and motion of the air in the atmosphere. These equations represent the relationships between the temperature, density, and wind speeds of the air in the atmosphere. The final equations are a set of nonlinear partial differential equations which require a numerical solution. There are several methods used to accomplish a numerical solution to these equations.

Models of the ocean can be developed in much the same way as models of the atmosphere. The differences include the fact that sea water is essentially incompressible. The models are much more complicated as the oceans are much more limited by the shape of the continents and so do not cover the entire Earth like the atmosphere does. To aid in the understanding of ocean circulation, simpler models of the main circulation of the oceans have been developed as "boxes" of sea water connected by flows of sea water between the boxes which are driven by differences in density between the boxes of sea water. The density of the sea water is a function of the temperature and salinity of the water in each part of the ocean. These box models show that there are multiple equilibrium states for the circulation of the ocean.

CONTENTS

ABSTRACT	iii
LIST OF FIGURES	vi
LIST OF TABLES	vii
CHAPTERS	
1. INTRODUCTION	1
2. ATMOSPHERIC CIRCULATION MODELS	3
2.1 Basic Physics	3
2.1.1 Wind Velocity	3
2.1.2 Rates of Change	4
2.1.3 Continuity/Conservation of Air	5
2.1.4 Hydrostatic Models	7
2.1.5 Geopotential	8
2.1.6 Potential Virtual Temperature	8
2.2 Thermodynamics Considerations	10
2.2.1 Thermodynamic Energy Equation	10
2.3 Newton's Law and Momentum	14
2.3.1 Conversion to Spherical Coordinates	14
2.3.1.1 Spherical Unit Vectors	15
2.3.1.2 Partial Derivatives of Spherical Unit Vectors	16
2.3.1.3 Converting Velocities	18
2.3.1.4 Gradient in Spherical Coordinates	18
2.3.2 Rotation of the Earth	20
2.3.2.1 Local Acceleration	23
2.3.2.2 Coriolis Forces	26
2.3.2.3 Gravitational and Centrifugal Forces	26
2.3.2.4 Pressure Gradient Forces	28
2.3.2.5 Viscous Forces and Turbulence	29
2.3.3 Complete Momentum Equation	30
2.4 Vertical Coordinate Conversion	31
2.4.1 Pressure or Isobaric Coordinate	32
2.4.1.1 Gradient for Pressure Coordinate	32
2.4.1.2 Continuity for the Pressure Coordinate	34
2.4.1.3 Total Derivative for the Pressure Coordinate	36
2.4.2 Sigma Pressure Coordinate	36
2.4.2.1 Gradient for Sigma Pressure Coordinate	38

2.4.2.2	Continuity for the Sigma Pressure Coordinate	39
2.4.3	Surface Air Pressure	40
2.4.4	Vertical Wind Velocity	41
2.4.5	Thermodynamic Equation	41
2.4.6	Horizontal Momentum	42
2.5	Final Equations	43
2.6	Numerical Solutions	45
2.6.1	Finite Difference Methods	45
2.6.2	Spectral Methods	48
3.	OCEANIC CIRCULATION MODELS	50
3.1	Stommel 2-Box Model	54
3.1.1	Equations for Stommel's 2-Box Model	57
3.1.2	Equilibrium Points	58
3.1.3	Numerical Modeling	62
3.2	3-Box Models	66
3.2.1	Welander 3-Box Model	66
3.2.1.1	Equations for Welander 3-Box Model	67
3.2.1.2	Equilibrium Points	68
3.2.1.3	Numerical Modeling	70
3.2.2	Rooth's 3-Box Model	73
3.2.2.1	Equations for Rooth's 3-Box Model	73
3.2.2.2	Equilibrium Points	76
3.2.2.3	Numerical Modeling	81
3.3	Models with More Boxes	85
	APPENDIX: SALT WATER DENSITY	87
	REFERENCES	90

LIST OF FIGURES

2.1	How the movement of air particles conserves mass	5
2.2	The basis vectors for spherical coordinates	14
2.3	The pressure gradient forces within a cube of air	29
2.4	The pressure coordinate system	32
2.5	Pressure coordinate surfaces of constant pressure.	33
2.6	The sigma pressure coordinate system	37
2.7	Sigma coordinate surfaces of constant measure	38
2.8	The Arakawa C-Grid	47
3.1	The simplified global thermohaline circulation of sea water	51
3.2	The original Stommel 2-box model	54
3.3	The modified 2-box model	56
3.4	The 2-box model's bifurcation diagram	61
3.5	The THC strengths for changes to the freshwater flux	63
3.6	The THC strengths for short-term changes to the freshwater flux	64
3.7	Welander's 3-box model of thermohaline circulation	67
3.8	Welander model with a 134% increase in the freshwater flux	72
3.9	Welander model with a short-term 134% increase in the freshwater flux	73
3.10	Welander model with a 201% increase in the freshwater flux	74
3.11	Welander model with a short-term 201% increase in the freshwater flux	75
3.12	Rooth's 3-box model of thermohaline circulation	76
3.13	Rooth's 3-box model with changes to the freshwater flux	83
3.14	Rooth's 3-box model with short-term changes to the freshwater flux	84
3.15	A 4-box model of thermohaline circulation	86
3.16	A 6-box model of thermohaline circulation	86
A.1	The density of salt water	88
A.2	The density of salt water for selected temperatures and salinities	89

LIST OF TABLES

2.1 Reasons for diabatic heating	13
3.1 Parameters for box models	53

CHAPTER 1

INTRODUCTION

This thesis is about some of the techniques which are used when developing models of atmospheric and oceanic circulation. These types of models can be used for short-term weather forecasting or for long-term climate modeling.

There are no basic differences between the types of equations used for climate modeling and weather prediction. Weather prediction is for a much shorter-time period and requires a much higher resolution than what is required for a climate model [10]. That is, time steps in a model used for weather prediction are usually for a much shorter duration than the time steps used in a climate model. Also, the physical dimensions of the cells used for the numerical solutions of the equations for a weather forecasting model are much smaller than what is used for a climate model. Note that weather prediction requires a much more exact result than a climate model. For instance, misforecasting the track of a storm by 100 miles results in a poor weather forecast. However, a climate model needs only to produce a long-term average forecast over a period of at least a decade and sometimes much longer. Because of this, while it remains difficult to forecast the weather for a period of 1 to 2 weeks, climate models can give a good forecast of the average values of the weather system - the climate - for hundreds of years into the future.

The first part of this thesis covers the development of some of the partial differential equations used in models of atmospheric circulation. The models are a combination of physical laws and the mathematics used to represent the effects of those physical laws. The equations can be difficult to develop as they make use of a number of simplifications so that the resulting partial differential equations (PDEs) can be solved numerically.

The second part of the thesis discusses simplified models of the thermohaline

circulation of the oceans. This is the oceanic circulation caused by the differences in density which are the result of the differences in temperature and salinity of regions of the ocean. The simplified models are “box models,” the first of which was developed by Henry Stommel in 1961 [15]. These are high-level models of the oceanic circulation which is driven by heat and salinity differences across the oceans. The thermohaline circulation is responsible for moving both heat and salinity within the oceans of the Earth and has a major effect on the climate of the Earth. An example of this circulation is the Gulf Stream current which flows along the surface of the Atlantic Ocean just off the coast of North America and which is responsible for keeping the climate of Northern Europe warmer than it would be otherwise. The thermohaline circulation of the oceans is responsible for the warming or cooling of different areas of the Earth as heat is moved to different parts of the ocean.

CHAPTER 2

ATMOSPHERIC CIRCULATION MODELS

Atmospheric circulation models are used to predict the movement of atmospheric air. They can be used for weather prediction, or for climate predictions. The equations of the movement of the air are developed from physical properties of the air. These equations represent the changes in the attributes of the air as a series of partial differential equations (PDE's).

2.1 Basic Physics

To begin the development of the equations used for atmospheric modeling, some basic definitions are needed for the physical properties of the air to be modeled. Some of these definitions simply to settle which symbols are used for which physical attributes. Others delve deeper into the physics required to fully describe the flow of the atmosphere.

The initial definitions are all in the context of a set of Cartesian coordinates. That is, in the context of a set of x , y , and z coordinates with the orthogonal basis vectors \mathbf{i} , \mathbf{j} , and \mathbf{k} . The definitions will eventually be extended so that they work in a context of spherical coordinates on the surface of the rotating Earth.

2.1.1 Wind Velocity

The wind velocity is one of the main outputs of these models. The position of a parcel of air is given in the usual x , y , and z coordinates, while the velocity of the parcel of air is given in terms of the x , y , and z components of the velocity, the variables u , v , and w are used for the velocity components. The position and wind velocity using the Cartesian basis vectors are:

$$\mathbf{x} = x\mathbf{i} + y\mathbf{j} + z\mathbf{k} \qquad \text{Position} \qquad (2.1)$$

$$\mathbf{v} = u\mathbf{i} + v\mathbf{j} + w\mathbf{k} \quad \text{Velocity} \quad (2.2)$$

The vector variable \mathbf{v} represents the wind velocity as a vector. Each of the variables u , v , and w are the time derivatives of each of the Cartesian coordinates x , y , and z , respectively, of a parcel of air and are the scalar components of the \mathbf{v} velocity vector.

2.1.2 Rates of Change

There are two ways to measure the rate of change of an attribute of a parcel of air as it circulates in the atmosphere. An attribute of that parcel of air can be any of temperature, density, wind speed, or other measurable values. The first way to measure the rate of change of the attribute is to measure the rate of change within the air parcel as that air parcel changes position in the atmosphere. This is referred to as a Lagrangian frame of reference. The second way is to measure the rate of change of that attribute at a fixed point in the atmosphere as various air parcels move past that fixed point, this is referred to as an Eulerian frame of reference. Using the Lagrangian frame of reference, the rate of change of an attribute N (such as temperature, density, etc.) associated with that parcel of air is measured as the total derivative of that attribute with respect to time or $\frac{dN}{dt}$. Using the chain rule for derivatives the total derivative of this attribute with respect to time becomes:

$$\frac{dN}{dt} = \frac{\partial N}{\partial t} \frac{dt}{dt} + \frac{\partial N}{\partial x} \frac{dx}{dt} + \frac{\partial N}{\partial y} \frac{dy}{dt} + \frac{\partial N}{\partial z} \frac{dz}{dt} \quad (2.3)$$

$$= \frac{\partial N}{\partial t} + u \frac{\partial N}{\partial x} + v \frac{\partial N}{\partial y} + w \frac{\partial N}{\partial z} \quad (2.4)$$

While the left side of this equation makes use of a Lagrangian frame of reference, the right side of this equation uses an Eulerian frame of reference. Generalizing this equation to use the gradient operator gives the total derivative as an operator:

$$\frac{dN}{dt} = \frac{\partial N}{\partial t} + \mathbf{v} \cdot \nabla N \quad \text{Using the gradient} \quad (2.5)$$

$$\frac{d}{dt} = \frac{\partial}{\partial t} + \mathbf{v} \cdot \nabla \quad \text{Total derivative as an operator} \quad (2.6)$$

This is the total derivative of an attribute of air, it can be interpreted as the change in the value of the attribute over time within the parcel of air, as well as the values added or subtracted from that attribute as air moves into or out of the

boundaries of the parcel of air being measured. The total derivative of an attribute will be used at many points in the development of the partial differential equations used for atmospheric circulation.

2.1.3 Continuity/Conservation of Air

For these models, the atmosphere will be divided into a three-dimensional set of cells of air. As the air circulates between these cells, many of the attributes of that parcel of air will be conserved. The main attribute which is conserved is the mass or density of the air. For the mass of a parcel of air, this means that the initial mass of the air in a cell, plus the mass of the air entering the cell during a time period, and minus the mass of the air leaving the cell during the time period gives the final mass of air in the cell at the end of the time period. Figure 2.1 shows a diagram of this for a small cube of air with a wind velocity parallel to the x -axis.

For the mass of an air parcel, the measured attribute is the density of the air, which is the mass of the air per unit volume. Here, the variable N will be used to emphasize that these equations work for any conserved attribute of the parcel of air

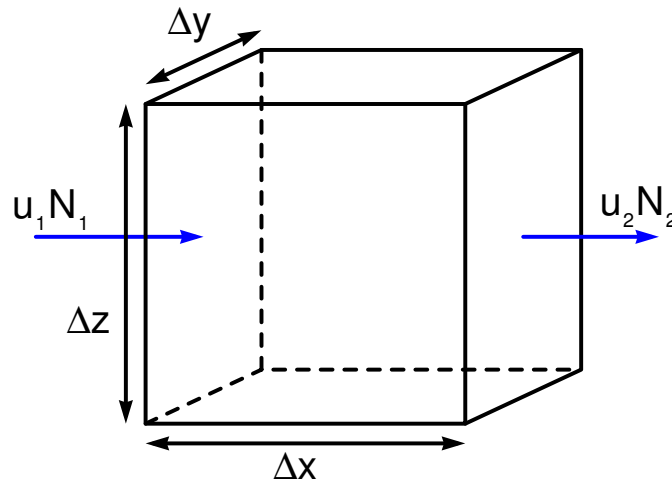


Figure 2.1. How the movement of air particles conserves mass. This shows the movement of air particles into and out of a cube with a wind velocity parallel to the x -axis. The variables u_1 and u_2 are the wind velocities (parallel to the x -axis) and the variables N_1 and N_2 are the densities of the air at either side of the cube.

and not just mass or density. If the density of the air particles is N_1 on the left side of the cube and the velocity of the air particles on the left of the cube is u_1 , then the mass of the air entering the cube on the left side of the cube is the product $u_1 N_1 \Delta y \Delta z \Delta t$. In the same way, the mass of air leaving the cube on the right side is the product $u_2 N_2 \Delta y \Delta z \Delta t$. Since the mass of the air within the cube is the product of the density of the air and the volume of the cube, these values can be put together to show that the change of the density of the air within the cube depends on the densities of the air at either face of the cube and the velocity of the air at that face:

$$\Delta N \Delta x \Delta y \Delta z = u_1 N_1 \Delta y \Delta z \Delta t - u_2 N_2 \Delta y \Delta z \Delta t \quad (2.7)$$

Equation (2.7) can be changed to a partial differential equation. First, divide the equation by the product $\Delta x \Delta y \Delta z \Delta t$, and then take the limit as both Δx and Δt approach zero. The resulting equation is a partial differential equation for the continuity or conservation of the mass of the air:

$$\frac{\Delta N}{\Delta t} = - \left(\frac{u_2 N_2 - u_1 N_1}{\Delta x} \right) \quad \text{After dividing by } \Delta x \Delta y \Delta z \Delta t \quad (2.8)$$

$$\frac{\partial N}{\partial t} = - \frac{\partial}{\partial x} (uN) \quad \text{Limit as } \Delta x \rightarrow 0 \text{ and } \Delta t \rightarrow 0 \quad (2.9)$$

Equation (2.9) is the continuity equation for a gas affected by a velocity in only the x direction. This equation was developed using the density of the air, but N could be any conserved attribute of a parcel of air. Equation (2.9) can be extended for use in three dimensions through a similar analysis as what was used to derive this equation:

$$\frac{\partial N}{\partial t} = -\nabla \cdot (\mathbf{v}N) \quad (2.10)$$

$$= -N(\nabla \cdot \mathbf{v}) - (\mathbf{v} \cdot \nabla)N \quad \text{Expanding the gradient of the product} \quad (2.11)$$

This relationship is used to model attributes of a cell of air which are conserved in the circulation model. For instance, the continuity equation for air, that is, how the density of the air varies with time is:

$$\frac{\partial \rho}{\partial t} = -\nabla \cdot (\mathbf{v}\rho) = -\rho(\nabla \cdot \mathbf{v}) - (\mathbf{v} \cdot \nabla)\rho \quad (2.12)$$

Equation (2.12) shows two ways to represent the continuity or conservation of air. It can be interpreted as the change in the mass per unit volume or density of the air

within a parcel which is driven by the masses of air entering or leaving the parcel of air under consideration.

2.1.4 Hydrostatic Models

The variation of air pressure with altitude can be estimated in different ways. One of the most common of these is referred to as the “hydrostatic assumption.” The hydrostatic assumption is that the density of the air in the atmosphere decreases as a monotone function of the altitude. The use of the hydrostatic assumption in a model means that the vertical velocities and accelerations of the atmosphere are assumed to be very small compared to the horizontal velocities and accelerations. This assumption is a good approximation when a model averages the air pressure over a large enough horizontal area (an area greater than about 5 km²) and outside of any storms [5]. The usual values of vertical velocities in the atmosphere are several orders of magnitude below the values of the horizontal velocities. Using the equation for hydrostatic air pressure results in a simple relationship between the pressure at an altitude and the altitude. This relationship is used to convert equations to make use of the hydrostatic assumption:

$$dp = -\rho g dz \tag{2.13}$$

The hydrostatic assumption will be used for most of the equations developed in this thesis. The hydrostatic assumption for a model can be used to remove the $\frac{dw}{dt}$ term from the momentum equation.

Another assumption about air pressure which has been used in atmospheric circulation models is the anelastic assumption. This alternative was designed to remove acoustic or sound waves from the modeled processes in the atmosphere [1] [9]. The main result of using the anelastic assumption is the removal of the $\frac{\partial \rho}{\partial t}$ term from the continuity equation for air [5]. Another assumption similar to the anelastic assumption is the Boussinesq approximation, which is a subset of the anelastic assumption and which can be used for shallow flows of a fluid.

2.1.5 Geopotential

Geopotential is the amount of work required against gravity to raise a parcel of air from sea level to a given altitude. It represents the potential energy of a parcel of air due to its altitude in the atmosphere. The value of the geopotential of a unit mass of air is the integral of the force of gravity over the height that the air must be raised to go to its altitude:

$$\Phi(z) = \int_0^z g(z) dz \quad (2.14)$$

Near the surface of the Earth, the geopotential can be approximated as simply gz because the value of g is approximately constant over the height of most atmospheric models. The value of g differs by about 0.39 % at an altitude of 25 km and about 1.55 % at 100 km [5]. Approximating the value of g as a constant introduces only a small error into a model.

Geopotential is used when calculating the momentum of a parcel of air in the atmosphere. It can be used to evaluate the force of gravity on that parcel of air.

2.1.6 Potential Virtual Temperature

The virtual temperature of a parcel of moist air is the temperature which a parcel of dry air would need to have in order to be at the same pressure and density as the parcel of moist air. Using virtual temperature is a way to scale the temperature of a parcel of air in order to simplify calculations involving moist air. The virtual temperature can be calculated from the temperature of the parcel of air and the value of the specific humidity q_v , which is the ratio of the mass of the water vapor content to the total mass of the parcel of air:

$$T_v \approx T(1 + 0.608q_v) \quad (2.15)$$

Note that the constant 0.608 in equation (2.15) is the ratio $\frac{M_d - M_v}{M_d}$ with M_d being the molecular weight of dry air (grams per mole), which is approximately $28.966 \text{ g mol}^{-1}$, and M_v is the molecular weight of water vapor, which is approximately 18.02 g mol^{-1} . The variable q_v is the specific humidity of the moist air, which is the ratio of the mass of the water vapor to the total mass of the moist air. For dry air,

q_v is zero so that the virtual temperature will be the same as the temperature of a dry air sample, $T_v = T$.

The potential temperature θ_p of a parcel of air is the temperature which that parcel would obtain if it were brought from its original pressure at its original altitude to a pressure of 1000 hPa adiabatically, that is, without losing or gaining any energy from its surrounding environment. The potential temperature of a parcel of air can be evaluated by considering a parcel of air and its change of temperature given a change of pressure. The variable $c_{p,m}$ is the specific heat of moist air at a constant pressure, and ρ is the density of the air. From the ideal gas law, the relationship $p = R_m \rho T$ or $\rho = \frac{p}{R_m T}$ can be used to simplify the relationship. The variable R_m represents the specific gas constant for the moist air, which is the ideal gas constant R divided by the molar mass of the moist air. Integrating the resulting differential equation gives an equation for the change in temperature of a parcel of air as the pressure of the parcel is changed, this equation is often referred to as Poisson's equation [5]:

$$c_{p,m} \rho dT = dp \quad (2.16)$$

$$c_{p,m} \frac{p}{R_m T} dT = dp \quad (2.17)$$

$$\frac{dT}{T} = \frac{R_m}{c_{p,m}} \frac{dp}{p} \quad (2.18)$$

$$T = T_0 \left(\frac{p}{p_0} \right)^{R_m/c_{p,m}} \quad (2.19)$$

Equation (2.19) can be simplified by making use of the relationship for the specific heat of moist air in terms of the specific heat of dry air, which is $c_{p,m} = \frac{M_d c_{p,d} + M_v c_{p,v}}{M_d + M_v} \approx c_{p,d}(1 + 0.856q_v)$ and another relationship between the specific gas constant for moist air and the specific constant for dry air, which is $R_m = R_d \left(1 + \frac{M_d - M_v}{M_d} q_v \right) \approx R_d(1 + 0.608q_v)$. The simplified form of equation (2.19) is:

$$T = T_0 \left(\frac{p}{p_0} \right)^{R_d(1+0.608q_v)/[c_{p,d}(1+0.856q_v)]} \quad (2.20)$$

$$\approx T_0 \left(\frac{p}{p_0} \right)^{\kappa(1-0.251q_v)} \quad (2.21)$$

$$\kappa = \frac{R_d}{c_{p,d}} = \frac{c_{p,d} - c_{v,d}}{c_{p,d}} \approx 0.286 \quad (2.22)$$

The variable $c_{p,d}$ is the specific heat of dry air at a constant pressure and $c_{v,d}$ is the specific heat of dry air at a constant volume. These specific heat values are the amount of energy required to raise the temperature of a unit mass of the substance by one degree Kelvin keeping either the pressure or volume constant.

Potential virtual temperature θ_v is a combination of the concepts of virtual temperature and potential temperature, it is the temperature of a parcel of air in which all moisture is converted to dry air and then the pressure is brought to 1000 hPa.

$$\theta_{p,m} = T \left(\frac{1000 \text{ hPa}}{p} \right)^{\kappa(1-0.251q_v)} \quad \text{For moist air} \quad (2.23)$$

$$\theta_p = T \left(\frac{1000 \text{ hPa}}{p} \right)^{\kappa} \quad \text{For dry air} \quad (2.24)$$

The pressure of 1000 hPa is a reference pressure of 1000 hecto pascals. This is near to 1013.25 hPa, which is about the average air pressure at sea level on the Earth. For dry air, the potential temperature and potential virtual temperature will be the same value.

Potential virtual temperature is used to simplify the equations used for the thermodynamics of the atmosphere. Converting from temperature to potential virtual temperature simplifies the equations for thermodynamics.

2.2 Thermodynamics Considerations

2.2.1 Thermodynamic Energy Equation

The laws of thermodynamics or how changes in heat and energy affect the parcels of air in the atmosphere play a large role in how the circulation of the air is modeled. The first law of thermodynamics, or the conservation of energy for a parcel of air, is:

$$dQ^* = dU^* + dW^* \quad (2.25)$$

The term dQ^* is the diabatic heating term or the energy transferred between the air parcel and its environment. The dU^* term is the change in the internal energy of the parcel. The dW^* term is the work either done by (negative) or on the parcel of air (positive). Dividing this equation by the mass of the parcel of air gives the energy per unit mass of the parcel of the air:

$$\frac{dQ^*}{M} = \frac{dU^*}{M} + \frac{dW^*}{M} \quad \text{Dividing by the mass of the parcel of air} \quad (2.26)$$

$$dQ = dU + dW \quad \text{Simplified to the energy per unit mass of air} \quad (2.27)$$

Equation (2.27) is in terms of the energy per unit mass of the air. The terms dU and dW can be further evaluated in terms of other attributes of the parcel of air in question. When a parcel of air changes its volume, the work done is the product of the pressure at the boundary of the parcel of air and the volume of the air. That work now done, can be stated in terms of a new variable, $\alpha = \frac{1}{\rho}$, the reciprocal of density, as:

$$dW = \frac{dW^*}{M} = \frac{p dV}{M} = p d\alpha \quad (2.28)$$

The change in the internal energy of a parcel of air dU is the change in temperature multiplied by the energy required to change its temperature by 1 Kelvin.

$$dU = \left(\frac{\partial Q}{\partial T} \right) dT = c_{v,m} dT \quad (2.29)$$

The constant $c_{v,m}$ is the specific heat of moist air at constant volume. Note that the specific heat of dry air at a constant volume varies by less than 0.2% for temperatures of 200 to 300 K [5], so that using a constant value for the specific heat values will only incorporate a small error into the models. Combining equations (2.28) and (2.29) with equation (2.27), the equation for the first law of thermodynamics has now become:

$$dQ = c_{v,m} dT + p d\alpha \quad (2.30)$$

The ideal gas law is a combination of Boyle's law, Charles' law, and Avrogradro's law. The ideal gas law is the equation $pV = nRT$, where p is the pressure of the gas, V is the volume of the gas, n is the number of moles of the gas, R is the ideal gas constant or $8.3144621 \text{ J mol}^{-1} \text{ K}^{-1}$, and T is the temperature of the gas in Kelvins. The constant R_m is the specific gas constant for moist air or the ideal gas constant R divided by the molar mass of the moist air. Converting the ideal gas law to make use of R_m changes it to $pV = nm_a R_m T$, with m_a the molar mass or grams per mole of the gas. The product nm_a is the number of moles of the gas times the molar mass of the gas, which is simply the mass of the gas. Using this and then making use of the variable $\alpha = \frac{1}{\rho}$ gives:

$$p = \frac{M}{V} R_m T = \rho R_m T \quad \text{The converted ideal gas law} \quad (2.31)$$

$$p\alpha = R_m T \quad \text{Using } \alpha = \frac{1}{\rho} = \frac{V}{M} \quad (2.32)$$

$$p d\alpha = R_m dT - \alpha dp \quad \text{Differentiating and simplifying} \quad (2.33)$$

Substituting equation (2.33) into equation (2.30) gives a new expression for the energy per unit mass of the air. Note that the value of $c_{p,m} = c_{v,m} + R_m$, or that the specific heat of moist air at a constant pressure is equal to the sum of the specific heat of moist air at a constant volume and the specific gas constant of the moist air. The expression for the unit mass of the air becomes:

$$dQ = c_{v,m} dT + R_m dT - \alpha dp \quad (2.34)$$

$$= (c_{v,m} + R_m) dT - \alpha dp \quad (2.35)$$

$$= c_{p,m} dT - \alpha dp \quad (2.36)$$

This equation can be expressed as an approximation using virtual temperature by making use of equation (2.15) and the relationship $c_{p,m} = c_{p,d}(1 + 0.856q_v)$. Note that the constant 0.856 is approximately the value of $\frac{M_d c_{p,d} + M_v c_{p,v}}{M_d + M_v}$, where M_d is the molar mass of dry air, M_v is the molar mass of water vapor, $c_{p,d}$ is the specific heat of dry air, and $c_{p,v}$ is the specific heat of water vapor. Because the specific humidity, q_v , is between 0 and 1, equation (2.36) can be approximated as:

$$dQ = \frac{c_{p,d}(1 + 0.856q_v)}{(1 + 0.608q_v)} dT_v - \alpha dp \quad (2.37)$$

$$\approx c_{p,d} dT_v - \alpha dp \quad (2.38)$$

Dividing equation (2.38) by dt , using $\alpha = \frac{1}{\rho}$, and rearranging terms gives another form of the thermodynamic energy equation:

$$\frac{dT_v}{dt} = \frac{1}{c_{p,m}} \frac{dQ}{dt} + \frac{1}{c_{p,m}\rho} \frac{dp}{dt} \quad (2.39)$$

Equation (2.39) can be further simplified by using potential virtual temperature rather than virtual temperature. Differentiating the definition of potential virtual temperature for dry air, equation (2.24), with respect to time results in a relationship between the derivatives of virtual temperature and potential virtual temperature:

$$\frac{d\theta_v}{dt} = \frac{dT_v}{dt} \left(\frac{1000}{p} \right)^\kappa + \kappa T_v \left(\frac{1000}{p} \right)^{\kappa-1} \left(-\frac{1000}{p^2} \right) \frac{dp}{dt} \quad (2.40)$$

$$= \frac{\theta_v}{T_v} \frac{dT_v}{dt} - \frac{\kappa \theta_v}{p} \frac{dp}{dt} \quad (2.41)$$

$$\frac{dT_v}{dt} = \frac{T_v}{\theta_v} \frac{d\theta_v}{dt} + \frac{\kappa T_v}{p} \frac{dp}{dt} \quad \text{Solving for } \frac{dT_v}{dt} \quad (2.42)$$

Making use of (2.42) and the relationships $\kappa = \frac{R}{c_{p,m}}$ and $p = \rho R T_v$ will reduce equation (2.39) to an equation involving only potential virtual temperature:

$$\frac{T_v}{\theta_v} \frac{d\theta_v}{dt} + \frac{R T_v}{c_{p,m} \rho R T_v} \frac{dp}{dt} = \frac{1}{c_{p,m}} \frac{dQ}{dt} + \frac{1}{c_{p,m} \rho} \frac{dp}{dt} \quad (2.43)$$

$$\frac{d\theta_v}{dt} = \frac{\theta_v}{c_{p,m} T_v} \frac{dQ}{dt} + \frac{\theta_v}{c_{p,m} \rho T_v} \frac{dp}{dt} - \frac{\theta_v}{c_{p,m} \rho T_v} \frac{dp}{dt} \quad (2.44)$$

$$= \frac{\theta_v}{c_{p,m} T_v} \frac{dQ}{dt} \quad (2.45)$$

$$\frac{\partial \theta_v}{\partial t} + (\mathbf{v} \cdot \nabla) \theta_v = \frac{\theta_v}{c_{p,m} T_v} \frac{dQ}{dt} \quad \text{Using the total derivative} \quad (2.46)$$

Equation (2.46) can be expanded to include the effects of eddy turbulence [5]. The result of this transformation is that the equation becomes:

$$\frac{\partial \theta_v}{\partial t} + (\mathbf{v} \cdot \nabla) \theta_v = \frac{\theta_v}{c_{p,d}} \frac{dQ}{dt} + \frac{1}{\rho} (\nabla \cdot \rho \mathbf{K}_h \nabla) \theta_v \quad (2.47)$$

The variable \mathbf{K}_h represents the eddy diffusion tensor for energy.

The expression $\frac{dQ}{dt}$ is the sum of a series of diabatic heating rates [5]. This sum includes the reasons shown in Table 2.1. Any model of the atmosphere must have ways to incorporate energy inputs and outflows which correspond to each of the reasons shown in this table. Some of the reasons in the table come from daily or seasonal variations of sunlight and heating. These always require additional preparation for the model to represent actual physical conditions.

Table 2.1. Reasons for diabatic heating

Term in Sum	Reason for energy change
$Q_{c/e}$	condensational growth (evaporation)
$Q_{f/m}$	freezing (melting)
$Q_{dp/s}$	depositional growth (sublimation)
Q_{solar}	solar radiation (heating)
Q_{ir}	infra-red radiation (cooling)

2.3 Newton's Law and Momentum

2.3.1 Conversion to Spherical Coordinates

The equations developed to this point are equations which disregard the curvature of the Earth's surface. They make use of the Cartesian x , y , and z coordinates and the related basis vectors. For use in a global model of Earth's atmosphere, these equations should be converted for use with spherical coordinates. To do this, the x and y coordinates will be changed to λ and φ coordinates where λ is the equivalent of longitude ranging from 0 to 2π and φ is the equivalent of latitude ranging from $-\frac{\pi}{2}$ to $\frac{\pi}{2}$. The third coordinate will be the height above the center of the Earth, initially this will be the variable r to prevent confusion with the Cartesian z coordinate, but eventually this will be converted back to being the z variable. Along with this, the basis vectors \mathbf{i} , \mathbf{j} , and \mathbf{k} used for Cartesian coordinates will be converted to new basis vectors \mathbf{i}_λ , \mathbf{j}_φ , and \mathbf{k}_r . The vector \mathbf{i}_λ always points to the East at the surface of the Earth, \mathbf{j}_φ always points to the North at the surface of the Earth, and \mathbf{k}_r always points upwards in the vertical direction, again, at the surface of the Earth. Figure 2.2 shows the orientation of these new basis vectors.

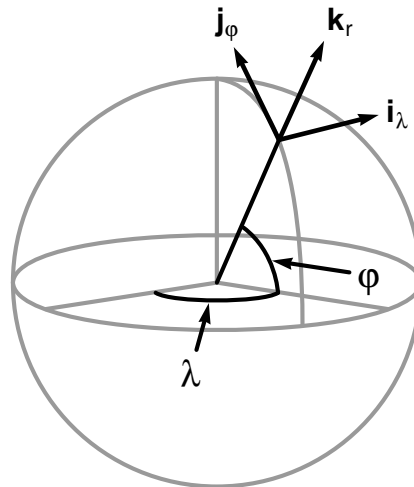


Figure 2.2. The basis vectors for spherical coordinates.

2.3.1.1 Spherical Unit Vectors

The equations (2.50) can be used to convert between Cartesian coordinates and spherical coordinates. These transformation equations make use of the two-parameter inverse tangent function so that there is no confusion about the quadrants of the angles involved. This function is equivalent to the “atan2” function available in many computer programming languages and spreadsheets. If x is greater than 0, then the value of $\arctan(y, x)$ is the same as $\tan^{-1} \frac{y}{x}$ so that $\arctan(y, x)$ is between $-\frac{\pi}{2}$ and $\frac{\pi}{2}$ for this case. If x is less than 0, then $\arctan(y, x) = \tan^{-1} \frac{y}{x} + \pi$. If x equals 0, then the value of $\arctan(y, x)$ is either $-\frac{\pi}{2}$ when $y < 0$, or $\frac{\pi}{2}$ when $y > 0$. In this way, the value of $\arctan(y, x)$ gives a unique angle with the quadrant correctly determined. Note that if both x and y are equal to zero, then the value of $\arctan(y, x)$ is undefined.

$$r = \sqrt{x^2 + y^2 + z^2} \qquad x = r \cos \lambda \cos \varphi \qquad (2.48)$$

$$\lambda = \arctan(y, x) \qquad y = r \sin \lambda \cos \varphi \qquad (2.49)$$

$$\varphi = \arctan \left(z, \sqrt{x^2 + y^2} \right) \qquad z = r \sin \varphi \qquad (2.50)$$

The unit vectors for spherical coordinates can be calculated in terms of the Cartesian unit vectors by making use of these transformation equations. To begin this process, the spherical unit vector \mathbf{k}_r is a unit vector with the direction which points away from the origin. Using the transformation equations (2.50), this unit vector can be calculated as:

$$\mathbf{k}_r = \frac{\mathbf{r}}{r} = \frac{x\mathbf{i} + y\mathbf{j} + z\mathbf{k}}{r} = \mathbf{i} \cos \lambda \cos \varphi + \mathbf{j} \sin \lambda \cos \varphi + \mathbf{k} \sin \varphi \qquad (2.51)$$

The spherical unit vector \mathbf{i}_λ can be found by noting that it is a unit vector which is orthogonal to both the \mathbf{k}_r spherical unit vector and the Cartesian \mathbf{k} vector. This unit vector can be found through the use of a vector cross product of the \mathbf{k} and \mathbf{k}_r vectors. The \mathbf{k} vector should be first in the cross product so that the value of λ increases as a position on the surface of the Earth moves in the direction of the \mathbf{i}_λ basis vector:

$$\mathbf{k} \times \mathbf{k}_r = \begin{vmatrix} \mathbf{i} & \mathbf{j} & \mathbf{k} \\ 0 & 0 & 1 \\ \cos \lambda \cos \varphi & \sin \lambda \cos \varphi & \sin \varphi \end{vmatrix} = -\mathbf{i} \sin \lambda \cos \varphi + \mathbf{j} \cos \lambda \cos \varphi \qquad (2.52)$$

$$\|\mathbf{k} \times \mathbf{k}_r\| = \left\| -\mathbf{i} \sin \lambda \cos \varphi + \mathbf{j} \cos \lambda \cos \varphi \right\| = \cos \varphi \quad (2.53)$$

$$\mathbf{i}_\lambda = \frac{\mathbf{k} \times \mathbf{k}_r}{\|\mathbf{k} \times \mathbf{k}_r\|} = \frac{-\mathbf{i} \sin \lambda \cos \varphi + \mathbf{j} \cos \lambda \cos \varphi}{\cos \varphi} = -\mathbf{i} \sin \lambda + \mathbf{j} \cos \lambda \quad (2.54)$$

Finally, the \mathbf{j}_φ unit vector must be orthogonal to both the \mathbf{k}_r and \mathbf{i}_λ unit vectors. Again, the value of this unit vector can be calculated through the use of a vector cross product between these other two orthogonal unit vectors. The \mathbf{k}_r vector must be first in the cross product so that the value of φ increases as a position on the surface of the Earth moves in the direction of the \mathbf{j}_φ unit vector. Note that this vector is a unit vector; the norm of this vector will be 1 because it is the cross product of 2 orthogonal unit vectors:

$$\mathbf{j}_\varphi = \mathbf{k}_r \times \mathbf{i}_\lambda = \begin{vmatrix} \mathbf{i} & \mathbf{j} & \mathbf{k} \\ \cos \lambda \cos \varphi & \sin \lambda \cos \varphi & \sin \varphi \\ -\sin \lambda & \cos \lambda & 0 \end{vmatrix} \quad (2.55)$$

$$= -\mathbf{i} \cos \lambda \sin \varphi - \mathbf{j} \sin \lambda \sin \varphi + \mathbf{k} \cos \varphi \quad (2.56)$$

These three equations (2.51), (2.54), and (2.56) for \mathbf{i}_λ , \mathbf{j}_φ , and \mathbf{k}_r in terms of \mathbf{i} , \mathbf{j} , and \mathbf{k} can be solved for the Cartesian unit vectors to give these equations:

$$\mathbf{i} = -\mathbf{i}_\lambda \sin \lambda - \mathbf{j}_\varphi \cos \lambda \sin \varphi + \mathbf{k}_r \cos \lambda \cos \varphi \quad (2.57)$$

$$\mathbf{j} = \mathbf{i}_\lambda \cos \lambda - \mathbf{j}_\varphi \sin \lambda \sin \varphi + \mathbf{k}_r \sin \lambda \cos \varphi \quad (2.58)$$

$$\mathbf{k} = \mathbf{j}_\varphi \cos \varphi + \mathbf{k}_r \sin \varphi \quad (2.59)$$

These expressions for the Cartesian basis vectors in terms of the spherical basis vectors will be used to calculate the partial derivatives of the spherical unit vectors with respect to the spherical coordinate values.

2.3.1.2 Partial Derivatives of Spherical Unit Vectors

The partial derivatives of the spherical unit vectors with respect to the spherical coordinate variables will be needed for converting the gradient from Cartesian coordinates to spherical coordinates. Each of these nine partial derivatives can be calculated through the use of the equations developed in the last section. The partial derivatives of the \mathbf{i}_λ vector with respect to each of the spherical coordinates can be found by taking the corresponding partial derivatives of equation (2.54) and then

substituting for the values of the Cartesian unit vectors as per equations (2.59), (2.57), and (2.58):

$$\begin{aligned} \frac{\partial \mathbf{i}_\lambda}{\partial \lambda} &= -(-\mathbf{i}_\lambda \sin \lambda - \mathbf{j}_\varphi \cos \lambda \sin \varphi + \mathbf{k}_r \cos \lambda \cos \varphi) \cos \lambda \\ &\quad - (\mathbf{i}_\lambda \cos \lambda - \mathbf{j}_\varphi \sin \lambda \sin \varphi + \mathbf{k}_r \sin \lambda \cos \varphi) \sin \lambda \end{aligned} \quad (2.60)$$

$$= \mathbf{j}_\varphi \sin \varphi - \mathbf{k}_r \cos \varphi \quad (2.61)$$

$$\frac{\partial \mathbf{i}_\lambda}{\partial \varphi} = 0 \quad (2.62)$$

$$\frac{\partial \mathbf{i}_\lambda}{\partial r} = 0 \quad (2.63)$$

In the same way, the partial derivatives of \mathbf{j}_φ and \mathbf{k}_r can be calculated using equations (2.56) and (2.51):

$$\begin{aligned} \frac{\partial \mathbf{j}_\varphi}{\partial \lambda} &= (-\mathbf{i}_\lambda \sin \lambda - \mathbf{j}_\varphi \cos \lambda \sin \varphi + \mathbf{k}_r \cos \lambda \cos \varphi) \sin \lambda \sin \varphi \\ &\quad - (\mathbf{i}_\lambda \cos \lambda - \mathbf{j}_\varphi \sin \lambda \sin \varphi + \mathbf{k}_r \sin \lambda \cos \varphi) \cos \lambda \sin \varphi \end{aligned} \quad (2.64)$$

$$= -\mathbf{i}_\lambda \sin \varphi \quad (2.65)$$

$$\begin{aligned} \frac{\partial \mathbf{j}_\varphi}{\partial \varphi} &= -(-\mathbf{i}_\lambda \sin \lambda - \mathbf{j}_\varphi \cos \lambda \sin \varphi + \mathbf{k}_r \cos \lambda \cos \varphi) \cos \lambda \cos \varphi \\ &\quad - (\mathbf{i}_\lambda \cos \lambda - \mathbf{j}_\varphi \sin \lambda \sin \varphi + \mathbf{k}_r \sin \lambda \cos \varphi) \sin \lambda \cos \varphi \\ &\quad - (\mathbf{j}_\varphi \cos \varphi + \mathbf{k}_r \sin \varphi) \sin \varphi \end{aligned} \quad (2.66)$$

$$= -\mathbf{k}_r \quad (2.67)$$

$$\frac{\partial \mathbf{j}_\varphi}{\partial r} = 0 \quad (2.68)$$

$$\begin{aligned} \frac{\partial \mathbf{k}_r}{\partial \lambda} &= -(-\mathbf{i}_\lambda \sin \lambda - \mathbf{j}_\varphi \cos \lambda \sin \varphi + \mathbf{k}_r \cos \lambda \cos \varphi) \sin \lambda \cos \varphi \\ &\quad + (\mathbf{i}_\lambda \cos \lambda - \mathbf{j}_\varphi \sin \lambda \sin \varphi + \mathbf{k}_r \sin \lambda \cos \varphi) \cos \lambda \cos \varphi \end{aligned} \quad (2.69)$$

$$= -\mathbf{i}_\lambda \cos \varphi \quad (2.70)$$

$$\begin{aligned} \frac{\partial \mathbf{k}_r}{\partial \varphi} &= -(-\mathbf{i}_\lambda \sin \lambda - \mathbf{j}_\varphi \cos \lambda \sin \varphi + \mathbf{k}_r \cos \lambda \cos \varphi) \cos \lambda \sin \varphi \\ &\quad - (\mathbf{i}_\lambda \cos \lambda - \mathbf{j}_\varphi \sin \lambda \sin \varphi + \mathbf{k}_r \sin \lambda \cos \varphi) \sin \lambda \sin \varphi \\ &\quad + (\mathbf{j}_\varphi \cos \varphi + \mathbf{k}_r \sin \varphi) \cos \varphi \end{aligned} \quad (2.71)$$

$$= \mathbf{j}_\varphi \quad (2.72)$$

$$\frac{\partial \mathbf{k}_r}{\partial r} = 0 \quad (2.73)$$

These partial derivatives will be used to convert the gradient operator to spherical

coordinates.

2.3.1.3 Converting Velocities

The horizontal measurements x (East/West) and y (North/South) when measured at the surface of the Earth are replaced with the spherical coordinates λ and φ . Note that x and y are now the local East/West and North/South directions as measured at the surface of the Earth, not the corresponding Cartesian coordinates. Also, the local z direction is outward from the center of the Earth and not the Cartesian z coordinate. This means that the z coordinate is now the r coordinate which was initially used for spherical coordinates, and there is no conversion here for the z coordinate as it is not replaced by an angle measurement. The local x and y coordinates are related to the λ and φ coordinates by simply being multiples (proportional to the z coordinate) of each other, respectively. The derivatives of the local horizontal coordinates are related by:

$$dx = (z \cos \varphi) d\lambda \quad (2.74)$$

$$dy = z d\varphi \quad (2.75)$$

Converting horizontal velocities into spherical coordinates makes use of these relationships as:

$$u = \frac{dx}{dt} = z \cos \varphi \frac{d\lambda}{dt} \quad (2.76)$$

$$v = \frac{dy}{dt} = z \frac{d\varphi}{dt} \quad (2.77)$$

$$w = \frac{dz}{dt} \quad (2.78)$$

With these conversions, the local wind velocity can be converted to the corresponding spherical coordinate representation. The local wind velocity makes use of the local x and y coordinate values where these are the local East/West and North/South wind velocities relative to the surface of the Earth.

2.3.1.4 Gradient in Spherical Coordinates

The gradient operator in Cartesian coordinates is:

$$\nabla = \mathbf{i} \frac{\partial}{\partial x} + \mathbf{j} \frac{\partial}{\partial y} + \mathbf{k} \frac{\partial}{\partial z} \quad (2.79)$$

The same equation applies when the values of x , y , and z are the local coordinates at the surface of the Earth and the basis vectors used in the gradient are the spherical basis vectors. With the derivatives for velocities given in (2.78), the gradient operator in spherical coordinates is transformed to:

$$\nabla = \mathbf{i}_\lambda \frac{1}{z \cos \varphi} \frac{\partial}{\partial \lambda} + \mathbf{j}_\varphi \frac{1}{z} \frac{\partial}{\partial \varphi} + \mathbf{k}_r \frac{\partial}{\partial z} \quad (2.80)$$

However, applying the gradient operator for the divergence of a vector function like velocity, that is, when calculating a value such as $\nabla \cdot \mathbf{v}$, the derivatives of the spherical basis vectors become involved as well because these basis vectors do not have a constant direction so their derivatives are not zero. These basis vectors do remain orthogonal; the inner products $\mathbf{i}_\lambda \cdot \mathbf{j}_\varphi$, $\mathbf{i}_\lambda \cdot \mathbf{k}_r$, and $\mathbf{j}_\varphi \cdot \mathbf{k}_r$ are all equal to zero because of this orthogonality. To calculate $\nabla \cdot \mathbf{v}$ in spherical coordinates using (2.80) and $\mathbf{v} = \mathbf{i}_\lambda u + \mathbf{j}_\varphi v + \mathbf{k}_r w$:

$$\nabla \cdot \mathbf{v} = \left(\mathbf{i}_\lambda \frac{1}{z \cos \varphi} \frac{\partial}{\partial \lambda} + \mathbf{j}_\varphi \frac{1}{z} \frac{\partial}{\partial \varphi} + \mathbf{k}_r \frac{\partial}{\partial z} \right) \cdot (\mathbf{i}_\lambda u + \mathbf{j}_\varphi v + \mathbf{k}_r w) \quad (2.81)$$

$$\begin{aligned} &= \left(\frac{1}{z \cos \varphi} \frac{\partial u}{\partial \lambda} + \mathbf{i}_\lambda \frac{u}{z \cos \varphi} \cdot \frac{\partial \mathbf{i}_\lambda}{\partial \lambda} + \mathbf{i}_\lambda \frac{v}{z \cos \varphi} \cdot \frac{\partial \mathbf{j}_\varphi}{\partial \lambda} + \mathbf{i}_\lambda \frac{w}{z \cos \varphi} \cdot \frac{\partial \mathbf{k}_r}{\partial \lambda} \right) \\ &+ \left(\frac{1}{z} \frac{\partial v}{\partial \varphi} + \mathbf{j}_\varphi \frac{u}{z} \cdot \frac{\partial \mathbf{i}_\lambda}{\partial \varphi} + \mathbf{j}_\varphi \frac{v}{z} \cdot \frac{\partial \mathbf{j}_\varphi}{\partial \varphi} + \mathbf{j}_\varphi \frac{w}{z} \cdot \frac{\partial \mathbf{k}_r}{\partial \varphi} \right) \\ &+ \left(\frac{\partial w}{\partial z} + \mathbf{k}_r u \cdot \frac{\partial \mathbf{i}_\lambda}{\partial z} + \mathbf{k}_r v \cdot \frac{\partial \mathbf{j}_\varphi}{\partial z} + \mathbf{k}_r w \cdot \frac{\partial \mathbf{k}_r}{\partial z} \right) \end{aligned} \quad (2.82)$$

Substituting the values of the partial derivatives into (2.82) (and using z in place of r) gives the value of the gradient in spherical coordinates:

$$\begin{aligned} \nabla \cdot \mathbf{v} &= \left(\frac{1}{z \cos \varphi} \frac{\partial u}{\partial \lambda} + \mathbf{i}_\lambda \frac{u}{z \cos \varphi} \cdot (\mathbf{j}_\varphi \sin \varphi - \mathbf{k}_r \cos \varphi) + \mathbf{i}_\lambda \frac{v}{z \cos \varphi} \cdot (-\mathbf{i}_\lambda \sin \varphi) \right. \\ &\quad \left. + \mathbf{i}_\lambda \frac{w}{z \cos \varphi} \cdot (\mathbf{i}_\lambda \cos \varphi) \right) \\ &+ \left(\frac{1}{z} \frac{\partial v}{\partial \varphi} + \mathbf{j}_\varphi \frac{u}{z} \cdot \mathbf{0} + \mathbf{j}_\varphi \frac{v}{z} \cdot (-\mathbf{k}_r) + \mathbf{j}_\varphi \frac{w}{z} \cdot \mathbf{j}_\varphi \right) \\ &+ \left(\frac{\partial w}{\partial z} + \mathbf{k}_r u \cdot \mathbf{0} + \mathbf{k}_r v \cdot \mathbf{0} + \mathbf{k}_r w \cdot \mathbf{0} \right) \end{aligned} \quad (2.83)$$

$$= \left(\frac{1}{z \cos \varphi} \frac{\partial u}{\partial \lambda} - \frac{v \sin \varphi}{z \cos \varphi} + \frac{w}{z} \right) + \left(\frac{1}{z} \frac{\partial v}{\partial \varphi} + \frac{w}{z} \right) + \frac{\partial w}{\partial z} \quad (2.84)$$

$$= \frac{1}{z \cos \varphi} \frac{\partial u}{\partial \lambda} + \left(\frac{1}{z} \frac{\partial v}{\partial \varphi} - \frac{v \sin \varphi}{z \cos \varphi} \right) + \left(2 \frac{w}{z} + \frac{\partial w}{\partial z} \right) \quad (2.85)$$

$$= \frac{1}{z \cos \varphi} \frac{\partial u}{\partial \lambda} + \frac{1}{z \cos \varphi} \frac{\partial}{\partial \varphi} (v \cos \varphi) + \frac{1}{z^2} \frac{\partial}{\partial z} (wz^2) \quad (2.86)$$

For modeling the atmosphere, the value of z can be taken as a constant relative to the radius of the Earth, R_e , without introducing too large an error. The maximum height above sea level used in most models is on the order of 50 to 100 kilometers while the radius of the Earth, R_e , is about 6371 kilometers. Taking $z \approx R_e$ being approximately a constant changes the last term in equation 2.86 to:

$$\nabla \cdot \mathbf{v} = \frac{1}{R_e \cos \varphi} \frac{\partial u}{\partial \lambda} + \frac{1}{R_e \cos \varphi} \frac{\partial}{\partial \varphi} (v \cos \varphi) + \frac{\partial w}{\partial z} \quad (2.87)$$

This definition of the gradient in spherical coordinates is used later to find $\nabla \cdot (\mathbf{v}_h)$ and $\nabla \cdot (\mathbf{v}_h \pi)$ where π is the difference between the pressure at the surface of the Earth and the pressure at the maximum height of the model. The variable \mathbf{v}_h is the horizontal velocity or no \mathbf{k}_r component). These divergences are:

$$\nabla \cdot (\mathbf{v}_h) = \frac{1}{R_e \cos \varphi} \frac{\partial}{\partial \lambda} (u) + \frac{1}{R_e \cos \varphi} \frac{\partial}{\partial \varphi} (v \cos \varphi) \quad (2.88)$$

$$\nabla \cdot (\mathbf{v}_h \pi) = \frac{1}{R_e \cos \varphi} \frac{\partial}{\partial \lambda} (u\pi) + \frac{1}{R_e \cos \varphi} \frac{\partial}{\partial \varphi} (v\pi \cos \varphi) \quad (2.89)$$

2.3.2 Rotation of the Earth

The motion of a parcel of air in the atmosphere depends on the forces applied to that parcel of air. The acceleration of the parcel of air is proportional to the vector sum of those forces. If the Earth were not rotating, the parcel of air in the atmosphere would be moving in an inertial reference frame when its motion is measured using a coordinate system based on the surface of the Earth. An inertial reference frame is a frame of reference or a coordinate system which is not accelerating or rotating. This means that the motion of the air appears to be affected by forces due to the rotation of the Earth when viewed from a position rotating with the surface of the Earth.

Because the Earth is rotating, a frame of reference based on coordinates measured from a point on the surface of the Earth is being measured in an accelerating frame of reference, or a noninertial frame of reference. Sometimes the effects of the rotation of the Earth can be seen in everyday events. The direction in which a large storm in the atmosphere, such as a hurricane, rotates is determined by rotation of the Earth

and the hemisphere in which the storm is located. A hurricane can be described as a large area of lower pressure in the atmosphere, so that air tends to move toward the center of the storm. Hurricanes in the northern hemisphere rotate counter-clockwise while hurricanes in the southern hemisphere rotate clockwise. The movement of the air in a storm like this is affected by the rotation of the Earth when the movement of the air is measured based on the location of a point on the surface of the Earth.

Any observer at a fixed point in space (or a nonaccelerating point in space) observing a parcel of air in the atmosphere of the Earth would be observing from an inertial reference frame. If the parcel of air is moving at a velocity \mathbf{v} relative to the surface of the Earth, the Earth is rotating with an angular velocity vector $\boldsymbol{\Omega}$, and \mathbf{R}_e is the radius vector from the center of the Earth to the parcel of air, then the observer in the inertial reference frame would see the parcel of air moving with absolute velocity of:

$$\mathbf{v}_{\text{inertial}} = \mathbf{v}_{\text{rotating}} + \boldsymbol{\Omega} \times \mathbf{R}_e \quad (2.90)$$

Note that for the Earth, $|\boldsymbol{\Omega}| = \Omega \approx 2\pi/86164 \approx 7.292 \times 10^{-5}$ radians per second where 86164 seconds is the approximate length of a sidereal day. The vector $\boldsymbol{\Omega}$ is parallel to the axis of rotation of the Earth and points to the North so that $\boldsymbol{\Omega} = \Omega \mathbf{k}$. To use this equation to determine the relationship between the observed inertial acceleration and the acceleration in the rotating frame of reference, let $\mathbf{X}_{\text{rotating}} = x \mathbf{i}_\lambda + y \mathbf{j}_\varphi + z \mathbf{k}_r$ be the position of a particle relative to a point on the surface of the Earth. Now the velocity as seen from a rotating position on the surface of the Earth is just the time derivative of this value:

$$\left(\frac{d\mathbf{X}}{dt} \right)_{\text{rotating}} = \frac{dx}{dt} \mathbf{i}_\lambda + \frac{dy}{dt} \mathbf{j}_\varphi + \frac{dz}{dt} \mathbf{k}_r \quad (2.91)$$

This is what the rotating (noninertial) observer on the surface of the Earth would see as the velocity of the particle. In order to convert this to the inertial reference frame, the same derivative would need to take the variation of the unit vectors due to the rotation into account. This conversion will make use of equations (2.51), (2.54), and (2.56), and the fact that $\boldsymbol{\Omega} = \Omega \mathbf{k}$ and $\frac{d\lambda}{dt} = \Omega$. The derivatives of these unit vectors,

in the inertial reference frame with φ and z both constant as they would be for an object rotating with the surface of the Earth, are:

$$\left(\frac{d\mathbf{i}_\lambda}{dt}\right)_{\text{inertial}} = \frac{d}{dt}(-\mathbf{i} \sin \lambda + \mathbf{j} \cos \lambda) = (-\mathbf{i} \cos \lambda - \mathbf{j} \sin \lambda) \frac{d\lambda}{dt} \quad (2.92)$$

$$= \begin{vmatrix} \mathbf{i} & \mathbf{j} & \mathbf{k} \\ 0 & 0 & \Omega \\ -\sin \varphi & \cos \varphi & 0 \end{vmatrix} = \boldsymbol{\Omega} \times \mathbf{i}_\lambda \quad (2.93)$$

$$\left(\frac{d\mathbf{j}_\varphi}{dt}\right)_{\text{inertial}} = \frac{d}{dt}(-\mathbf{i} \cos \lambda \sin \varphi - \mathbf{j} \sin \lambda \sin \varphi + \mathbf{k} \cos \varphi) \quad (2.94)$$

$$= (\mathbf{i} \sin \lambda \sin \varphi - \mathbf{j} \cos \lambda \sin \varphi) \frac{d\lambda}{dt} = \boldsymbol{\Omega} \times \mathbf{j}_\varphi \quad (2.95)$$

$$\left(\frac{d\mathbf{k}_r}{dt}\right)_{\text{inertial}} = \frac{d}{dt}(\mathbf{i} \cos \lambda \cos \varphi + \mathbf{j} \sin \lambda \cos \varphi + \mathbf{k} \sin \varphi) \quad (2.96)$$

$$= (-\mathbf{i} \sin \lambda \cos \varphi + \mathbf{j} \cos \lambda \cos \varphi) \frac{d\lambda}{dt} = \boldsymbol{\Omega} \times \mathbf{k}_r \quad (2.97)$$

Taking the derivative of the position in the inertial frame of reference and making use of the chain rule for derivatives gives:

$$\begin{aligned} \left(\frac{d\mathbf{X}}{dt}\right)_{\text{inertial}} &= \frac{dx}{dt} \mathbf{i}_\lambda + x \left(\frac{d\mathbf{i}_\lambda}{dt}\right)_{\text{inertial}} + \frac{dy}{dt} \mathbf{j}_\varphi + y \left(\frac{d\mathbf{j}_\varphi}{dt}\right)_{\text{inertial}} \\ &\quad + \frac{dz}{dt} \mathbf{k}_r + z \left(\frac{d\mathbf{k}_r}{dt}\right)_{\text{inertial}} \end{aligned} \quad (2.98)$$

$$= \frac{dx}{dt} \mathbf{i}_\lambda + \frac{dy}{dt} \mathbf{j}_\varphi + \frac{dz}{dt} \mathbf{k}_r + \boldsymbol{\Omega} \times (x \mathbf{i}_\lambda + y \mathbf{j}_\varphi + z \mathbf{k}_r) \quad (2.99)$$

$$= \left(\frac{d\mathbf{X}}{dt}\right)_{\text{rotating}} + \boldsymbol{\Omega} \times \mathbf{X} \quad (2.100)$$

$$\left(\frac{d}{dt}\right)_{\text{inertial}} = \left[\left(\frac{d}{dt}\right)_{\text{rotating}} + \boldsymbol{\Omega} \times \right] \quad \text{The derivative as an operator} \quad (2.101)$$

Using (2.90), and taking its derivative in the inertial frame of reference through the use of equation (2.101), gives the acceleration in the inertial frame of reference:

$$\left(\frac{d\mathbf{v}}{dt}\right)_{\text{inertial}} = \left[\left(\frac{d}{dt}\right)_{\text{rotating}} + \boldsymbol{\Omega} \times \right] (\mathbf{v} + \boldsymbol{\Omega} \times \mathbf{R}_e) \quad (2.102)$$

$$= \left(\frac{d\mathbf{v}}{dt}\right)_{\text{rotating}} + \boldsymbol{\Omega} \times \left(\frac{d\mathbf{R}_e}{dt}\right)_{\text{rotating}} + \boldsymbol{\Omega} \times \mathbf{v} + \boldsymbol{\Omega} \times \boldsymbol{\Omega} \times \mathbf{v} \quad (2.103)$$

The value of $\left(\frac{d\mathbf{R}_e}{dt}\right)_{\text{rotating}}$ is approximately equal to the velocity of the particle \mathbf{v} when the vertical component of \mathbf{v} is small compared to the horizontal component,

which is usually the case in the atmosphere. With that change, the last equation becomes:

$$\mathbf{a}_{\text{inertial}} = \left(\frac{d\mathbf{v}}{dt} \right)_{\text{inertial}} = \left(\frac{d\mathbf{v}}{dt} \right)_{\text{rotating}} + 2\boldsymbol{\Omega} \times \mathbf{v} + \boldsymbol{\Omega} \times \boldsymbol{\Omega} \times \mathbf{v} \quad (2.104)$$

$$= \mathbf{a}_\ell + \mathbf{a}_c + \mathbf{a}_r \quad (2.105)$$

The three components of $\mathbf{a}_{\text{inertial}}$ are \mathbf{a}_ℓ , which is the local (noninertial) acceleration; \mathbf{a}_c , which is the Coriolis acceleration; and \mathbf{a}_r , which is the centripetal acceleration.

The total acceleration of a parcel of air is due to the different forces acting on the parcel of air. These forces are due to gravity (\mathbf{F}_g), the pressure gradient force (\mathbf{F}_p), and forces caused by the molecular viscosity of the air (\mathbf{F}_v). Taking M as the mass of the parcel of air, the effects of these forces can be related to the inertial acceleration of the air parcel through Newton's second law:

$$\mathbf{a}_\ell + \mathbf{a}_c + \mathbf{a}_r = \frac{1}{M}(\mathbf{F}_g + \mathbf{F}_p + \mathbf{F}_v) \quad (2.106)$$

Because the motion of the parcel of air will be calculated relative to a position on the surface of the Earth, only the local acceleration is useful as an output from any model. To better show the relationship between the local acceleration and the forces involved, the Coriolis and centripetal accelerations will be converted to forces by setting them equal to an equivalent force divided by the mass of the parcel of air. Also, the centripetal force will be treated as a negative force so that it becomes an apparent centrifugal force. With that, the local acceleration becomes:

$$\mathbf{a}_\ell = \frac{1}{M}(\mathbf{F}_r - \mathbf{F}_c + \mathbf{F}_g + \mathbf{F}_p + \mathbf{F}_v) \quad (2.107)$$

Each of the terms in this equation will be treated differently in the following sections.

2.3.2.1 Local Acceleration

The local acceleration is the total derivative of the velocity of the air parcel in the rotating frame of reference:

$$\mathbf{a}_\ell = \frac{d\mathbf{v}}{dt} = \frac{\partial \mathbf{v}}{\partial t} + (\mathbf{v} \cdot \nabla)\mathbf{v} \quad (2.108)$$

Equation (2.108) shows that the local acceleration is due to the acceleration at that

point plus any flux of acceleration due to air moving in or out of the cell or parcel of air. Expanding this equation in Cartesian coordinates is not difficult, it becomes:

$$\mathbf{i} \frac{du}{dt} + \mathbf{j} \frac{dv}{dt} + \mathbf{k} \frac{dw}{dt} = \left(\frac{\partial}{\partial t} + u \frac{\partial}{\partial x} + v \frac{\partial}{\partial y} + w \frac{\partial}{\partial z} \right) (\mathbf{i}u + \mathbf{j}v + \mathbf{k}w) \quad (2.109)$$

$$= \mathbf{i} \left(\frac{\partial u}{\partial t} + u \frac{\partial u}{\partial x} + v \frac{\partial u}{\partial y} + w \frac{\partial u}{\partial z} \right) + \mathbf{j} \left(\frac{\partial v}{\partial t} + u \frac{\partial v}{\partial x} + v \frac{\partial v}{\partial y} + w \frac{\partial v}{\partial z} \right) \quad (2.110)$$

$$+ \mathbf{k} \left(\frac{\partial w}{\partial t} + u \frac{\partial w}{\partial x} + v \frac{\partial w}{\partial y} + w \frac{\partial w}{\partial z} \right) \quad (2.111)$$

Expanding this same equation in spherical coordinates requires more work. The left side becomes:

$$\frac{d\mathbf{v}}{dt} = \frac{d}{dt} (\mathbf{i}_\lambda u + \mathbf{j}_\varphi v + \mathbf{k}_r w) \quad (2.112)$$

$$= \mathbf{i}_\lambda \frac{du}{dt} + u \frac{d\mathbf{i}_\lambda}{dt} + \mathbf{j}_\varphi \frac{dv}{dt} + v \frac{d\mathbf{j}_\varphi}{dt} + \mathbf{k}_r \frac{dw}{dt} + w \frac{d\mathbf{k}_r}{dt} \quad (2.113)$$

Now, the time derivatives of the spherical basis vectors are needed because these basis vectors are not constant. Because $dx = (R_e \cos \varphi) d\lambda$ and $dy = R_e d\varphi$, the total derivative in spherical coordinates is:

$$\frac{d}{dt} = \frac{\partial}{\partial t} + \frac{u}{R_e \cos \varphi} \frac{\partial}{\partial \lambda} + \frac{v}{R_e} \frac{\partial}{\partial \varphi} + w \frac{\partial}{\partial z} \quad (2.114)$$

This can be applied to find the total derivatives of \mathbf{i}_λ , \mathbf{j}_φ , and \mathbf{k}_r . Note that in the rotating frame of reference, the derivatives of the spherical basis vectors with respect to time will all be zero.

$$\frac{d\mathbf{i}_\lambda}{dt} = \frac{\partial \mathbf{i}_\lambda}{\partial t} + \frac{u}{R_e \cos \varphi} \frac{\partial \mathbf{i}_\lambda}{\partial \lambda} + \frac{v}{R_e} \frac{\partial \mathbf{i}_\lambda}{\partial \varphi} + w \frac{\partial \mathbf{i}_\lambda}{\partial z} \quad (2.115)$$

$$= 0 + \frac{u}{R_e \cos \varphi} (\mathbf{j}_\varphi \sin \varphi - \mathbf{k}_r \cos \varphi) + \frac{v}{R_e} \cdot (0) + w \cdot (0) \quad (2.116)$$

$$= \mathbf{j}_\varphi \frac{u \tan \varphi}{R_e} - \mathbf{k}_r \frac{u}{R_e} \quad (2.117)$$

$$\frac{d\mathbf{j}_\varphi}{dt} = \frac{\partial \mathbf{j}_\varphi}{\partial t} + \frac{u}{R_e \cos \varphi} \frac{\partial \mathbf{j}_\varphi}{\partial \lambda} + \frac{v}{R_e} \frac{\partial \mathbf{j}_\varphi}{\partial \varphi} + w \frac{\partial \mathbf{j}_\varphi}{\partial z} \quad (2.118)$$

$$= 0 + \frac{u}{R_e \cos \varphi} (-\mathbf{i}_\lambda \sin \varphi) + \frac{v}{R_e} (-\mathbf{k}_r) + w \cdot (0) \quad (2.119)$$

$$= -\mathbf{i}_\lambda \frac{u \tan \varphi}{R_e} - \mathbf{k}_r \frac{v}{R_e} \quad (2.120)$$

$$\frac{d\mathbf{k}_r}{dt} = \frac{\partial \mathbf{k}_r}{\partial t} + \frac{u}{R_e \cos \varphi} \frac{\partial \mathbf{k}_r}{\partial \lambda} + \frac{v}{R_e} \frac{\partial \mathbf{k}_r}{\partial \varphi} + w \frac{\partial \mathbf{k}_r}{\partial z} \quad (2.121)$$

$$= 0 + \frac{u}{R_e \cos \varphi} (\mathbf{i}_\lambda \cos \varphi) + \frac{v}{R_e} (\mathbf{j}_\varphi) + w \cdot (0) \quad (2.122)$$

$$= \mathbf{i}_\lambda \frac{u}{R_e} + \mathbf{j}_\varphi \frac{v}{R_e} \quad (2.123)$$

Substituting these values into the total derivative for spherical coordinates (2.113) gives:

$$\frac{d\mathbf{v}}{dt} = \mathbf{i}_\lambda \frac{du}{dt} + u \left(\mathbf{j}_\varphi \frac{u \tan \varphi}{R_e} - \mathbf{k}_r \frac{u}{R_e} \right) + \mathbf{j}_\varphi \frac{dv}{dt} + v \left(-\mathbf{i}_\lambda \frac{u \tan \varphi}{R_e} - \mathbf{k}_r \frac{v}{R_e} \right) + \mathbf{k}_r \frac{dw}{dt} \quad (2.124)$$

$$+ w \left(\mathbf{i}_\lambda \frac{u}{R_e} + \mathbf{j}_\varphi \frac{v}{R_e} \right) \quad (2.125)$$

$$= \mathbf{i}_\lambda \left(\frac{du}{dt} - \frac{uv \tan \varphi}{R_e} + \frac{uw}{R_e} \right) + \mathbf{j}_\varphi \left(\frac{dv}{dt} + \frac{u^2 \tan \varphi}{R_e} + \frac{uv}{R_e} \right) \quad (2.126)$$

$$+ \mathbf{k}_r \left(\frac{dw}{dt} - \frac{u^2}{R_e} - \frac{v^2}{R_e} \right) \quad (2.127)$$

To further simplify this expression, note that the terms $\frac{uw}{R_e}$ and $\frac{uv}{R_e}$ are small for large scale motions because w is much smaller than either u or v . These two terms can be removed without incorporating too much of an error. To keep from adding energy to the system, the $\frac{u^2}{R_e}$ and $\frac{v^2}{R_e}$ must also be removed from the vertical expression when the other terms are removed [5]. Now the local acceleration in spherical coordinates as a total derivative is:

$$\frac{d\mathbf{v}}{dt} = \mathbf{i}_\lambda \left(\frac{du}{dt} - \frac{uv \tan \varphi}{R_e} \right) + \mathbf{j}_\varphi \left(\frac{dv}{dt} + \frac{u^2 \tan \varphi}{R_e} \right) + \mathbf{k}_r \left(\frac{dw}{dt} \right) \quad (2.128)$$

Expanding equation (2.128) by making use of the total derivatives of u , v , and w gives the velocity in the rotating frame of reference:

$$\begin{aligned} \frac{d\mathbf{v}}{dt} = & \mathbf{i}_\lambda \left(\frac{\partial u}{\partial t} + \frac{u}{R_e \cos \varphi} \frac{\partial u}{\partial \lambda} + \frac{v}{R_e} \frac{\partial u}{\partial \varphi} + w \frac{\partial u}{\partial w} - \frac{uv \tan \varphi}{R_e} \right) \\ & + \mathbf{j}_\varphi \left(\frac{\partial v}{\partial t} + \frac{u}{R_e \cos \varphi} \frac{\partial v}{\partial \lambda} + \frac{v}{R_e} \frac{\partial v}{\partial \varphi} + w \frac{\partial v}{\partial w} + \frac{u^2 \tan \varphi}{R_e} \right) \\ & + \mathbf{k}_r \left(\frac{\partial w}{\partial t} + \frac{u}{R_e \cos \varphi} \frac{\partial w}{\partial \lambda} + \frac{v}{R_e} \frac{\partial w}{\partial \varphi} + w \frac{\partial w}{\partial w} \right) \end{aligned} \quad (2.129)$$

Equation (2.129) is the local acceleration of a parcel of air as seen by an observer rotating with the Earth.

2.3.2.2 Coriolis Forces

Coriolis forces are apparent forces acting on a moving parcel of air as seen from the rotating reference frame which are caused by the rotation of the Earth. Note that from a point on the Earth's surface, the spherical basis vectors will be oriented at an angle to the axis of rotation of the Earth. That angle will be equal to φ or the latitude of the point on the surface of the Earth. Stated differently, the value of $\mathbf{\Omega}$ is $\mathbf{\Omega} \mathbf{k} = \mathbf{j}_\varphi \Omega \cos \varphi + \mathbf{k}_r \Omega \sin \varphi$ in terms of the spherical basis vectors. To find the value of the acceleration due to the Coriolis forces:

$$\mathbf{a}_r = \frac{\mathbf{F}_r}{M} = 2\mathbf{\Omega} \times \mathbf{v} = 2\Omega \begin{vmatrix} \mathbf{i}_\lambda & \mathbf{j}_\varphi & \mathbf{k}_r \\ 0 & \cos \varphi & \sin \varphi \\ u & v & w \end{vmatrix} \quad (2.130)$$

$$= \mathbf{i}_\lambda 2\Omega(w \cos \varphi - v \sin \varphi) + \mathbf{j}_\varphi 2\Omega u \sin \varphi - \mathbf{k}_r 2\Omega u \cos \varphi \quad (2.131)$$

Further simplifications to equation (2.131) are that because the vertical velocities are much smaller than horizontal velocities for any model with a sufficiently large time scale; the $2\Omega w \cos \varphi$ term can be removed from the \mathbf{i}_λ portion of this equation. Since the vertical component of the Coriolis forces is much smaller than the vertical component of gravitational or pressure gradient forces, the component for the \mathbf{k}_r term can also be ignored and removed [5].

$$\mathbf{a}_r \approx -\mathbf{i}_\lambda 2\Omega v \sin \varphi + \mathbf{j}_\varphi 2\Omega u \sin \varphi \quad (2.132)$$

This leads to an approximation of the Coriolis forces as $f = 2\Omega \sin \varphi$ and the Coriolis forces become:

$$\frac{\mathbf{F}_r}{M} \approx -\mathbf{i}_\lambda f v + \mathbf{j}_\varphi f u = f \begin{vmatrix} \mathbf{i}_\lambda & \mathbf{j}_\varphi & \mathbf{k}_r \\ 0 & 0 & 1 \\ u & v & 0 \end{vmatrix} = f \mathbf{k}_r \times \mathbf{v}_h \quad (2.133)$$

With the approximations used here, the Coriolis forces become very easy to calculate.

2.3.2.3 Gravitational and Centrifugal Forces

The force of gravity acts on all parcels of air in the atmosphere. The Earth itself is not actually a sphere, it can be modeled more accurately as an oblate spheroid. Calculating the actual gravitational attraction that a parcel of air experiences should take the shape of the Earth into account. However, the Earth is usually modeled as

a perfect sphere in order to simplify the calculations. With the Earth as a perfect sphere, the acceleration due to gravity is:

$$\mathbf{a}_g = \frac{\mathbf{F}_g}{M} = -\mathbf{k}_r g \quad (2.134)$$

The constant $g \approx 9.81 \text{ m s}^{-2}$ is derived from Newton's law of gravitation; the force between two bodies is:

$$\mathbf{F} = -\mathbf{r} \frac{GM_1M_2}{\|\mathbf{r}\|^3} \quad (2.135)$$

The variable G is the gravitational constant, $G \approx 6.6720 \times 10^{-11} \text{ m}^3 \text{ kg}^{-1} \text{ s}^{-1}$ and M_1 and M_2 are the masses of the two bodies. For the force exerted on a parcel of air by the Earth:

$$\frac{\mathbf{F}_g}{M} = -\mathbf{k}_r \frac{GM_e}{R_e^2} \quad (2.136)$$

$$g = \frac{GM_e}{R_e^2} \quad (2.137)$$

The Centrifugal force acting on a parcel of air is an apparent force. Its value as a force per unit mass is:

$$-\mathbf{a}_r = \frac{\mathbf{F}_r}{M} = -\boldsymbol{\Omega} \times (\boldsymbol{\Omega} \times \mathbf{R}_e) \quad (2.138)$$

To evaluate this, first evaluate $\boldsymbol{\Omega} \times \mathbf{R}_e$. Again, note that the angle between \mathbf{R}_e and $\boldsymbol{\Omega}$ is the angle φ of the position on the surface of the Earth corresponding to \mathbf{R}_e . This cross product is:

$$\boldsymbol{\Omega} \times \mathbf{R}_e = \Omega \begin{vmatrix} \mathbf{i}_\lambda & \mathbf{j}_\varphi & \mathbf{k}_r \\ 0 & \cos \varphi & \sin \varphi \\ 0 & 0 & R_e \end{vmatrix} = \mathbf{i}_\lambda R_e \Omega \cos \varphi \quad (2.139)$$

Now the value of $-\mathbf{a}_r$ becomes:

$$-\boldsymbol{\Omega} \times (\boldsymbol{\Omega} \times \mathbf{R}_e) = -\Omega \begin{vmatrix} \mathbf{i}_\lambda & \mathbf{j}_\varphi & \mathbf{k}_r \\ 0 & \cos \varphi & \sin \varphi \\ R_e \Omega \cos \varphi & 0 & 0 \end{vmatrix} \quad (2.140)$$

$$= -\mathbf{j}_\varphi R_e \Omega^2 \cos \varphi \sin \varphi + \mathbf{k}_r R_e \Omega^2 \cos^2 \varphi \quad (2.141)$$

The vector in equation (2.141) is approximately vertical, or in the direction of the \mathbf{k}_r vector. When the \mathbf{j}_φ component of this vector is larger then the value of

$\cos\varphi$ will be small so the overall effect of this vector can be approximated as a vertical force. Using this, the effects of the gravitational and centrifugal forces can be combined into an effective gravitational force. Both act approximately along the vertical direction. Together they can be approximated as variations in the constant g based on the position of the parcel of air and variations in the centrifugal forces. The geopotential is the vector $\mathbf{\Phi}(z) = \mathbf{k}_r \Phi(z)$, where the value of $\Phi(z)$ can be calculated via equation (2.14) which is:

$$\Phi(z) = \int_0^z g(s) ds \quad (2.142)$$

For simplicity in the modeling, the value of g is taken to be a constant. With the assumption that the value of g is a constant, the value of $\Phi = gz$ and $\nabla\Phi = \mathbf{k}_r \frac{\partial\Phi}{\partial z} \approx \mathbf{k}_r g$. With this, the value of the gravitational and centrifugal forces can be approximated as:

$$\frac{\mathbf{F}_g}{M} = -\mathbf{k}_r g = -\nabla\Phi \quad (2.143)$$

Using these approximations, the gravitational and centrifugal forces are combined into a single term which eases the calculation of the force.

2.3.2.4 Pressure Gradient Forces

These are the forces which cause parcels of air to move from regions of high pressure to regions of low pressure. From Figure 2.3, the pressures on either side of the cube can be approximated through the use of a Taylor series which is formed for the center of the cube. The pressure on the left is $p_c - \frac{\partial p}{\partial x} \frac{\Delta x}{2}$ and on the right the pressure is $p_c + \frac{\partial p}{\partial x} \frac{\Delta x}{2}$ where p_c is the pressure at the center of the cube and Δx is the width of the cube in the x -direction. Taking the sum of these pressures (times the areas of the corresponding sides of the cube) and dividing by the mass of the parcel of air gives:

$$\frac{F_p}{M} = \frac{(p_c - \frac{\partial p}{\partial x} \frac{\Delta x}{2}) \Delta y \Delta z - (p_c + \frac{\partial p}{\partial x} \frac{\Delta x}{2}) \Delta y \Delta z}{\rho \Delta x \Delta y \Delta z} \approx -\frac{1}{\rho} \frac{\partial p}{\partial x} \quad (2.144)$$

This can be generalized into three dimensions in Cartesian coordinates and then spherical coordinates as:

$$\frac{\mathbf{F}_p}{M} = -\frac{1}{\rho} \nabla p \quad (2.145)$$

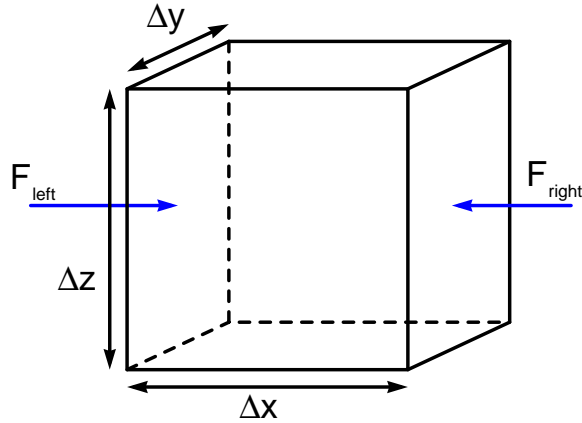


Figure 2.3. The pressure gradient forces within a cube of air. This shows the pressure gradient forces acting on two sides of a cube of air.

$$= -\frac{1}{\rho} \left(\mathbf{i}_\lambda \frac{1}{R_e \cos \varphi} \frac{\partial p}{\partial \lambda} + \mathbf{j}_\varphi \frac{1}{R_e} \frac{\partial p}{\partial \varphi} + \mathbf{k}_r \frac{\partial p}{\partial z} \right) \quad (2.146)$$

2.3.2.5 Viscous Forces and Turbulence

The viscous forces in a parcel of air are the forces caused by the air's resistance to changes in motion. These forces arise from the collisions of air molecules with other molecules in the air and with stationary surfaces. When a collision is between two molecules of a gas, the molecules generally do not lose energy because the chemical bonds in the molecules do not break, the molecules simply rebound with the same total kinetic energy. However, when a molecule of a gas collides with a stationary surface, that molecule may lose energy. This is one reason why the wind speed of the atmosphere is reduced to zero at the surface of the Earth.

The dynamic viscosity of air is represented by the variable η . The viscous force vector per unit mass of air is [5]:

$$\frac{\mathbf{F}_v}{M} = \frac{\eta}{\rho} \nabla^2 \mathbf{v} \quad (2.147)$$

The viscous forces in the atmosphere are usually quite small except near the surface of the Earth.

Turbulence is caused by wind shear or a shearing stress caused by differences in the velocities of nearby parcels of air. For instance, when a wind encounters a

solid object, some of the momentum and energy of the wind is lost through collisions between the molecules of air and the object. This means that on the downwind side of the object, the air molecules which have collided with the object will have a lower velocity, but other air molecules which have not been in collisions will remain at their full velocity. The shear stress caused by these differences in velocity will result in eddies or rotating motions in the air downwind of the object. These types of effects can also be caused by buoyancy. For instance, if a surface is heated, the air near it will tend to rise while other air above it will tend to fall. Again, the differences in velocities of the many parcels of air will give rise to eddies. These rotating motions are turbulence in the atmosphere.

When a model has cells with sides of a few millimeters or less, then the model will be able to identify these turbulent motions without any special treatment. However, for atmospheric circulation models, the size of the side of a cell is several kilometers. For these models, the effects of turbulence must be handled as “subgrid” effects or via parameterization. This is accomplished by making use of a tensor \mathbf{K}_m to describe the effects of the turbulence. The turbulence force per unit mass of a parcel of air is [5]:

$$\frac{\mathbf{F}_t}{M} = -\frac{1}{\rho}(\nabla \cdot \rho \mathbf{K}_m \nabla) \mathbf{v} \quad (2.148)$$

In this way, the effects of turbulence due to changes in the motion of the air which occurs at a much finer resolution than what is used for most atmospheric circulation models, can be included in a model.

2.3.3 Complete Momentum Equation

The complete momentum equation with both viscous forces and turbulence ignored and f the factor for Coriolis forces is:

$$\frac{d\mathbf{v}}{dt} = -f\mathbf{k}_r \times \mathbf{v} - \nabla\Phi - \frac{1}{\rho}\nabla p + \frac{\eta}{\rho}\nabla^2\mathbf{v} + \frac{1}{\rho}(\nabla \cdot \rho \mathbf{K}_m \nabla) \mathbf{v} \quad (2.149)$$

The forces from viscosity are usually very small for models with an atmospheric resolution. Because of that, the viscosity term is usually dropped from this equation for atmospheric models:

$$\frac{d\mathbf{v}}{dt} = -f\mathbf{k}_r \times \mathbf{v} - \nabla\Phi - \frac{1}{\rho}\nabla p + \frac{1}{\rho}(\nabla \cdot \rho \mathbf{K}_m \nabla) \mathbf{v} \quad (2.150)$$

These are the equations are used for the calculations for wind velocity in an atmospheric circulation model. However, the altitude coordinate will be changed in order to simplify the equations to some extent.

2.4 Vertical Coordinate Conversion

The use of altitude for the vertical coordinate has disadvantages when working with models of the atmosphere [13]. The measurement of altitude which is the vertical coordinate of a spherical coordinate system is just the measure of the altitude from the center of the Earth or alternatively the measurement of the altitude above (or below) some arbitrary altitude such as mean sea level. The disadvantage of using an altitude coordinate measured in this way is that a surface of constant altitude may intersect the surface of the Earth. To overcome this disadvantage, the altitude coordinate will be converted to an intermediate coordinate system based on the air pressure at that altitude, and then to the sigma-pressure coordinate system which is based on the ratio of the pressure at an altitude to the pressure at the surface of the Earth just below that point in the atmosphere. Converting to the final sigma-pressure coordinate means that the vertical coordinate varies from a constant zero at the highest altitude of the model to a constant 1 at the surface of the Earth. When the sigma-pressure coordinate is used as the vertical coordinate, a surface with a constant sigma-pressure value will not intersect the surface of the Earth, because the sigma-pressure coordinate at the surface of the Earth is a constant 1 irregardless of the altitude of the surface at that point. When either of the intermediate pressure-altitude or the sigma-pressure coordinates is used, the actual altitude of the highest portion of the atmosphere included in the model becomes variable. The top of the atmosphere in the model becomes the altitude at which the air pressure reaches the minimum value specified for the model. The actual altitude at which that occurs may vary based on how the air pressure varies for different regions in the model. Also, the use of either of these two pressure related coordinates requires using the hydrostatic assumption so that the air pressure is a monotone strictly decreasing function of the altitude.

2.4.1 Pressure or Isobaric Coordinate

The pressure coordinate is an alternative way to define the coordinate positions of the tops and bottoms of layers of the atmosphere. The pressure coordinate is simply the air pressure at that point in the atmosphere. Using this vertical coordinate system requires making use of the hydrostatic assumption, that is, the value of the air pressure must be a (strictly) monotone decreasing function. This vertical coordinate system is only used as an intermediate coordinate system to aid in the conversion to the final sigma-pressure coordinate system. Using this coordinate system, the boundary of a layer of the atmosphere is a surface with constant pressure. Figure 2.4 is an illustration of how this coordinate differs from the z altitude coordinate. Note that a surface of constant pressure can still intersect the surface of the Earth.

2.4.1.1 Gradient for Pressure Coordinate

Figure 2.5 can be used to calculate a gradient using the pressure coordinate. The dashed lines show surfaces of constant pressure which vary in terms of altitude. The value of some attribute of the atmosphere ξ which could be any of density, temperature, or some other variable, varies with distance in the x direction as:

$$\frac{\xi_3 - \xi_1}{x_2 - x_1} = \frac{\xi_2 - \xi_1}{x_2 - x_1} + \frac{\xi_3 - \xi_2}{x_2 - x_1} = \frac{\xi_2 - \xi_1}{x_2 - x_1} + \left(\frac{p_2 - p_1}{x_2 - x_1} \right) \left(\frac{\xi_2 - \xi_3}{p_1 - p_2} \right) \quad (2.151)$$

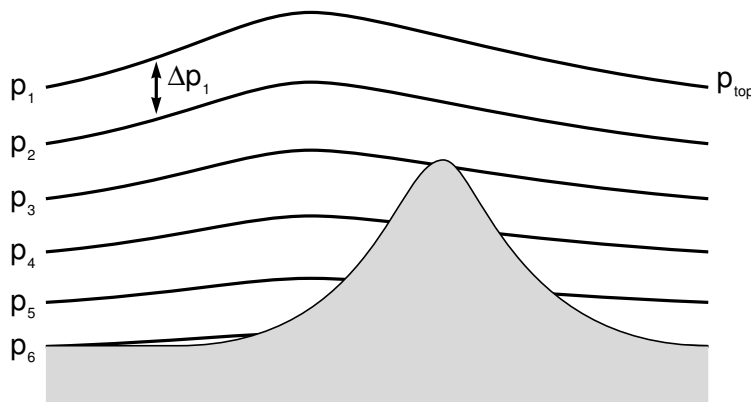


Figure 2.4. The pressure coordinate system. This shows how the pressure coordinate is used as a vertical coordinate. Note that the pressure is not a constant value at the surface of the Earth. Also, the altitude of the top of the model atmosphere may vary with the pressure.

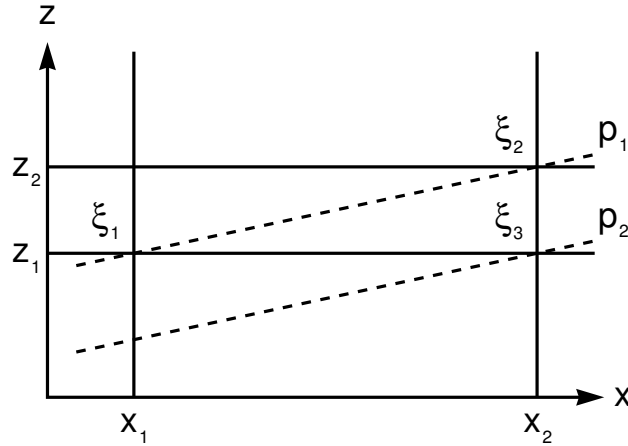


Figure 2.5. Pressure coordinate surfaces of constant pressure. The value of ξ is an attribute of the atmosphere such as density, temperature, or other measurements. The dashed lines p_1 and p_2 represent surfaces of constant pressure.

Taking the limit as both $x_2 - x_1 \rightarrow 0$ and $p_2 - p_1 \rightarrow 0$ changes the individual rational expressions in equation (2.151) to differentials. Each of the resulting differentials has had a particular variable held to a constant value. The differentials, with subscripts indicating which variable has been held constant, are:

$$\left(\frac{\partial \xi}{\partial x}\right)_z = \frac{\xi_3 - \xi_1}{x_2 - x_1} \quad \left(\frac{\partial \xi}{\partial x}\right)_p = \frac{\xi_2 - \xi_1}{x_2 - x_1} \quad (2.152)$$

$$\left(\frac{\partial p}{\partial x}\right)_z = \frac{p_2 - p_1}{x_2 - x_1} \quad \left(\frac{\partial \xi}{\partial p}\right)_x = \frac{\xi_2 - \xi_3}{p_1 - p_2} \quad (2.153)$$

Putting these differentials into equation (2.151) gives the value of a differential with respect to the x coordinate. This can be expanded in three dimensions as the gradient over a surface of constant pressure altitude, which is an expression involving the gradient over a surface of constant pressure:

$$\left(\frac{\partial \xi}{\partial x}\right)_z = \left(\frac{\partial \xi}{\partial x}\right)_p + \left(\frac{\partial p}{\partial x}\right)_z \left(\frac{\partial \xi}{\partial p}\right)_x \quad (2.154)$$

$$\left(\frac{\partial}{\partial x}\right)_z = \left(\frac{\partial}{\partial x}\right)_p + \left(\frac{\partial p}{\partial x}\right)_z \left(\frac{\partial}{\partial p}\right)_x \quad \text{As a generalized operator} \quad (2.155)$$

$$\nabla_z = \nabla_p + \nabla_z(p) \frac{\partial}{\partial p} \quad \text{Expanded to three dimensions} \quad (2.156)$$

In equation (2.156), these notations for gradients on a surface of constant altitude and gradients on a surface of constant pressure have been used:

$$\nabla_z = \mathbf{i} \frac{\partial}{\partial x} + \mathbf{j} \frac{\partial}{\partial y} \quad \text{Horizontal gradient} \quad (2.157)$$

$$\nabla_p = \mathbf{i} \left(\frac{\partial}{\partial x} \right)_p + \mathbf{j} \left(\frac{\partial}{\partial y} \right)_p \quad \text{Horizontal gradient for pressure coordinate} \quad (2.158)$$

Equation (2.156) can be used to find the partial derivatives of a variable along a surface of constant pressure. The operator in equation (2.155) can be used to take derivatives with respect to time as well:

$$\left(\frac{\partial}{\partial t} \right)_z = \left(\frac{\partial}{\partial t} \right)_p + \left(\frac{\partial p}{\partial t} \right)_z \left(\frac{\partial}{\partial p} \right)_t \quad (2.159)$$

Also, from the approximation of geopotential, which is $\Phi = gz$ from equation (2.14) with g held constant, the gradient of geopotential along a surface of constant altitude is zero. The partial derivative $\frac{\partial p}{\partial z} = -\rho g$. With these, the gradient of air pressure along a surface of constant altitude is:

$$\nabla_z p = -\frac{\partial p}{\partial \Phi} \nabla_p \Phi = -\frac{\partial p}{\partial \Phi} \nabla_p \Phi = \rho \nabla_p \Phi \quad (2.160)$$

2.4.1.2 Continuity for the Pressure Coordinate

Using the equation for the continuity or conservation of air (2.11), taking the partial derivative along a surface of constant Cartesian altitude z and using $\mathbf{v}_h = u\mathbf{i} + v\mathbf{j}$ gives:

$$\left(\frac{\partial \rho}{\partial t} \right)_z = -\rho \left(\nabla_z \cdot \mathbf{v}_h + \frac{\partial w}{\partial z} \right) - (\mathbf{v}_h \cdot \nabla_z) \rho - w \frac{\partial \rho}{\partial z} \quad (2.161)$$

To simplify this expression, evaluate $\nabla_z \cdot \mathbf{v}_h$:

$$\nabla_z \cdot \mathbf{v}_h = \nabla_p \cdot \mathbf{v}_h + \nabla_z(p) \cdot \frac{\partial \mathbf{v}_h}{\partial p} \quad (2.162)$$

Substituting equation (2.162) into equation (2.161) and then using the hydrostatic assumption from equation (2.13), for the continuity of air at a constant Cartesian altitude, equation (2.161) can be simplified to:

$$\left(\frac{\partial \rho}{\partial t} \right)_z = -\rho \left(\nabla_p \cdot \mathbf{v}_h + \nabla_z(p) \cdot \frac{\partial \mathbf{v}_h}{\partial p} + \frac{\partial w}{\partial z} \right) - (\mathbf{v}_h \cdot \nabla_z) \rho - w \frac{\partial \rho}{\partial z} \quad (2.163)$$

$$= -\rho \left(\nabla_p \cdot \mathbf{v}_h + \nabla_z(p) \cdot \frac{\partial \mathbf{v}_h}{\partial p} \right) - (\mathbf{v}_h \cdot \nabla_z) \rho - \rho \frac{\partial w}{\partial z} - w \frac{\partial \rho}{\partial z} \quad (2.164)$$

$$= -\rho \left(\nabla_p \cdot \mathbf{v}_h + \nabla_z(p) \cdot \frac{\partial \mathbf{v}_h}{\partial p} \right) - (\mathbf{v}_h \cdot \nabla_z) \rho - \frac{\partial}{\partial z}(\rho w) \quad (2.165)$$

$$= -\rho \left(\nabla_p \cdot \mathbf{v}_h + \nabla_z(p) \cdot \frac{\partial \mathbf{v}_h}{\partial p} \right) - (\mathbf{v}_h \cdot \nabla_z) \rho + g\rho \frac{\partial}{\partial p}(\rho w) \quad (2.166)$$

The vertical scalar velocity for the pressure coordinate w_p is the rate of change of the pressure per second and is measured in hPa per second. It is the total derivative of p with respect to time. The total derivative can be simplified by making use of the hydrostatic assumption, equation (2.13):

$$w_p = \frac{dp}{dt} = \left(\frac{\partial p}{\partial t} \right)_z + (\mathbf{v} \cdot \nabla) p \quad \text{Total/material derivative} \quad (2.167)$$

$$= \left(\frac{\partial p}{\partial t} \right)_z + (\mathbf{v}_h \cdot \nabla_z) p + w \frac{\partial p}{\partial z} \quad \text{Horizontal/vertical split} \quad (2.168)$$

$$= -g\rho \left(\frac{\partial z}{\partial t} \right)_z + (\mathbf{v}_h \cdot \nabla_z) p - g\rho w \quad \text{Using a hydrostatic model} \quad (2.169)$$

To find the continuity/conservation equation for air in the pressure-altitude coordinates, take the partial derivative of w_p with respect to the altitude coordinate z :

$$\frac{\partial w_p}{\partial z} = -g \left(\frac{\partial \rho}{\partial t} \right)_z + \nabla_z(p) \cdot \frac{\partial \mathbf{v}_h}{\partial z} + (\mathbf{v}_h \cdot \nabla_z) \frac{\partial p}{\partial z} - g \frac{\partial}{\partial z}(\rho w) \quad (2.170)$$

Then substitute for the hydrostatic assumption which is $dp = -\rho g dz$ or equation (2.13):

$$-g\rho \frac{\partial w_p}{\partial p} = -g \left(\frac{\partial \rho}{\partial t} \right)_z - g\rho \nabla_z(p) \cdot \frac{\partial \mathbf{v}_h}{\partial p} - (\mathbf{v}_h \cdot \nabla_z)(g\rho) + g^2 \rho \frac{\partial}{\partial p}(\rho w) \quad (2.171)$$

$$\rho \frac{\partial w_p}{\partial p} = \left(\frac{\partial \rho}{\partial t} \right)_z + \rho \nabla_z(p) \cdot \frac{\partial \mathbf{v}_h}{\partial p} + (\mathbf{v}_h \cdot \nabla_z) \rho - g\rho \frac{\partial}{\partial p}(\rho w) \quad (2.172)$$

Substituting equation (2.166) into the last equation gives:

$$\begin{aligned} \rho \frac{\partial w_p}{\partial p} &= -\rho \left(\nabla_p \cdot \mathbf{v}_h + \nabla_z(p) \cdot \frac{\partial \mathbf{v}_h}{\partial p} \right) && \text{Substituting} \\ &\quad - (\mathbf{v}_h \cdot \nabla_z) \rho + g\rho \frac{\partial}{\partial p}(\rho w) \\ &\quad + \rho \nabla_z(p) \cdot \frac{\partial \mathbf{v}_h}{\partial p} + (\mathbf{v}_h \cdot \nabla_z) \rho - g\rho \frac{\partial}{\partial p}(\rho w) && (2.173) \end{aligned}$$

$$= -\rho (\nabla_p \cdot \mathbf{v}_h) \quad \text{Simplifying} \quad (2.174)$$

$$\frac{\partial w_p}{\partial p} = -(\nabla_p \cdot \mathbf{v}_h) \quad (2.175)$$

This is the continuity/conservation equation for air in pressure-altitude coordinates.

2.4.1.3 Total Derivative for the Pressure Coordinate

The total derivative operator for Cartesian coordinates is:

$$\frac{d}{dt} = \left(\frac{\partial}{\partial t} \right)_z + (\mathbf{v}_h \cdot \nabla_z) + w \frac{\partial}{\partial z} \quad (2.176)$$

Substituting for $\left(\frac{\partial}{\partial t} \right)_z$ using (2.159) and then using (2.156) for the horizontal gradient ∇_z results in:

$$\frac{d}{dt} = \left(\frac{\partial}{\partial t} \right)_p + \left(\frac{\partial p}{\partial t} \right)_z \left(\frac{\partial}{\partial p} \right)_t + \mathbf{v}_h \cdot \left(\nabla_p + \nabla_z(p) \frac{\partial}{\partial p} \right) + w \frac{\partial}{\partial z} \quad (2.177)$$

$$= \left(\frac{\partial}{\partial t} \right)_p + \left(\frac{\partial p}{\partial t} \right)_z \left(\frac{\partial}{\partial p} \right)_t + (\mathbf{v}_h \cdot \nabla_p) + [\mathbf{v}_h \cdot \nabla_z(p)] \frac{\partial}{\partial p} + w \frac{\partial}{\partial z} \quad (2.178)$$

$$= \left(\frac{\partial}{\partial t} \right)_p + \left(\frac{\partial p}{\partial t} \right)_z \left(\frac{\partial}{\partial p} \right)_t + (\mathbf{v}_h \cdot \nabla_p) + [\mathbf{v}_h \cdot \nabla_z(p)] \frac{\partial}{\partial p} - g\rho w \frac{\partial}{\partial p} \quad (2.179)$$

From (2.168), the vertical velocity w can be written in terms of the vertical velocity in pressure coordinates as:

$$w = \frac{\left(\frac{\partial p}{\partial t} \right)_z + (\mathbf{v}_h \cdot \nabla_p) - w_p}{g\rho} \quad (2.180)$$

Combining these last two gives the total differential in pressure-altitude coordinates as:

$$\frac{d}{dt} = \left(\frac{\partial}{\partial t} \right)_p + (\mathbf{v}_h \cdot \nabla_p) + w_p \frac{\partial}{\partial p} \quad (2.181)$$

2.4.2 Sigma Pressure Coordinate

To ease calculations, a new variable, σ , will be used in place of both the altitude and the pressure vertical coordinate systems. To make conversion to the σ coordinate easier, the equations are first converted to the pressure coordinate and then to the σ coordinate. The σ coordinate is defined as the ratio between the total pressure difference from top to bottom of the modeled portion of the atmosphere and the difference between the pressure at the top of the modeled portion of the atmosphere and the pressure at the altitude in question:

$$\sigma = \frac{p - p_{\text{top}}}{p_{\text{surf}} - p_{\text{top}}} = \frac{p - p_{\text{top}}}{\pi} \quad (2.182)$$

$$p = p_{\text{top}} + \pi\sigma \quad \text{An alternate definition} \quad (2.183)$$

Note that the variable π is $\pi = p_{\text{surf}} - p_{\text{top}}$ or the difference between the surface pressure and the constant top pressure for the model. The value of π will vary from point to point in the model while the value of p_{top} is a constant for the model even when the actual altitude of the top of the model may vary. The sigma pressure coordinate is an alternative way to define the location of the tops and bottoms of layers in a model. The σ coordinate can be any value between 0 and 1. The value of 1 will occur at the surface of the Earth. The value of σ is zero at the top of the model, but the actual vertical altitude of the top of the model may vary with time. Note that the top of the model is defined by the constant pressure value to be found at the top of the model. That is, a model of the atmosphere is defined as a model of the atmosphere up to the altitude where the air pressure takes on a preassigned minimum value for that particular model. The actual top of the atmosphere modeled may vary in altitude as the pressure in a region of the model varies. Surfaces of a constant σ value do not intersect the ground surface, see Figure 2.6. This makes the sigma-pressure coordinate more useful than other vertical coordinate systems for modeling atmospheric interactions.

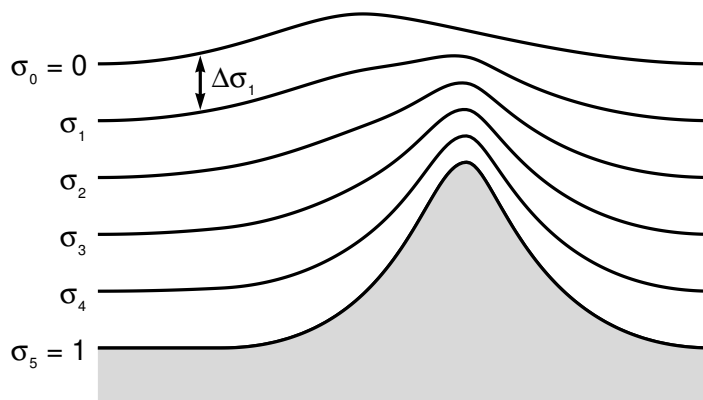


Figure 2.6. The sigma pressure coordinate system. This shows how the sigma pressure coordinate is used as a vertical coordinate. Note that the sigma pressure coordinate is a constant 1.0 at the surface of the Earth. The sigma pressure coordinate is zero at the top of the model which may vary in actual altitude.

2.4.2.1 Gradient for Sigma Pressure Coordinate

To calculate a gradient using the sigma pressure coordinate, use Figure 2.7. The value of some variable ξ varies with distance in the x direction as:

$$\frac{\xi_3 - \xi_1}{x_2 - x_1} = \frac{\xi_2 - \xi_1}{x_2 - x_1} + \frac{\xi_3 - \xi_2}{x_2 - x_1} = \frac{\xi_2 - \xi_1}{x_2 - x_1} + \left(\frac{\sigma_2 - \sigma_1}{x_2 - x_1} \right) \left(\frac{\xi_2 - \xi_3}{\sigma_1 - \sigma_2} \right) \quad (2.184)$$

Allowing $x_2 - x_1 \rightarrow 0$ and $\sigma_2 - \sigma_1 \rightarrow 0$ allows this equation to be approximated with differentials in the same way that this was done for the pressure coordinate. The differentials are:

$$\left(\frac{\partial \xi}{\partial x} \right)_p = \frac{\xi_3 - \xi_1}{x_2 - x_1} \quad \left(\frac{\partial \xi}{\partial x} \right)_\sigma = \frac{\xi_2 - \xi_1}{x_2 - x_1} \quad (2.185)$$

$$\left(\frac{\partial \sigma}{\partial x} \right)_p = \frac{\sigma_2 - \sigma_1}{x_2 - x_1} \quad \left(\frac{\partial \xi}{\partial \sigma} \right)_x = \frac{\xi_2 - \xi_3}{\sigma_1 - \sigma_2} \quad (2.186)$$

Now the expression for the differential becomes:

$$\left(\frac{\partial \xi}{\partial x} \right)_p = \left(\frac{\partial \xi}{\partial x} \right)_\sigma + \left(\frac{\partial \sigma}{\partial x} \right)_p \left(\frac{\partial \xi}{\partial \sigma} \right)_x \quad (2.187)$$

$$\nabla_p = \nabla_\sigma + \nabla_p(\sigma) \frac{\partial}{\partial \sigma} \quad \text{As an operator} \quad (2.188)$$

The value of $\nabla_p(\sigma)$ along a surface of constant pressure can be calculated using equation (2.182). Also, the gradient of pressure on a surface of constant pressure is

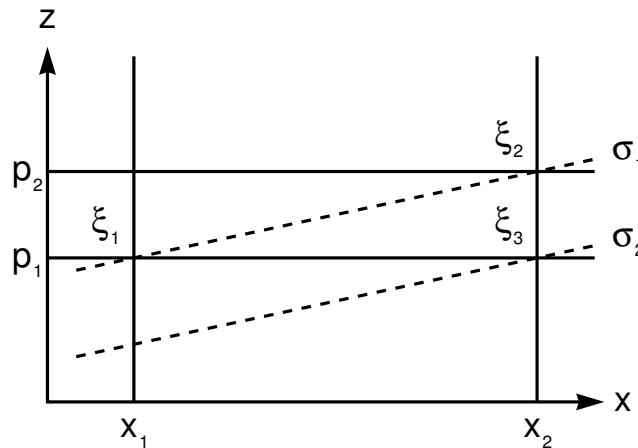


Figure 2.7. Sigma coordinate surfaces of constant measure. The value of ξ is an attribute of the atmosphere such as density, temperature, or other values. The horizontal lines represent surfaces of constant pressure. The dashed lines σ_1 and σ_2 represent surfaces of constant σ values.

zero or $\nabla_p(p) = \nabla_p(p_{\text{top}}) = 0$, and the gradients of the difference between the surface pressure and the top pressure, π , are the same irregardless of which of the altitude coordinates is being used; $\nabla_z(\pi) = \nabla_p(\pi) = \nabla_\sigma(\pi)$:

$$\nabla_p(\sigma) = \nabla_p\left(\frac{p - p_{\text{top}}}{\pi}\right) \quad (2.189)$$

$$= (p - p_{\text{top}})\nabla_p\left(\frac{1}{\pi}\right) + \frac{1}{\pi}\nabla_p(p - p_{\text{top}}) \quad \text{Gradient of a product} \quad (2.190)$$

$$= (p - p_{\text{top}})\nabla_p\left(\frac{1}{\pi}\right) \quad \text{Removing zero terms} \quad (2.191)$$

$$= (p - p_{\text{top}})\left(-\frac{1}{\pi^2}\right)\nabla_p(\pi) \quad \text{Expanding the function composition} \quad (2.192)$$

$$= -\frac{\sigma}{\pi}\nabla_p(\pi) \quad (2.193)$$

$$= -\frac{\sigma}{\pi}\nabla_\sigma(\pi) \quad (2.194)$$

Substituting this into equation (2.184) gives the equation for gradient conversion from pressure-altitude to sigma-pressure coordinates:

$$\nabla_p = \nabla_\sigma - \frac{\sigma}{\pi}\nabla_\sigma(\pi)\frac{\partial}{\partial\sigma} \quad (2.195)$$

2.4.2.2 Continuity for the Sigma Pressure Coordinate

The continuity/conservation equation for air in the pressure coordinate system along with the hydrostatic equation and the total derivative of the sigma-pressure coordinate are used to generate the continuity/conservation equation for air in the sigma-pressure coordinate. Substituting the partial derivative of air pressure with respect to σ , $\frac{\partial p}{\partial\sigma} = \pi$, which is the difference between the surface pressure and the constant top pressure, and the gradient conversion to sigma-pressure (2.195) into the continuity equation for air in the pressure coordinate (2.175) gives:

$$\frac{\partial w_p}{\partial p} + \nabla_\sigma \cdot \mathbf{v}_h - \frac{\sigma}{\pi}\nabla_\sigma(\pi)\frac{\partial \mathbf{v}_h}{\partial\sigma} = 0 \quad \text{Using gradient conversion} \quad (2.196)$$

$$\frac{1}{\pi}\frac{\partial w_p}{\partial\sigma} + \nabla_\sigma \cdot \mathbf{v}_h - \frac{\sigma}{\pi}\nabla_\sigma(\pi)\frac{\partial \mathbf{v}_h}{\partial\sigma} = 0 \quad \text{Using } \frac{\partial p}{\partial\sigma} = \pi \quad (2.197)$$

Now an expression is needed for $\frac{\partial w_p}{\partial\sigma}$. The vertical scalar velocity in the sigma-

pressure coordinate is $\dot{\sigma} = \frac{d\sigma}{dt}$. Substituting $p = p_{\text{top}} + \pi\sigma$ into the equation $w_p = \frac{dp}{dt}$ gives:

$$w_p = \frac{dp}{dt} = \sigma \frac{d\pi}{dt} + \pi \frac{d\sigma}{dt} = \sigma \frac{d\pi}{dt} + \pi \dot{\sigma} \quad (2.198)$$

The total derivative operator with respect to σ can be generated in a similar manner to that for pressure in the pressure-coordinate system and is:

$$\frac{d}{dt} = \left(\frac{\partial}{\partial t} \right)_{\sigma} + \mathbf{v}_h \cdot \nabla_{\sigma} + \dot{\sigma} \frac{\partial}{\partial \sigma} \quad (2.199)$$

Now the total derivative of π can be calculated and substituted into (2.198) for:

$$w_p = \sigma \left[\left(\frac{\partial \pi}{\partial t} \right)_{\sigma} + \mathbf{v}_h \cdot \nabla_{\sigma}(\pi) + \dot{\sigma} \frac{\partial \pi}{\partial \sigma} \right] + \dot{\sigma} \pi \quad (2.200)$$

$$= \sigma \left[\left(\frac{\partial \pi}{\partial t} \right)_{\sigma} + \mathbf{v}_h \cdot \nabla_{\sigma}(\pi) \right] + \dot{\sigma} \pi \quad (2.201)$$

Then the partial derivative of this last equation with respect to σ is:

$$\frac{\partial w_p}{\partial \sigma} = \left(\frac{\partial \pi}{\partial t} \right)_{\sigma} + \mathbf{v}_h \cdot \nabla_{\sigma}(\pi) + \sigma \nabla_{\sigma}(\pi) \cdot \frac{\partial \mathbf{v}_h}{\partial \sigma} + \pi \frac{\partial \dot{\sigma}}{\partial \sigma} \quad (2.202)$$

Substituting this value into (2.197) gives:

$$\left(\frac{\partial \pi}{\partial t} \right)_{\sigma} + \nabla_{\sigma} \cdot (\mathbf{v}_h \pi) + \pi \frac{\partial \dot{\sigma}}{\partial \sigma} = 0 \quad (2.203)$$

This is the equation for continuity or conservation in the sigma-pressure coordinate system.

2.4.3 Surface Air Pressure

One of the first calculations in a time step of a model is to calculate the surface air pressure for a vertical column of the atmosphere. What is actually calculated is the value of $\pi = p_{\text{surf}} - p_{\text{top}}$ with p_{top} being a constant value specific to the model. This surface pressure is needed in many other calculations in each time step of a model.

To calculate the surface air pressure, take the integral of equation (2.203) over all of the layers of σ . Note that for the rightmost integral, the values of $\dot{\sigma}$ are zero at both the top and the bottom of the layers. This is because the vertical velocity is zero at the surface. While the vertical velocity will not be exactly zero at the top of

the model where $\sigma = 0$, it will be approximated as zero at the boundary at the top of the model:

$$\int_0^1 \left(\frac{\partial \pi}{\partial t} \right)_\sigma d\sigma = -\nabla_\sigma \cdot \int_0^1 (\mathbf{v}_h \pi) d\sigma - \pi \int_0^1 d\dot{\sigma} \quad (2.204)$$

$$= -\nabla_\sigma \cdot \int_0^1 (\mathbf{v}_h \pi) d\sigma \quad (2.205)$$

$$\left(\frac{\partial \pi}{\partial t} \right)_\sigma = - \int_0^1 \nabla_\sigma \cdot (\mathbf{v}_h \pi) d\sigma \quad (2.206)$$

Expanding the value of $\nabla_\sigma \cdot (\mathbf{v}_h \pi)$ using (2.89) and multiplying by $R_e^2 \cos \varphi$ gives this equation, which can be used to calculate the surface air pressure π :

$$R_e^2 \cos \varphi \left(\frac{\partial \pi}{\partial t} \right)_\sigma = - \int_0^1 \left[\frac{\partial}{\partial \lambda} (R_e u \pi) + \frac{\partial}{\partial \varphi} (R_e v \pi \cos \varphi) \right] d\sigma \quad (2.207)$$

2.4.4 Vertical Wind Velocity

To calculate the vertical wind velocity at any σ level, take the integral of (2.203) from the top of the model where $\sigma = 0$ to the σ value for the layer in question. This gives:

$$\pi \int_0^\sigma d\dot{\sigma} = -\nabla_\sigma \cdot \int_0^\sigma (\mathbf{v}_h \pi) d\sigma - \int_0^\sigma \left(\frac{\partial \pi}{\partial t} \right)_\sigma d\sigma \quad (2.208)$$

$$\dot{\sigma} \pi = -\nabla_\sigma \cdot \int_0^\sigma (\mathbf{v}_h \pi) d\sigma - \sigma \left(\frac{\partial \pi}{\partial t} \right)_\sigma \quad (2.209)$$

This last equation can be used to calculate the vertical wind velocity $\dot{\sigma}$ at any σ -level of the model. Note that this equation requires the value of π , which can be calculated once the surface pressure has been calculated. The value of $\frac{\partial \pi}{\partial t}$ will be calculated through the use of (2.207) prior to using this equation. Again, expanding the value of $\nabla_\sigma \cdot (\mathbf{v}_h \pi)$ using (2.89) and multiplying by $R_e^2 \cos \varphi$ gives the next equation, which can be used to calculate the vertical wind velocity at any σ -level of the model:

$$R_e^2 \dot{\sigma} \pi \cos \varphi = - \int_0^\sigma \left[\frac{\partial}{\partial \lambda} (R_e u \pi) + \frac{\partial}{\partial \varphi} (R_e v \pi \cos \varphi) \right] d\sigma - R_e^2 \sigma \cos \varphi \left(\frac{\partial \pi}{\partial t} \right)_\sigma \quad (2.210)$$

2.4.5 Thermodynamic Equation

Changing equation (2.47) to make use of a total derivative and then changing that total derivative to a total derivative in sigma-pressure coordinates gives:

$$\frac{d\theta_v}{dt} = \frac{\theta_v}{c_{p,d}} \frac{dQ}{dt} + \frac{1}{\rho} (\nabla \cdot \rho \mathbf{K}_h \nabla) \theta_v \quad (2.211)$$

$$\left(\frac{\partial\theta_v}{\partial t}\right)_\sigma + (\mathbf{v}_h \cdot \nabla_\sigma)\theta_v + \dot{\sigma}\frac{\partial\theta_v}{\partial\sigma} = \frac{\theta_v}{c_{p,d}}\frac{dQ}{dt} + \frac{1}{\rho}(\nabla \cdot \rho\mathbf{K}_h\nabla)\theta_v \quad (2.212)$$

Multiplying equation (2.212) by π , multiplying equation (2.203) by θ_v , and adding the results yields the flux form of the thermodynamic equation:

$$\begin{aligned} \pi \left[\left(\frac{\partial\theta_v}{\partial t}\right)_\sigma + (\mathbf{v}_h \cdot \nabla_\sigma)\theta_v + \dot{\sigma}\frac{\partial\theta_v}{\partial\sigma} \right] + \theta_v \left[\left(\frac{\partial\pi}{\partial t}\right)_\sigma + \nabla_\sigma \cdot (\mathbf{v}_h\pi) + \pi\frac{\partial\dot{\sigma}}{\partial\sigma} \right] \\ = \pi \left[\frac{\theta_v}{c_{p,d}}\frac{dQ}{dt} + \frac{1}{\rho}(\nabla \cdot \rho\mathbf{K}_h\nabla)\theta_v \right] \end{aligned} \quad (2.213)$$

$$\begin{aligned} \pi \left(\frac{\partial\theta_v}{\partial t}\right)_\sigma + \theta_v \left(\frac{\partial\pi}{\partial t}\right)_\sigma + \pi(\mathbf{v}_h \cdot \nabla_\sigma)\theta_v + \theta_v\nabla_\sigma \cdot (\mathbf{v}_h\pi) + \pi\dot{\sigma}\frac{\partial\theta_v}{\partial\sigma} + \theta_v\pi\frac{\partial\dot{\sigma}}{\partial\sigma} \\ = \pi \left[\frac{\theta_v}{c_{p,d}}\frac{dQ}{dt} + \frac{1}{\rho}(\nabla \cdot \rho\mathbf{K}_h\nabla)\theta_v \right] \end{aligned} \quad (2.214)$$

$$\begin{aligned} \left(\frac{\partial}{\partial t}(\pi\theta_v)\right)_\sigma + \nabla_\sigma \cdot (\mathbf{v}_h\pi\theta_v) + \pi\frac{\partial}{\partial\sigma}(\dot{\sigma}\theta_v) \\ = \pi \left[\frac{\theta_v}{c_{p,d}}\frac{dQ}{dt} + \frac{1}{\rho}(\nabla \cdot \rho\mathbf{K}_h\nabla)\theta_v \right] \end{aligned} \quad (2.215)$$

Converting the gradient to spherical coordinates via (2.88) and multiplying by $R_e^2 \cos \varphi$ gives the flux form of the thermodynamic energy equation in spherical-sigma-pressure coordinates:

$$\begin{aligned} R_e^2 \cos \varphi \left[\frac{\partial}{\partial t}(\pi\theta_v) \right]_\sigma + \left[\frac{\partial}{\partial\lambda}(R_e u \pi\theta_v) + \frac{\partial}{\partial\varphi}(R_e v \pi\theta_v \cos \varphi) \right] + R_e^2 \pi \cos \varphi \frac{\partial}{\partial\sigma}(\dot{\sigma}\theta_v) \\ = \pi R_e^2 \cos \varphi \left[\frac{\theta_v}{c_{p,d}}\frac{dQ}{dt} + \frac{1}{\rho}(\nabla \cdot \rho\mathbf{K}_h\nabla)\theta_v \right] \end{aligned} \quad (2.216)$$

2.4.6 Horizontal Momentum

The equation for horizontal momentum can be found by applying the total derivative with respect to σ , equation (2.199), to equation (2.150) for the horizontal velocity.

That gives:

$$\left(\frac{\partial\mathbf{v}_h}{\partial t}\right)_\sigma + (\mathbf{v}_h \cdot \nabla_\sigma)\mathbf{v}_h + \dot{\sigma}\frac{\partial\mathbf{v}_h}{\partial\sigma} = -f\mathbf{k}_r \times \mathbf{v}_h - \frac{1}{\rho}\nabla_z p + \frac{1}{\rho}(\nabla \cdot \rho\mathbf{K}_m\nabla)\mathbf{v}_h \quad (2.217)$$

To get the value of $\nabla_z p$ in terms of σ , make use of (2.160) and (2.194) to get:

$$\frac{1}{\rho}\nabla_z p = \nabla_p \Phi = \nabla_\sigma \Phi - \frac{\sigma}{\pi}\nabla_\sigma(\pi)\frac{\partial\Phi}{\partial\sigma} \quad (2.218)$$

Substituting this into (2.217) gives:

$$\left(\frac{\partial\mathbf{v}_h}{\partial t}\right)_\sigma + (\mathbf{v}_h \cdot \nabla_\sigma)\mathbf{v}_h + \dot{\sigma}\frac{\partial\mathbf{v}_h}{\partial\sigma} = -f\mathbf{k} \times \mathbf{v}_h - \nabla_\sigma \Phi + \frac{\sigma}{\pi}\nabla_\sigma(\pi)\frac{\partial\Phi}{\partial\sigma}$$

$$+ \frac{1}{\rho} (\nabla \cdot \rho \mathbf{K}_m \nabla) \mathbf{v}_h \quad (2.219)$$

To convert equation (2.219) to spherical coordinates, first find an expression for $\frac{\partial \Phi}{\partial \sigma}$. Using the ideal gas law, $p = \rho R_m T_v$, the relationship $R_m = \kappa c_{p,d}$, the relationship between virtual temperature and potential virtual temperature $T_v = \theta_v \left(\frac{1000}{p}\right)^\kappa = \theta_v P$ and the derivative $\frac{\partial p}{\partial \sigma} = \pi$ where $\pi = p_{\text{surf}} - p_{\text{top}}$. Using these gives $\frac{\partial \Phi}{\partial \sigma}$ as:

$$\frac{\partial \Phi}{\partial \sigma} = g \frac{\partial z}{\partial \sigma} = -\frac{1}{\rho} \frac{\partial p}{\partial \sigma} = -\frac{\pi}{\rho} \quad (2.220)$$

$$= -\frac{\pi R_m T_v}{p} = -\frac{\pi \kappa c_{p,d} \theta_v \left(\frac{1000}{p}\right)^\kappa}{p} = -\pi c_{p,d} \theta_v \frac{\partial P}{\partial p} \quad (2.221)$$

Substituting this into equation (2.219) changes the horizontal momentum equation to:

$$\begin{aligned} & \left(\frac{\partial \mathbf{v}_h}{\partial t} \right)_\sigma + (\mathbf{v}_h \cdot \nabla_\sigma) \mathbf{v}_h + \dot{\sigma} \frac{\partial \mathbf{v}_h}{\partial \sigma} \\ & = -f \mathbf{k} \times \mathbf{v}_h - \nabla_\sigma \Phi - \sigma c_{p,d} \theta_v \frac{\partial P}{\partial p} \nabla_\sigma (\pi) + \frac{1}{\rho} (\nabla \cdot \rho \mathbf{K}_m \nabla) \mathbf{v}_h \end{aligned} \quad (2.222)$$

Converting equation (2.222) fully to spherical coordinates gives these equations for the horizontal momentum:

$$\begin{aligned} & R_e^2 \cos \varphi \left[\frac{\partial}{\partial t} (\pi u) \right]_\sigma + \left[\frac{\partial}{\partial \lambda} (\pi u^2 R_e) + \frac{\partial}{\partial \varphi} (\pi u v R_e \cos \varphi) \right]_\sigma + \pi R_e^2 \cos \varphi \frac{\partial}{\partial \sigma} (\dot{\sigma} u) \\ & = \pi u v R_e \sin \varphi + \pi f v R_e^2 \cos \varphi - R_e \left(\pi \frac{\partial \Phi}{\partial \lambda} + \sigma c_{p,d} \theta_v \frac{\partial P}{\partial \sigma} \frac{\partial \pi}{\partial \lambda} \right)_\sigma \\ & + R_e^2 \cos \varphi \frac{\pi}{\rho} (\nabla \cdot \rho \mathbf{K}_m \nabla) u \end{aligned} \quad (2.223)$$

$$\begin{aligned} & R_e^2 \cos \varphi \left[\frac{\partial}{\partial t} (\pi v) \right]_\sigma + \left[\frac{\partial}{\partial \lambda} (\pi u v R_e) + \frac{\partial}{\partial \varphi} (\pi v^2 R_e \cos \varphi) \right]_\sigma + \pi R_e^2 \cos \varphi \frac{\partial}{\partial \sigma} (\dot{\sigma} v) \\ & = -\pi u^2 R_e \sin \varphi - \pi f u R_e^2 \cos \varphi - R_e \left(\pi \frac{\partial \Phi}{\partial \varphi} + \sigma c_{p,d} \theta_v \frac{\partial P}{\partial \sigma} \frac{\partial \pi}{\partial \varphi} \right)_\sigma \\ & + R_e^2 \cos \varphi \frac{\pi}{\rho} (\nabla \cdot \rho \mathbf{K}_m \nabla) v \end{aligned} \quad (2.224)$$

2.5 Final Equations

For each time step of a model, the variables for the model should be solved for in a specific order [5]. First, the surface air pressure should be found for each

vertical column in the model. Second, the vertical wind velocity should be found for each cell in the model. The next step should be to solve for specific humidity and moist air mixing ratios, those equations are not detailed in this thesis. The potential virtual temperature is the next variable to be solved for each cell in the model. The geopotential is the next variable to be solved for. Finally, the horizontal wind velocities are found for each cell.

Equation (2.207) is used to calculate the surface air pressure:

$$R_e^2 \cos \varphi \left(\frac{\partial \pi}{\partial t} \right)_\sigma = - \int_0^1 \left[\frac{\partial}{\partial \lambda} (u \pi R_e) + \frac{\partial}{\partial \varphi} (v \pi R_e \cos \varphi) \right] d\sigma \quad (2.225)$$

Solving this integral equation numerically for the variable π requires the prior time-step's horizontal velocities.

Equation (2.210) can be used to calculate the vertical wind velocity:

$$\dot{\sigma} \pi R_e^2 \cos \varphi = - \int_0^\sigma \left[\frac{\partial}{\partial \lambda} (u \pi R_e) + \frac{\partial}{\partial \varphi} (v \pi R_e \cos \varphi) \right] d\sigma - \sigma R_e^2 \cos \varphi \left(\frac{\partial \pi}{\partial t} \right)_\sigma \quad (2.226)$$

The solution of this integral equation for the vertical wind velocity $\dot{\sigma}$ requires the prior time step's horizontal wind velocities and then the prior and current surface pressure values.

The thermodynamic energy equation is given in equation (2.216):

$$\begin{aligned} R_e^2 \cos \varphi \left[\frac{\partial}{\partial t} (\pi \theta_v) \right]_\sigma + \left[\frac{\partial}{\partial \lambda} (u \pi \theta_v R_e) + \frac{\partial}{\partial \varphi} (v \pi \theta_v R_e \cos \varphi) \right] + \pi R_e^2 \cos \varphi \frac{\partial}{\partial \sigma} (\dot{\sigma} \theta_v) \\ = \pi R_e^2 \cos \varphi \left[\frac{\nabla \cdot \rho \mathbf{K}_h \nabla \theta_v}{\rho} + \frac{\theta_v}{c_{p,d} T_v} \sum_{n=1}^N \frac{dQ_n}{dt} \right] \end{aligned} \quad (2.227)$$

This equation depends on the eddy turbulence definition for the model, which is the \mathbf{K}_h tensor, as well as the various energy inputs given by the Q_n values. It needs the current time-step's surface pressure values and the prior time-step's potential virtual temperatures and horizontal wind speeds in order to get solutions for this time-steps potential virtual temperatures.

The hydrostatic equation as used for numerical solutions is derived from relationships for the geopotential, potential virtual temperature with $P = \left(\frac{1000}{p} \right)^\kappa$, and equation (2.13):

$$d\Phi = -c_{p,d} \theta_v dP \quad (2.228)$$

Equations (2.223) and (2.224) are used to calculate the horizontal momentum:

$$\begin{aligned}
& R_e^2 \cos \varphi \left[\frac{\partial}{\partial t}(\pi u) \right]_{\sigma} + \left[\frac{\partial}{\partial \lambda}(\pi u^2 R_e) + \frac{\partial}{\partial \varphi}(\pi u v R_e \cos \varphi) \right]_{\sigma} + \pi R_e^2 \cos \varphi \frac{\partial}{\partial \sigma}(\dot{\sigma} u) \\
& = \pi u v R_e \sin \varphi + \pi f v R_e^2 \cos \varphi - R_e \left(\pi \frac{\partial \Phi}{\partial \lambda} + \sigma c_{p,d} \theta_v \frac{\partial P}{\partial \sigma} \frac{\partial \pi}{\partial \lambda} \right)_{\sigma} \\
& \quad + R_e^2 \cos \varphi \frac{\pi}{\rho} (\nabla \cdot \rho \mathbf{K}_m \nabla) u \tag{2.229}
\end{aligned}$$

$$\begin{aligned}
& R_e^2 \cos \varphi \left[\frac{\partial}{\partial t}(\pi v) \right]_{\sigma} + \left[\frac{\partial}{\partial \lambda}(\pi u v R_e) + \frac{\partial}{\partial \varphi}(\pi v^2 R_e \cos \varphi) \right]_{\sigma} + \pi R_e^2 \cos \varphi \frac{\partial}{\partial \sigma}(\dot{\sigma} v) \\
& = -\pi u^2 R_e \sin \varphi - \pi f u R_e^2 \cos \varphi - R_e \left(\pi \frac{\partial \Phi}{\partial \varphi} + \sigma c_{p,d} \theta_v \frac{\partial P}{\partial \sigma} \frac{\partial \pi}{\partial \varphi} \right)_{\sigma} \\
& \quad + R_e^2 \cos \varphi \frac{\pi}{\rho} (\nabla \cdot \rho \mathbf{K}_m \nabla) v \tag{2.230}
\end{aligned}$$

The exact usage of these equations depends on the grid being used and what scheme is being used for the numerical solution.

2.6 Numerical Solutions

The equations used for atmospheric circulation are the equations given in section 2.5. These equations do not have an analytical solution and so must be solved numerically. At least three methods can be used to solve equations of this nature. The first of the methods, finite differencing, is to approximate the values of the variables at discrete points within the model, and then approximate the variation of the variables via the earlier approximations. The second is spectral methods or making use of Fourier series for the values of the variables in the model. Finally, finite element methods can be used for the solution. However, these methods are not used for most atmospheric circulation models [16].

2.6.1 Finite Difference Methods

These methods obtain values of the variables in the model at discrete points within the model. For the simplest of these methods, the discrete points are spaced evenly about the model. For the more advanced models in use today, the discrete points are spaced unevenly based on the types of terrain or ocean surface at that point of the model. For these advanced models, areas over the surfaces of oceans may have cells with very large surface areas while areas over mountain ranges may have cells with

much smaller surface areas. In this way, a more advanced model can evaluate the variations involved with terrain which causes many of the variations in the climate in great detail while spending much less computing time evaluating variables in areas where the variables do not change quickly.

There are several ways to set where the variables are measured in a model. Most of these methods of measurements or the grids related to them are named for Akio Arakawa and were first presented by Arakawa and Lamb in 1977 [2]. For the Arakawa A-Grid, each variable is measured at the center of a cell, or alternatively at the corners or vertices of a cell. The remaining grid types have changes so that some variables are measured at the center of a cell and others are measured at vertices or at the sides of a cell.

The Arakawa C-Grid is the most successful of these grid types for rectangular cells. See Figure 2.8 for a representation of this grid. The air pressure and temperature are measured at the center of a cell while the horizontal wind velocities are measured at the horizontal sides of a cell. While not easily represented in Figure 2.8, the vertical wind velocities are measured on the top and bottom sides of a cell. This particular grid is the most used grid type for models that make use of rectangular or nearly rectangular cells. Other rectangular grid types have been used, the main differences are the locations of the measurements of the many variables.

Models which make use of hexagonal or triangular grids make use of an alternative means to measure the variables in the model. A hexagonal grid for the surface of the Earth can be constructed by starting with an icosahedron and then subdividing each triangular surface of the icosahedron into a triangular grid. This triangular grid is then “expanded” so that it is a roughly triangular grid on the surface of the Earth. The grid cells can be left as triangles or each set of 6 triangles can be joined to form a hexagon. Note that for a hexagonal grid, there will be 12 pentagonal cells, one at each vertex of the original icosahedron. There are hexagonal or triangular counterparts for each of the rectangular Arakawa grids. The main issues with these grids is that there are more instances of each value being measured in the model, or more places where a variable must be measured [11]. Also, the main idea behind the Arakawa C-Grid, that is, measuring some variables at the center of a cell and others at the sides of a

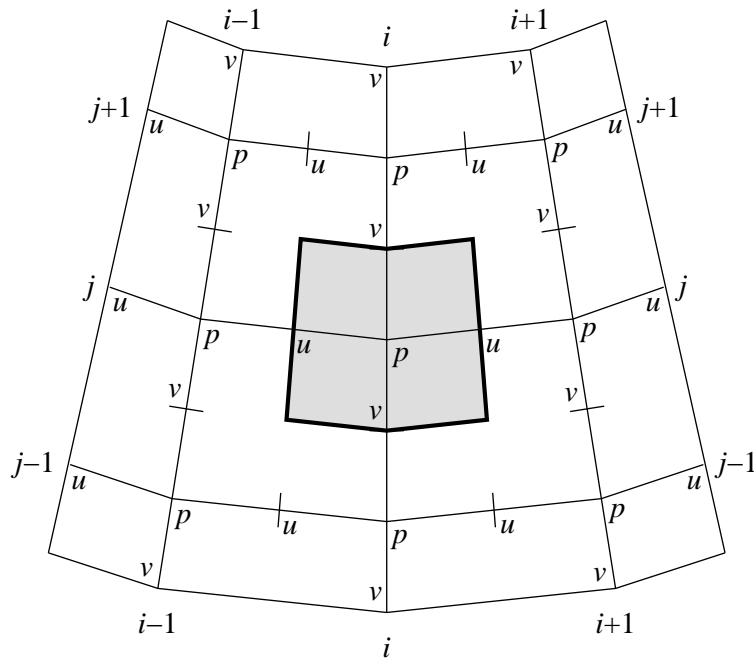


Figure 2.8. The Arakawa C-Grid. The shaded area represents a rectangular cell in the model with an approximation of the curvature of the Earth. The air pressure and other variables are measured at the center of a cell. Wind velocities are measured at the sides of a cell with the North/South wind velocity being measured at the upper and lower sides of a cell and the East/West wind velocity measured at the left and right sides of a cell. The vertical wind velocity is not measured at the center of a cell, but at the top and bottom sides of a cell.

cell, must be changed for these types of grids. When wind velocities are measured at the sides of the cells in a grid of this type, the measurement of the direction of the wind at the side of a cell can be changed. Some measurement schemes measure the perpendicular component of the wind at the side of the cell while others measure the parallel component of the wind at that side of the cell.

Using finite difference methods, the values of the variables can be calculated by approximating their values using Taylor's series based on the PDEs for the model. There are many ways to perform these calculations. Using a simple explicit Euler's method for the calculations, but without eddy diffusion terms [5], results in a solution which is unconditionally unstable when used for any length of time. More complicated implicit methods must be used to obtain solutions to these equations which are more

stable. One of the complications with implicit methods for these solutions is that when solving for vertical wind velocity, multiple vertical layers of the model must be used at once, which results in a much larger amount of computer memory being required for a numerical solution to be accomplished.

Finite differencing methods for a global model using a longitude/latitude grid all need to deal with singularities at the North and South poles of the model. One approach to this problem is to set the North/South wind velocities at the poles to zero. In this way, the singularity can be avoided, but the wind velocities near the poles may not be a good representation of the velocities for the physical Earth. Another issue related to this singularity is that the width of a cell should be large enough, or the time step should be small enough, so that a disturbance traveling at the speed of sound cannot cross a cell within a single time step. This can mean that for cells near the poles, the maximum time step must be smaller and smaller. From this, issues related to the singularity at the poles can become a part of the model for cells near the poles if the model's horizontal resolution is small enough, or the time step is large enough.

2.6.2 Spectral Methods

Spectral methods make use of Fourier expansions of the functions for the variables in the model. The horizontal variation of variables in the model are expressed in terms of orthogonal spherical harmonics. The use of spectral methods was not efficient enough to be used until faster computers and improvements in computer algorithms. Spectral methods were first adopted in the early 1970s for use in global circulation models [11].

The main advantage of a spectral method is that while it still requires the solution of a large set of linear equations to approximate the differences between time steps for a variable in the model, the linear system is usually much smaller than for a finite difference solution. However, the calculations required to set up the equations needed for a spectral method may be much more complicated than those needed for a finite difference method. This means that less computing time may be needed for a numerical solution using this method depending on how the solutions are accomplished.

This type of model can still have a singularity at the North and South poles. However, work done by Stephen Orszag in 1974 showed ways to overcome this singularity using specialized functions for the orthogonal spherical harmonics.

CHAPTER 3

OCEANIC CIRCULATION MODELS

Modeling oceanic circulation can be carried out in much the same manner as in atmospheric circulation models. That is, the content of the oceans can be divided into a three-dimensional set of cells of water, and the circulation of the water between those cells can be modeled in much the same way as it is for the atmosphere. Differences in the details of the models include the fact that, unlike air, salt water is essentially in-compressible. Also, terrain features take a much more predominant role in the models of oceanic circulation. This is because oceans do not cover the entire surface of the Earth like the atmosphere does — there are regions which are above sea level and so have no sea water present. The flow of ocean currents is very much affected by the extent of the continents and the contours of the seabed.

Models of ocean circulation can be constructed using equations similar to the ones used for atmospheric circulation. These models can be used to simulate oceanic circulation and how that circulation responds to changes in the environment of the Earth. Greatly simplified models can be created by modeling only the effects of the primary currents in the oceans. These are the surface and deep water currents that circulate heat and salinity about the oceans. These currents are called the thermohaline circulation (THC) of the oceans, see Figure 3.1. They mix the heat and salinity of the oceans on a global scale. The heat and salinity normally differ between regions of the oceans because of a greater heat input as well as greater evaporation in the equatorial regions. The ocean currents represented in Figure 3.1 are very stable given the modern day climate.

The thermohaline circulation can be modeled at a high level as a series of “boxes” of well-mixed sea water that are connected by currents, or flows of sea water from box-to-box. These types of models are called box models. Box models can be used

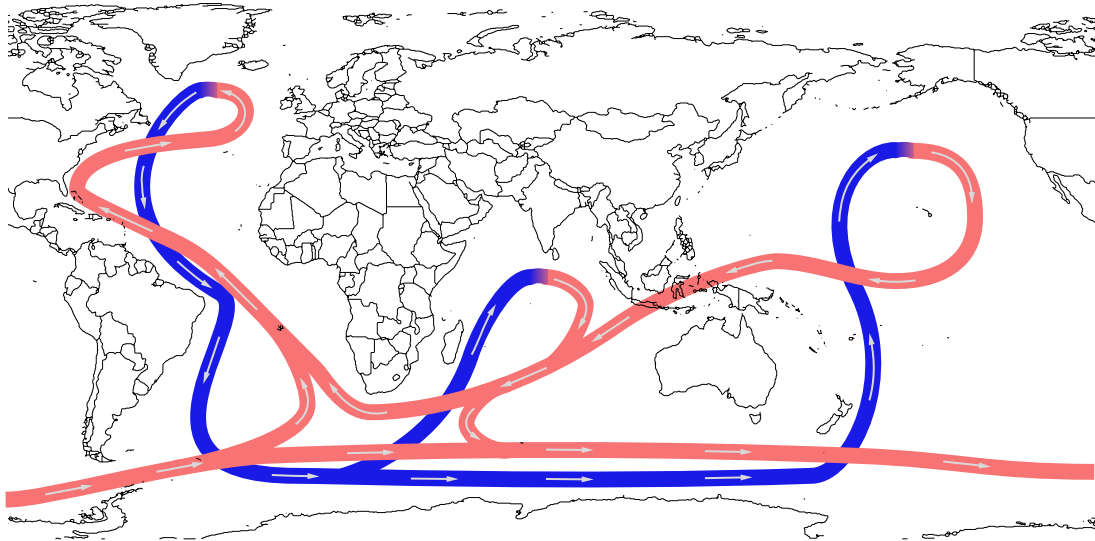


Figure 3.1. The simplified global thermohaline circulation of sea water. Red (light gray) represents warmer surface currents and blue (darker gray) represents colder deep currents.

to model theoretical effects of climate changes on the thermohaline circulation [14]. The earliest and simplest of these box models is the 2-box model developed by Henry Stommel in 1961 [15]. It represents a simplified model of the circulation between the tropical or equatorial Atlantic Ocean and the Northern Atlantic Ocean. More complicated box models add additional boxes in an attempt to better understand the relationships of the various currents to other factors such as temperature and evaporation/precipitation. These models have been used to study what effect a past or future change to the climate might have on the circulation of the oceans. For instance, Lucarini and Stone [7] studied the effects of increased evaporation in the equatorial Atlantic Ocean with increased precipitation in the Northern Atlantic and how this might affect the strength of the circulation currents in the Atlantic Ocean, which is seen today in the Gulf Stream and the corresponding deeper cold water currents.

In a box model of ocean circulation, the direction and magnitude of the flow of water between boxes is assumed to be driven by density differences between boxes. One or more of the flows in the model are the key flows which drive the circulation direction and strength for the entire model. The remaining flows have directions and

strengths so that the amount of sea water in each box remains constant, that is, the level of the sea water in each part of the ocean remains the same.

The key rates of flow of sea water between the the two boxes joined by the key flows are driven by differences in the density of the salt water in those boxes. The density of the salt water is affected by both the temperature and salinity of the water. The density is not a linear function of the temperature and salinity (see Appendix A for details on this), but it is approximately linear for the range of temperatures and salinities encountered in these models. The density of the salt water is modeled as the linear relationship to ease the numerical solutions to the differential equations involved:

$$\rho = \rho_0(1 - \alpha(T - T_0) + \beta(S - S_0)) \quad (3.1)$$

The values of T_0 , S_0 , and ρ_0 are reference temperature, salinity, and density measures. The value of ρ_0 is the density of the water when it has the reference temperature of T_0 and the reference salinity of S_0 . The values of $\alpha \approx 1.5 \times 10^{-4} \text{ K}^{-1}$ and $\beta \approx 8.0 \times 10^{-4} \text{ psu}^{-1}$ are approximations which make the linear relationship best fit the actual variation of density. Note that salinity is measured in “practical salinity units” (psu) rather than a percent of composition by weight. Practical salinity units are measured as a ratio of conductivities between the salt water and pure water, so a psu is a dimensionless measure [6]. The average salinity of the Earth’s oceans is about 35 psu. This is similar to the percent of salt in sea water, which is about 3.5% by weight of salt of all types, not just sodium chloride.

The parameters used in the box models for this thesis include the parameters shown in Table 3.1. These are the parameters which were used by Lucarini and Stone [7] to model changes in the flows of a 3-box model. In Table 3.1, the last twelve entries do not include a corresponding box number, because the box numbers for the various parts of the Atlantic change when the number of boxes in the model are changed.

The temperature restoring coefficient or λ is used to calculate the rate of heating or cooling for the salt water in a box. The difference between the target temperature for a box (τ_i) and the current temperature of the sea water in the box is multiplied

Table 3.1. Parameters for box models. These are the physical parameters used by Lucarini and Stone [7] in their study of how changes in the climate affect thermohaline circulation. Note that the last 12 parameters are four groups of three similar parameters for the northern, equatorial, and southern boxes, respectively. Because the box numbers change from model to model as used in this thesis, no box numbers are included as subscripts for these entries.

Variable	Meaning	Value
V	Ratio of equatorial box mass to high-latitude box	2
S_0	Average salinity	35 psu
α	Thermal expansion coefficient	$1.5 \times 10^{-4} \text{ K}^{-1}$
β	Haline expansion coefficient	$8.0 \times 10^{-4} \text{ psu}^{-1}$
λ	Temperature restoring coefficient	$25.8 \text{ W m}^{-2} \text{ K}^{-1}$
F	Total atmospheric freshwater flux, Northern Atlantic	0.41 Sv
F	Total atmospheric freshwater flux, equatorial Atlantic	-0.68 Sv
F	Total atmospheric freshwater flux, Southern Atlantic	0.27 Sv
τ	Target temperature, Northern Atlantic	0°C
τ	Target temperature, equatorial Atlantic	30°C
τ	Target temperature, Southern Atlantic	0°C
T	Temperature, Northern Atlantic	2.9°C
T	Temperature, equatorial Atlantic	28.4°C
T	Temperature, Southern Atlantic	0.3°C
S	Salinity, Northern Atlantic	34.7 psu
S	Salinity, equatorial Atlantic	35.6 psu
S	Salinity, Southern Atlantic	34.1 psu

by a constant derived from the value of λ to determine the amount of heating or cooling which occurs in a box over a time step. That constant is the product of this λ and the surface area of the Earth multiplied by the fractional portion of the Earth occupied by the Atlantic Ocean or $\varepsilon = \frac{1}{6}$, then divided by the total mass of water in all boxes and finally divided by the specific heat per unit mass of water. This calculation is performed for each box as each box has a unique target temperature and unique current temperature. Note that the value of ε is a good approximation for the surface area of the Atlantic Ocean but not for the surface area of the other

oceans. Also, the variable λ used in the differential equations for each box model is actually the product of the λ in this table with the other values as noted above.

The freshwater fluxes in Table 3.1 are the total amounts of the change of freshwater water for a box, where the differential equations used for each model refer to a flux per unit mass in a box. The conversion between total amounts of water for a box and the change in salinity for a box is accomplished by multiplying the flux value in the table by the total average density of the sea water for the entire model and then dividing by the mass of water in that particular box. This product results in a salinity change value for that box. This value is what is used in the differential equations that describe each model.

3.1 Stommel 2-Box Model

The 2-box model was originally developed by Henry Stommel in 1961 [15]. The model is an idealized view of the circulation of sea water in the Atlantic Ocean. The ocean in this model is composed of a northern box and an equatorial box which is presumably bounded to the South by a land mass. Figure 3.2 shows how the original model works. There are two flows of sea water between the northern and equatorial boxes. One flow is a surface flow and the other is a deep flow. The deep flow is the key flow and is driven by pressure differences in the densities of the sea water in the

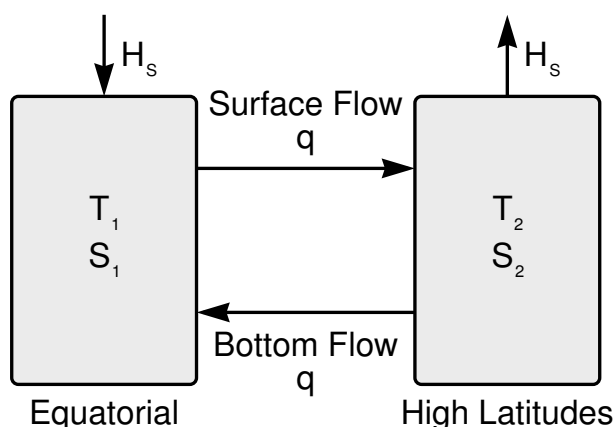


Figure 3.2. The original Stommel 2-box model. This is the original Stommel 2-box model of thermohaline circulation.

two boxes while the surface flow simply returns an equivalent volume of sea water to the box from which the deep flow removes water.

The amounts of freshwater and salt are constant for the total system. The original model as developed by Stommel has an amount of salt being added to the equatorial region and an equivalent amount of salt being removed from the polar region. This reflects the fact that water evaporates from the equatorial region of the ocean and then precipitation without as much evaporation adds freshwater to the northern region. These are modeled as salt being moved around the system in the original 2-box model. Also, in the original model, the salinity of a box relaxes toward the average salinity of the ocean bed for that box much in the same way that the temperature of a box relaxes toward the average temperature of the seabed for that box.

The first difference between the original Stommel model and the model used here is that the size of the two boxes of sea water are not the same. Like the 3-box model used by Lucarini and Stone [7], this model will assume that each box of sea water will have a unique size and that the ratio between the sizes of the equatorial box and the northern box is $V = \frac{M_2}{M_1}$, where M_i is the mass of the salt water in the box i . Taking the equatorial box as being the Atlantic Ocean between 30°S and 30°N and the high-latitude box as being the Atlantic Ocean above 30°N, the ratio $V \approx 2$.

For the model used here, the freshwater or salinity changes for each box caused by evaporation and precipitation will be modeled as changes in the freshwater content of that box rather than as changes in the amount of salt as was done in the original model as developed by Stommel, see Figure 3.3. This change is consistent with many other later box models and appears to be more consistent with the fact that it is freshwater which is moved about the system by evaporation and precipitation. The amount of freshwater removed by evaporation in the equatorial box will be balanced by the amount of freshwater added by precipitation in the high-latitude box. The variable H_S in Figure 3.2 represents salt addition or removal that will be replaced with variables F_1 and F_2 ; one of which is positive and the other negative. These values are derived from the values of the F s given in Table 3.1 by dividing the F value in the table by the mass of sea water in the box receiving (or losing) the freshwater. One complication with how the freshwater fluxes are handled in this model is that

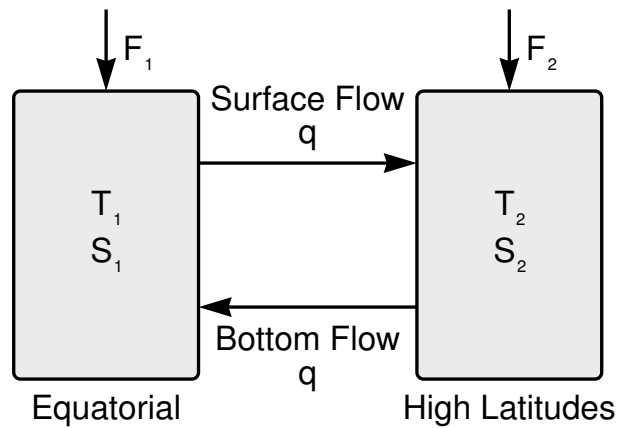


Figure 3.3. The modified 2-box model. This is the modified 2-box model of thermohaline circulation as used in this thesis. Rather than salt content being moved by evaporation/precipitation, an amount of freshwater is what is moved between boxes.

the magnitude of the flows of sea water should be changed to reflect the fact that the northern box would gain an amount of water over time due to precipitation and that the flows into and out of this box should combine to give a net flow of sea water from the northern box which reflects the increase of fresh water in that box. This is not accounted for in the model since the amount of water involved in precipitation is very small compared to the total amount of sea water in either box.

Because the evaporation and precipitation balance each other between the two boxes, the average salinity of the entire system will be a constant in the model. The salinity of each box will vary depending on the evaporation or precipitation and circulation of water between the two boxes.

The temperatures of the sea water in each box will warm or cool toward a target temperature for that box. The target temperatures for each box are $\tau_1 = 30^\circ\text{C}$ for the equatorial box and $\tau_2 = 0^\circ\text{C}$ for the high-latitude box. These particular target temperatures are in agreement with the model used by Lucarini and Stone [7]. The target temperature of 0°C may seem to be very cold, but sea water does not freeze at this temperature and the temperature of the high-latitude box cannot actually reach this temperature because of the warmer water flowing into that box from the equatorial box. The equations for the temperatures of the sea water in each box will

have a term which is proportional to the difference between the target temperature and the current temperature of the water in that box. In this way, the temperature of the sea water in a box will relax to the target temperature for that box in a manner similar to Newton's Law of Cooling.

Under current climatic conditions, the deep water flow will be from the high-latitude box with a higher density and to the equatorial box with a lower density. The surface flow will have the same magnitude but will be in the opposite direction. The rate of the flow is proportional to the difference in the density of the water in each box. Note that the equatorial box will have a higher salinity which raises its density, but also a higher temperature which lowers its density. The current conditions are referred to as a *T-mode* because density difference between the two boxes is predominately the effect of the temperature differences. The condition of the model would be referred to as *S-mode* when the density difference is dominated by the difference in the salinities. Using q as the rate of flow, the value of q can be expressed as:

$$q = k \left(\frac{\rho_1 - \rho_2}{\rho_0} \right) = k(\alpha(T_1 - T_2) - \beta(S_1 - S_2)) \quad (3.2)$$

The value of k will be set so that the rate of the main surface current in this model is flowing at the rate of about 15.5 Sv (Sverdrups or $1.0 \times 10^6 \text{ m}^3\text{s}^{-1}$), which is the approximate rate of flow of the Gulf Stream in the Atlantic Ocean [12]. The constant k is referred to as the hydraulic constant and represents the combined resistance to the flow of sea water between the boxes.

3.1.1 Equations for Stommel's 2-Box Model

This system, with the changes from the original Stommel 2-box model can be modeled as a series of differential equations that take into account the movement of sea water between boxes assuming immediate mixing within each box. The equations for this model are:

$$\frac{dT_1}{dt} = \lambda(\tau_1 - T_1) + \frac{|q|}{V}(T_2 - T_1) \quad (3.3)$$

$$\frac{dT_2}{dt} = \lambda(\tau_2 - T_2) + |q|(T_1 - T_2) \quad (3.4)$$

$$\frac{dS_1}{dt} = -F_1 + \frac{|q|}{V}(S_2 - S_1) \quad (3.5)$$

$$\frac{dS_2}{dt} = -F_2 + |q|(S_1 - S_2) \quad (3.6)$$

Note the use of absolute values in these equations, the mixing of the different types of sea water is not affected by the direction of the flow, only the magnitude of the flow. In these equations, the constant λ represents how quickly the temperature of the water in a box relaxes to the target temperature. The value of λ used here is based on the product of the value of λ given in Table 3.1 and one-sixth (ε) the surface area of the Earth, then divided by the total mass of sea water in the model and finally divided by the specific heat of water.

3.1.2 Equilibrium Points

For this model, the average salinity of the water in all boxes combined is a constant, or $V\frac{dS_1}{dt} + \frac{S_2}{dt} = 0$. Manipulating the differential equations (3.5) and (3.6) shows that this means that the freshwater flux for the first box is $F_1 = -\frac{F_2}{V}$.

The flow state with the surface current flowing from the equatorial region to the higher latitudes (as the Gulf Stream does today) is referred to as the northern sinking state. If the flow changes direction, that would be referred to as the southern sinking state. The equilibrium states of this system can be found by setting equations (3.4) and (3.6) to zero as they would be when the system is at equilibrium, subtracting β times equation (3.6) from α times equation (3.4), and then using equation (3.2) to simplify:

$$0 = \alpha[\lambda(\tau_2 - T_2) + |q|(T_1 - T_2)] - \beta[-F_2 + |q|(S_1 - S_2)] \quad (3.7)$$

$$0 = \alpha\lambda(\tau_2 - T_2) + \beta F_2 + \alpha|q|(T_1 - T_2) - \beta|q|(S_1 - S_2) \quad (3.8)$$

$$0 = \alpha\lambda(\tau_2 - T_2) + \beta F_2 + \frac{q|q|}{k} \quad (3.9)$$

$$q = \begin{cases} -\sqrt{k(\beta F_2 - \alpha\lambda(T_2 - \tau_2))} & \text{if } q < 0 \\ \sqrt{k(\alpha\lambda(T_2 - \tau_2) - \beta F_2)} & \text{if } q \geq 0 \end{cases} \quad (3.10)$$

Using the assumption that the temperatures of the two boxes will come to an equilibrium much more quickly than the salinities come to an equilibrium can be used to simplify this system of equations. The simplified system of equations can be

used to investigate the stability of the equilibrium solutions of the original system of equations. The differential equations for temperature can be eliminated because the two temperature variables would be nearly constant so their derivatives with respect to time are zero. The difference between these two temperatures will also be a constant of $\Delta T = T_1 - T_2$ and this difference will usually be greater than zero because of the target temperatures of the two boxes. Taking the difference of the two differential equations for salinity and using $\Delta S = S_1 - S_2$ results in a single differential equation in ΔS :

$$\frac{d(\Delta S)}{dt} = -\frac{V+1}{V}F_2 + \frac{V+1}{V}|q|\Delta S \quad (3.11)$$

$$= -\frac{V+1}{V}F_2 + \frac{V+1}{V}|k(\alpha\Delta T - \beta\Delta S)|\Delta S \quad (3.12)$$

To make this differential equation dimensionless, first replace ΔS with $\Delta S = \frac{\alpha\Delta T y}{\beta}$ and the equation becomes:

$$\frac{\alpha\Delta T}{\beta} \frac{dy}{dt} = -\frac{V+1}{V}F_2 + \frac{V+1}{V} \left| k \left(\alpha\Delta T - \beta \frac{\alpha\Delta T y}{\beta} \right) \right| \frac{\alpha\Delta T y}{\beta} \quad (3.13)$$

$$\frac{dy}{dt} = -\frac{V+1}{V}F_2 + \frac{V+1}{V}k\alpha|\Delta T||1-y|y \quad (3.14)$$

Then replace t with $t = \frac{V}{k\alpha|\Delta T|(V+1)}x$:

$$\frac{k\alpha|\Delta T|(V+1)}{V} \frac{dy}{dx} = -\frac{V+1}{V}F_2 + \frac{V+1}{V}k\alpha|\Delta T||1-y|y \quad (3.15)$$

$$\frac{dy}{dx} = -\frac{F_2}{k\alpha|\Delta T|} + |1-y|y \quad (3.16)$$

Finally, letting σ be $\sigma = \frac{F_2}{k\alpha|\Delta T|}$ results in a dimensionless differential equation. Note that $\sigma > 0$ because all components of this fraction are positive. In this model, the value of F_2 is the freshwater flux in the high-latitude box, which is positive as it must counteract the evaporation that occurs in the equatorial box:

$$\frac{dy}{dx} = -\sigma + |1-y|y \quad (3.17)$$

The equilibrium states of this differential equation can be found by solving this differential equation for y when $\frac{dy}{dx}$ is zero. The equation has several different solutions depending on the sign of $1-y$:

$$|1-y|y = \sigma \quad \text{The equation to be solved} \quad (3.18)$$

$$(1 - y)y = \sigma \quad \text{If } y < 1 \quad (3.19)$$

$$y = \frac{1}{2} \pm \frac{\sqrt{1 - 4\sigma}}{2} \quad (3.20)$$

$$(y - 1)y = \sigma \quad \text{If } y \geq 1 \quad (3.21)$$

$$y = \frac{1}{2} + \frac{\sqrt{1 + 4\sigma}}{2} \quad \text{Only the "+" works as } y \geq 1 \quad (3.22)$$

$$y = \begin{cases} \frac{1}{2} \pm \frac{\sqrt{1 - 4\sigma}}{2} & \text{if } y < 1 \\ \frac{1}{2} + \frac{\sqrt{1 + 4\sigma}}{2} & \text{if } y \geq 1 \end{cases} \quad (3.23)$$

To linearize this differential equation, let $y = y^* + u$, where y^* is a constant equilibrium point so that $|1 - y^*|y^* = \sigma$ and u is a small perturbation from the equilibrium point. Then find a first order approximation of the value of $\frac{du}{dx}$:

$$\frac{du}{dx} = |1 - (y^* + u)|(y^* + u) \quad (3.24)$$

$$= \begin{cases} y^* + u - (y^*)^2 - 2y^*u - u^2 & \text{if } y^* + u < 1 \\ -y^* - u + (y^*)^2 + 2y^*u + u^2 & \text{if } y^* + u \geq 1 \end{cases} \quad (3.25)$$

$$= \begin{cases} u - 2y^*u - u^2 & \text{if } y^* + u < 1 \\ -u + 2y^*u + u^2 & \text{if } y^* + u \geq 1 \end{cases} \quad (3.26)$$

$$\approx \begin{cases} u - 2y^*u & \text{if } y^* + u < 1 \\ -u + 2y^*u & \text{if } y^* + u \geq 1 \end{cases} \quad \text{First order approximation in } u \quad (3.27)$$

$$= \begin{cases} u(1 - 2y^*) & \text{if } y^* + u < 1 \\ -u(1 - 2y^*) & \text{if } y^* + u \geq 1 \end{cases} \quad (3.28)$$

Because y^* is an equilibrium point, equation 3.23 can be used to get its value in terms of σ . There are three ranges for y^* which are $[0, \frac{1}{2}]$, $(\frac{1}{2}, 1)$, and $[1, \infty)$. Each of these ranges has a different value for y in terms of σ . Combining equations (3.23) and (3.28) results in these differential equations for u .

$$\frac{du}{dx} = \begin{cases} u \left[1 - 2 \left(\frac{1}{2} - \frac{\sqrt{1 - 4\sigma}}{2} \right) \right] & \text{if } 0 \leq y^* \leq \frac{1}{2} \\ u \left[1 - 2 \left(\frac{1}{2} + \frac{\sqrt{1 - 4\sigma}}{2} \right) \right] & \text{if } \frac{1}{2} < y^* < 1 \\ -u \left[1 - 2 \left(\frac{1}{2} + \frac{\sqrt{1 + 4\sigma}}{2} \right) \right] & \text{if } y^* \geq 1 \end{cases} \quad (3.29)$$

$$= \begin{cases} u\sqrt{1 - 4\sigma} & \text{if } 0 \leq y^* \leq \frac{1}{2} \\ -u\sqrt{1 - 4\sigma} & \text{if } \frac{1}{2} < y^* < 1 \\ u\sqrt{1 + 4\sigma} & \text{if } y^* \geq 1 \end{cases} \quad (3.30)$$

From this, the differential equation (3.17) will be stable for $y \leq \frac{1}{2}$ and $y \geq 1$ and unstable otherwise. See Figure 3.4 for a bifurcation diagram of this system. The

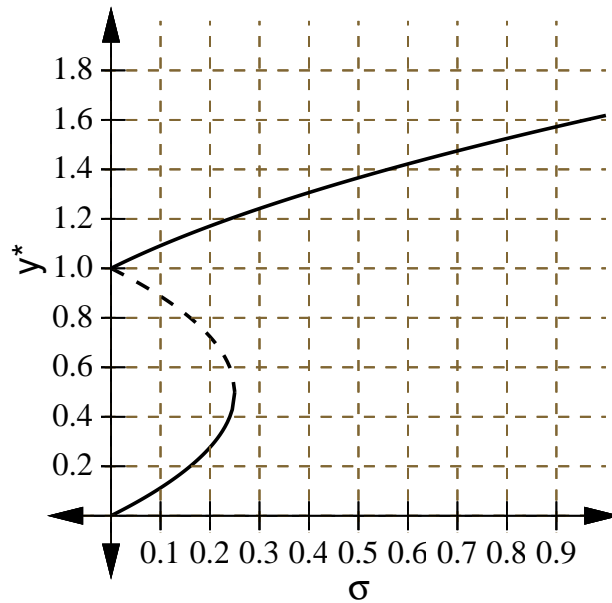


Figure 3.4. The 2-box model's bifurcation diagram. The lines represent stable equilibriums, the dashed line is for unstable equilibriums.

stable branch toward the top of the graph with $y^* \geq 1$, or $\Delta S = S_1 - S_2 > \frac{\alpha \Delta T}{\beta}$ with $\Delta T > 0$, the salinity of the content of the two boxes drives the flow, or the salinity term in equation (3.2) is greater than the temperature term. This is referred to the *S-mode* [6], where the surface flow is toward the equator. The lower stable branch with $y^* < \frac{1}{2}$, or $\Delta S = S_1 - S_2 < \frac{2\alpha \Delta T}{\beta}$, is when the temperatures of the boxes drive the flow. This is referred to as the *T-mode*, where the surface flow is away from the equator, like today's Gulf Stream current.

The analysis of the bifurcation diagram shows that according to this model, the thermohaline circulation can become unstable and even come to a different stable configuration which reverses the direction given major changes to the parameters of this system. Also, there may be no hysteresis for this system; a change to the parameters of the system which is subsequently reverted may not result in the system returning to its original state. In the bifurcation diagram, the lower stable curve is where the density difference is driven by the differences in temperatures rather than the differences in salinity, or what is referred to as *T-mode*. The upper stable curve is where the density difference is driven by the differences in salinities, what is referred

to as *S-mode*. Today, the circulation in the Atlantic Ocean is in *T-mode*. From the chart in Figure 3.4, if the value of $\sigma = \frac{F_2}{k\alpha|\Delta T|}$ is somehow gradually raised to where it is greater than $\frac{1}{4}$, that is, so that $F_2 > \frac{1}{4}k\alpha|\Delta T|$, then the system would be in a state such that it would tend to come to equilibrium on the upper stability curve in the bifurcation diagram. This would mean a reversal of the surface currents in the Atlantic Ocean so that the system would change to *S-mode*. If the value of the freshwater input to the Northern Atlantic, or F_2 , were then gradually reduced back to today's value, the system would remain in *S-mode* rather than return to *T-mode*. This type of change would reverse the direction of the surface and deep currents in the Atlantic Ocean. It could alter the climate of Eastern North America and Northern Europe by removing the warming effects of the Gulf Stream current in the Atlantic Ocean.

3.1.3 Numerical Modeling

A GNU Octave (Matlab compatible) model of this system was used as a quick way to to model changes in the freshwater flux, the values of F_1 and F_2 . The model makes use of a classical Runge-Kutta method to model the flows of sea water over 3000 years with a time step taken every year. Following the methods used in the article by Lucarini and Stone [7]. Figure 3.5 shows a graph of this system of equations where the freshwater flux is altered at different rates for the first 500 of 3000 years. The flux in the high-latitude box increases in each of the first 500 years with the flux in the equatorial box decreasing by a similar amount in those same 500 years according to:

$$F_{2,\text{current}} = \begin{cases} F_{2,\text{original}} + t\Delta F & \text{if } t \leq 500 \text{ years } (t \text{ in years}) \\ F_{2,\text{original}} + 500\Delta F & \text{if } t > 500 \text{ years} \end{cases} \quad (3.31)$$

Figure 3.6 shows this same increase over the first 500 years followed by 1000 years of that increased flux, and then followed by 500 years of the flux reducing by the same rate back to the original values. For this second graph, the flux in the high-latitude box changes according to:

$$F_{2,\text{current}} = \begin{cases} F_{2,\text{original}} + t\Delta F & \text{if } t \leq 500 \text{ years } (t \text{ in years}) \\ F_{2,\text{original}} + 500\Delta F & \text{if } 500 < t \leq 1500 \\ F_{2,\text{original}} + (2000 - t)\Delta F & \text{if } 1500 < t \leq 2000 \\ F_{2,\text{original}} & \text{if } t > 2000 \end{cases} \quad (3.32)$$

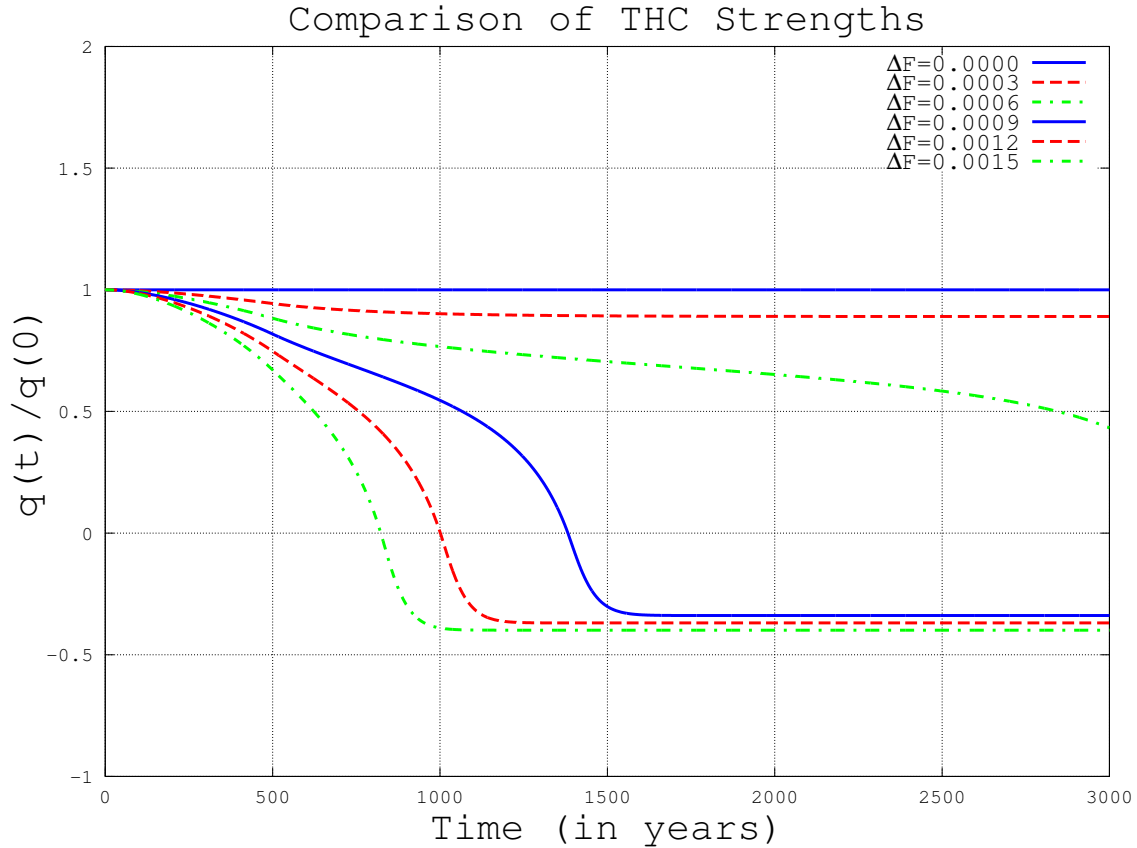


Figure 3.5. The THC strengths for changes to the freshwater flux. As the freshwater flux increases in the high-latitudes, the equilibrium state for the system has a smaller difference in temperatures. Each increment to ΔF adds 15% to the maximum freshwater flux in the northern box. For a high enough change in the freshwater flux, the system changes from *T-mode* to *S-mode* stability. Note that the curves graphed here are in the same order as the legend in the upper right corner.

In this way, the values of the freshwater fluxes are gradually increased from the initial equilibrium to the new values; then the system is allowed to settle into a new equilibrium; and then the values are gradually returned their initial values.

The values for the temperature and salinity were taken from the 3-box model of the Atlantic Ocean used by Lucarini and Stone [7], given in Table 3.1. However the values for temperature and salinity were not at an equilibrium in this 2-box model. The values for the initial temperatures and salinities were changed to:

$$T_1 = 28.838^\circ\text{C} \qquad S_1 = 35.613 \text{ psu} \qquad (3.33)$$

$$T_2 = 2.3268^\circ\text{C} \qquad S_2 = 34.073 \text{ psu} \qquad (3.34)$$

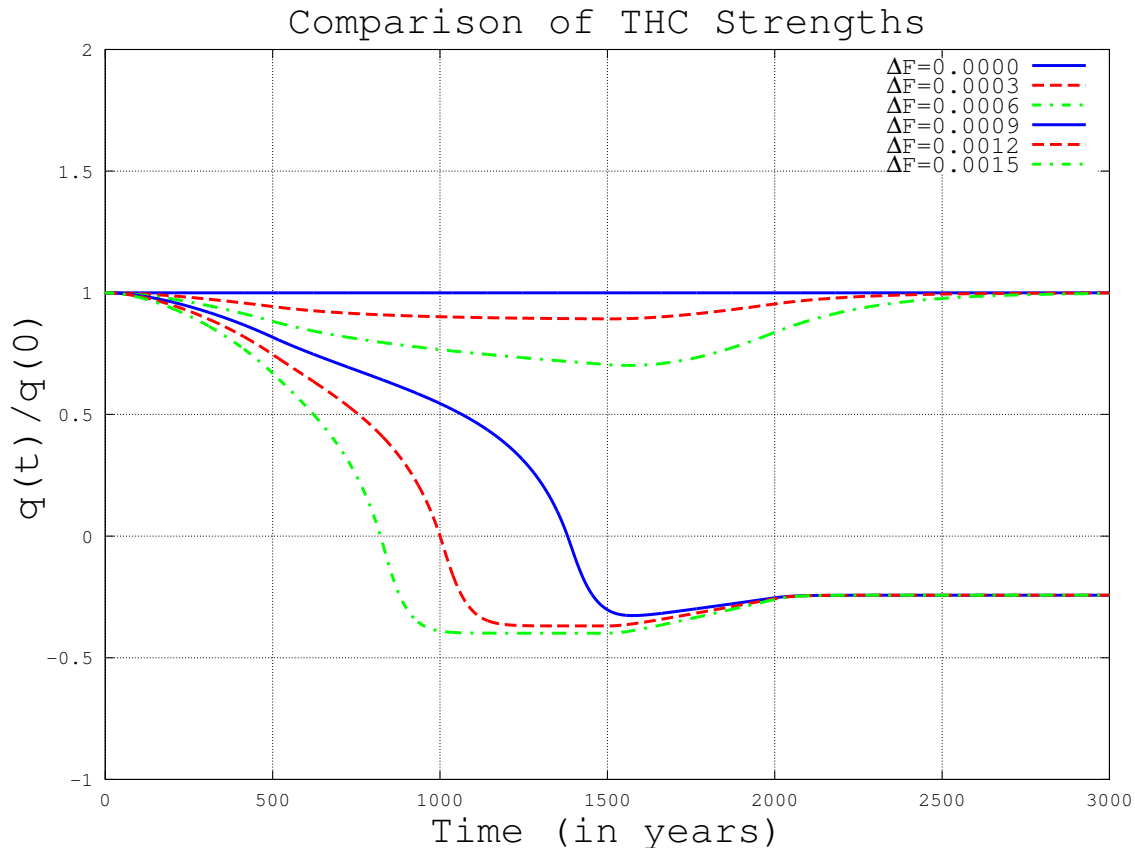


Figure 3.6. The THC strengths for short-term changes to the freshwater flux. Each increment to ΔF adds 15% to the maximum freshwater flux in the northern box. The freshwater fluxes are raised leading up to year 500 and then lowered back to the original values between years 1000 and 1500. For a high enough change in the freshwater flux, the system changes to different equilibrium states showing the lack of hysteresis in the system.

These values are similar to the physical properties of the Atlantic Ocean but not exact; however, they do start this model very closely to an equilibrium point. Another change from the values used by Lucarini and Stone is to the hydraulic constant k . In order to keep the rate of flow in the surface current at approximately 15.5 Sv, which is the approximate rate of flow in the surface current for today's Atlantic Ocean [12], the value of the hydraulic constant k was changed to $5.4120 \times 10^{-8} \text{ s}^{-1}$. This choice also makes the “overturning” rate of the model or the time needed to completely replace all of the sea water in the high-latitude box with incoming flows about 213 years. This agrees well with the actual overturning rate which is closer to about 250 years. Because of the assumption in a box model of oceanic circulation that the boxes

are well mixed, no prediction from a model which takes a much smaller amount of time than this overturning rate should be assumed to be reliable.

The graph in Figure 3.5 shows that for smaller increases in the freshwater flux, the system comes to an equilibrium which is still in *T-mode*, although with differing temperatures and salinities from the original equilibrium. The differences in the freshwater flux are such that when $\Delta F = 0.0003$ the change in the freshwater flux in the high-latitude box increases by a factor of 1.15, or an increase of 15%. The higher freshwater fluxes drive the system into a state where the differences in salinity drive the flows rather than the differences in temperature. This represents a change from *T-mode* to *S-mode* and includes a reversal of the direction of the surface flow in the Atlantic Ocean. Note that the third line from the top, where $\Delta F = 0.0006$, is actually coming to an equilibrium in *S-mode* with the flow directions reversed, but it needs close to 6000 years of model time to come close to its equilibrium rather than the 3000 years graphed here.

To demonstrate the lack of hysteresis in this system, Figure 3.6 is of the flows in the system when the freshwater flux in the high-latitude box is increased for 500 years, held steady at the higher rate for 1000 years, and then decreased back to the original value over the third 500 years. In the second graph, Figure 3.6, even though the parameters of the system are returned to their original values, the system can find a new equilibrium with a different value for the strength and direction of the new surface flow. The change in the freshwater flux in the high-latitude box, F_2 , is a change to the value of $\sigma = \frac{F_2}{k\alpha|\Delta T|}$. Note that while the value of ΔT is also changed, this difference remains somewhere between 25°C and 30°C, and nearer to 25°C. The change in the value of F_2 are in the range of an added 15% for each of the new values of ΔF . Once the value of σ is raised to be above $\frac{1}{4}$, the stability of the system shifts so that the only stable fixed point is one which corresponds to the upper stable curve in Figure 3.4, rather than the lower stable curve. The line in the second graph which corresponds to $\Delta F = 0.0006$, or an increase of 30% in the freshwater flux, changes the system to *S-mode*. For the curve for $\Delta F = 0.0006$, the system is changing to *S-mode*, but does not come close enough to the new equilibrium within the 500 years during which the freshwater flux remains at its maximum. Once the freshwater flux

begins to decrease, the system in this case returns to the equilibrium in *T-mode*.

This simple 2-box model shows that the thermohaline currents in the oceans can have multiple equilibrium values. If the parameters of the ocean circulation system are changed, the system may go through irreversible changes. The ocean circulation system may be altered to a new equilibrium state even if the parameters are changed and then revert back to the original parameters. The Stommel 2-box model does show that the circulation in the Atlantic Ocean has multiple equilibrium states. However, it cannot address some of the issues involved in modeling global circulation or even the circulation of the full Atlantic Ocean [14].

3.2 3-Box Models

While the Stommel 2-box model reveals some interesting points about the thermohaline circulation, it does appear to be too simple a model to represent the oceanic circulation for all of the Earth's oceans. In order to make a box model which is more representative of the total circulation of the oceans, more must be added to the model. The next step up in this sequence is to add another box to the 2-box model to make a 3-box model which represents the entire Atlantic Ocean. There are several different approaches to modeling ocean circulation with 3-box models. The main idea behind 3-box models is to model the Atlantic Ocean with two high-latitude boxes and an equatorial box. The Welander and Rooth 3-box models are presented here. The Rooth 3-box model appears to represent the circulation in the Atlantic better than the Welander 3-box model.

3.2.1 Welander 3-Box Model

The Welander 3-box model used here is similar to the Stommel 2-box model, but with a third box representing the Southern Atlantic Ocean added, see Figure 3.7. This is the Welander 3-box model used in Zhang (2007) [17]. It has flows to and from the equatorial region and both high-latitude regions, but no flow connecting the two high-latitude regions. This models the Atlantic Ocean as a symmetric basin, symmetric in that the high-latitude boxes and the circulation for these boxes are essentially the same.

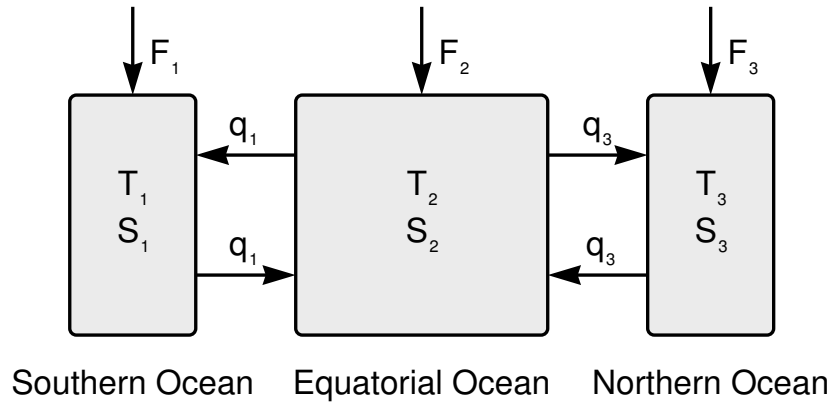


Figure 3.7. Welander's 3-box model of thermohaline circulation. The equatorial region has both surface and deep flows that connect to the polar regions.

3.2.1.1 Equations for Welander 3-Box Model

The equations for this model are this series of differential equations:

$$\frac{dT_1}{dt} = |q_1|(T_2 - T_1) + H_1 \quad (3.35)$$

$$\frac{dT_2}{dt} = \frac{|q_1|}{V}(T_1 - T_2) + \frac{|q_3|}{V}(T_3 - T_2) + H_2 \quad (3.36)$$

$$\frac{dT_3}{dt} = |q_3|(T_2 - T_3) + H_3 \quad (3.37)$$

$$\frac{dS_1}{dt} = |q_1|(S_2 - S_1) - F_1 \quad (3.38)$$

$$\frac{dS_2}{dt} = \frac{|q_1|}{V}(S_1 - S_2) + \frac{|q_3|}{V}(S_3 - S_2) - F_2 \quad (3.39)$$

$$\frac{dS_3}{dt} = |q_3|(S_2 - S_3) - F_3 \quad (3.40)$$

Note the use of absolute values in these equations in the same way as they were used in the equations for the Stommel 2-box model. The mixing of sea water between the equatorial box and either high-latitude box does not depend on the direction of the flow between the boxes, only the strength of the flow. The strengths of the two flows, q_1 and q_3 , depend on the densities of the salt water in the equatorial box and the corresponding the high-latitude box. These flows are given by:

$$q_1 = k(\alpha(T_2 - T_1) - \beta(S_2 - S_1)) \quad (3.41)$$

$$q_3 = k(\alpha(T_2 - T_3) - \beta(S_2 - S_3)) \quad (3.42)$$

Again, the variable k is a hydraulic constant that sets the strength of the flow based on the density differences. The value of k is assumed to be the same for flows in the northern and southern parts of the model. The values of α and β are the thermal and haline expansion coefficients used to estimate the density of salt water given its temperature and salinity.

3.2.1.2 Equilibrium Points

To find equilibrium points, assume that the temperatures of the boxes come to equilibrium more quickly than the salinities so that the temperatures can be assumed to be constant. The differences in the temperatures are $\Delta T_1 = T_2 - T_1$ and $\Delta T_3 = T_2 - T_3$. The total salinity is held constant so that $S_0 = S_1 + VS_2 + S_3$ and then $\frac{S_0}{V+2}$ is the constant average salinity of the entire system. The freshwater fluxes for the three boxes are related by $F_2 = -\frac{F_1 + F_3}{V}$. This system of differential equations can be reduced to a system of two differential equations dealing with the differences in salinity of the first and third boxes with the second box. The differences in the salinities of the boxes are $\Delta S_1 = S_2 - S_1$ and $\Delta S_3 = S_2 - S_3$. The system of differential equations for this model has been reduced to these two equations:

$$q_1 = k(\alpha\Delta T_1 - \beta\Delta S_1) \quad \text{Flow strengths} \quad (3.43)$$

$$q_3 = k(\alpha\Delta T_3 - \beta\Delta S_3) \quad (3.44)$$

$$\frac{d\Delta S_1}{dt} = -\frac{|q_1|}{V}\Delta S_1 - \frac{|q_3|}{V}\Delta S_3 + \frac{F_1 + F_3}{V} - |q_1|\Delta S_1 + F_1 \quad (3.45)$$

$$= -\frac{(V+1)|q_1|}{V}\Delta S_1 - \frac{|q_3|}{V}\Delta S_3 + \frac{V+1}{V}F_1 + \frac{1}{V}F_3 \quad (3.46)$$

$$\frac{d\Delta S_3}{dt} = -\frac{|q_1|}{V}\Delta S_1 - \frac{|q_3|}{V}\Delta S_3 + \frac{F_1 + F_3}{V} - |q_3|\Delta S_3 + F_3 \quad (3.47)$$

$$= -\frac{|q_1|}{V}\Delta S_1 - \frac{(V+1)|q_3|}{V}\Delta S_3 + \frac{1}{V}F_1 + \frac{V+1}{V}F_3 \quad (3.48)$$

There are four distinct equilibrium states for this model; these states come from the signs of the flow strengths q_1 and q_3 . To continue with a generalized solution for this system of equations, let Z_1 be -1 if $q_1 < 0$ and +1 if $q_1 \geq 0$, and let Z_3 have the same values depending on the sign of q_3 . With these new variables, the two differential equations become:

$$\frac{d\Delta S_1}{dt} = -\frac{Z_1(V+1)q_1}{V}\Delta S_1 - \frac{Z_3q_3}{V}\Delta S_3 + \frac{V+1}{V}F_1 + \frac{1}{V}F_3 \quad (3.49)$$

$$= -\frac{Z_1(V+1)k(\alpha\Delta T_1 - \beta\Delta S_1)}{V}\Delta S_1 - \frac{Z_3k(\alpha\Delta T_3 - \beta\Delta S_3)}{V}\Delta S_3 + \frac{V+1}{V}F_1 + \frac{1}{V}F_3 \quad (3.50)$$

$$= \frac{Z_1(V+1)k\beta}{V}\Delta S_1^2 - \frac{Z_1(V+1)k\alpha\Delta T_1}{V}\Delta S_1 + \frac{Z_3k\beta}{V}\Delta S_3^2 - \frac{Z_3k\alpha\Delta T_3}{V}\Delta S_3 + \frac{V+1}{V}F_1 + \frac{1}{V}F_3 \quad (3.51)$$

$$\frac{d\Delta S_3}{dt} = -\frac{Z_1q_1}{V}\Delta S_1 - \frac{Z_3(V+1)q_3}{V}\Delta S_3 + \frac{1}{V}F_1 + \frac{V+1}{V}F_3 \quad (3.52)$$

$$= -\frac{Z_1k(\alpha\Delta T_1 - \beta\Delta S_1)}{V}\Delta S_1 - \frac{Z_3(V+1)k(\alpha\Delta T_3 - \beta\Delta S_3)}{V}\Delta S_3 + \frac{1}{V}F_1 + \frac{V+1}{V}F_3 \quad (3.53)$$

$$= \frac{Z_1k\beta}{V}\Delta S_1^2 - \frac{Z_1k\alpha\Delta T_1}{V}\Delta S_1 + \frac{Z_3(V+1)k\beta}{V}\Delta S_3^2 - \frac{Z_3(V+1)k\alpha\Delta T_3}{V}\Delta S_3 + \frac{1}{V}F_1 + \frac{V+1}{V}F_3 \quad (3.54)$$

To simplify the solution for equilibrium points these two equations can be converted to two new variables $x = \Delta S_1 - \frac{\alpha\Delta T_1}{2\beta}$ and $y = \Delta S_3 - \frac{\alpha\Delta T_3}{2\beta}$ so that the differential equations become:

$$\begin{aligned} \frac{dx}{dt} &= \frac{Z_1(V+1)k\beta}{V}x^2 + \frac{Z_3k\beta}{V}y^2 \\ &+ \frac{V+1}{V}F_1 + \frac{1}{V}F_3 - \frac{k\alpha^2(Z_1(V+1)\Delta T_1^2 + Z_3\Delta T_3^2)}{4V\beta} \end{aligned} \quad (3.55)$$

$$\begin{aligned} \frac{dy}{dt} &= \frac{Z_1k\beta}{V}x^2 + \frac{Z_3(V+1)k\beta}{V}y^2 \\ &+ \frac{1}{V}F_1 + \frac{V+1}{V}F_3 - \frac{k\alpha^2(Z_1\Delta T_1^2 + Z_3(V+1)\Delta T_3^2)}{4V\beta} \end{aligned} \quad (3.56)$$

With these equations, the equilibrium points can be found by setting both derivatives equal to zero and solving the linear system of equations for the equilibrium values \bar{x}^2 and \bar{y}^2 , which gives:

$$\bar{x}^2 = \frac{\alpha^2\Delta T_1^2}{4\beta^2} - \frac{Z_1}{k\beta}F_1 \quad (3.57)$$

$$\bar{y}^2 = \frac{\alpha^2\Delta T_3^2}{4\beta^2} - \frac{Z_3}{k\beta}F_3 \quad (3.58)$$

Note that if either value Z_1 or Z_3 is greater than zero or equal to +1, then the

equilibrium points may not exist depending on the respective signs of the expressions in the right-hand sides of the equations above. The positive values of Z_1 and Z_3 correspond to the *T-mode* state of the Stommel 2-box model where the differences in temperature drive the direction of the flows. When the freshwater flux becomes large enough in one of the high-latitude boxes so that the equilibrium point does not exist, that portion of the model will switch to its *S-mode* so that the value of the corresponding q_i becomes negative. Converting the equilibrium values \bar{x} and \bar{y} back to $\Delta\bar{S}_1$ and $\Delta\bar{S}_3$ gives this solution for the equilibrium points:

$$\Delta\bar{S}_1 = \frac{\alpha\Delta T_1}{2\beta} \pm \sqrt{\frac{\alpha^2\Delta T_1^2}{4\beta^2} - \frac{Z_1}{k\beta}F_1} \quad (3.59)$$

$$\Delta\bar{S}_3 = \frac{\alpha\Delta T_3}{2\beta} \pm \sqrt{\frac{\alpha^2\Delta T_3^2}{4\beta^2} - \frac{Z_3}{k\beta}F_3} \quad (3.60)$$

This solution shows that there are multiple equilibrium solutions up to the point where the value within the radical becomes negative. This solution can be non-dimensionalized by allowing $X_1 = \frac{\beta\Delta S_1}{\alpha\Delta T_1}$ and $X_3 = \frac{\beta\Delta S_3}{\alpha\Delta T_3}$ and $F_1^* = \frac{\beta F_1}{k\alpha^2\Delta T_1^2}$ and $F_3^* = \frac{\beta F_3}{k\alpha^2\Delta T_3^2}$. The equilibrium solution becomes:

$$X_1 = \frac{1}{2} \pm \sqrt{\frac{1}{4} - Z_1 F_1^*} \quad (3.61)$$

$$X_3 = \frac{1}{2} \pm \sqrt{\frac{1}{4} - Z_3 F_3^*} \quad (3.62)$$

The values of the Z variables are the respective signs of the q values of the flows. This solution for the equilibrium points of this model shows that the model operates as if it were two different Stommel 2-box models. The temperature and salinity of the equatorial box can be affected by both high-latitude boxes, but once equilibrium is reached, the stability of either flow is determined in a similar manner to the Stommel 2-box model.

3.2.1.3 Numerical Modeling

A Gnu Octave script representing this model shows that the model also has two stable states under certain conditions, like the Stommel 2-box model. These models begin with the parameters used in the article by Lucarini and Stone [7]. However,

those parameters would not have this model in an equilibrium state. The initial temperatures and salinities required changes to:

$$T_1 = 2.8246^\circ \text{C} \qquad S_1 = 34.749 \text{ psu} \qquad (3.63)$$

$$T_2 = 26.960^\circ \text{C} \qquad S_2 = 35.338 \text{ psu} \qquad (3.64)$$

$$T_3 = 3.2548^\circ \text{C} \qquad S_3 = 34.576 \text{ psu} \qquad (3.65)$$

These parameter changes do not have the model beginning with the current state of the Atlantic Ocean, but do have the model starting in an equilibrium state. The main reason that the equilibrium values change is that the input to the Southern Atlantic comes from the equatorial box rather than from the Northern Atlantic, as is the case in Rooth's 3-box model. In addition, the hydraulic constant k was changed to the value 4.7169×10^{-8} so that the original northern surface flow from the equatorial box to the northern box is at a rate of about 15.5 Sv (Sverdrups or $10^6 \text{ m}^3 \text{ s}^{-1}$).

To show that there are two stable states, the freshwater flux in the high-latitude boxes was changed slowly over the course of time. For the northern box (box 3), the value of the freshwater flux was changed according to:

$$F_{3,\text{current}} = \begin{cases} F_{3,\text{original}} + t\Delta F & \text{if } t \leq 500 \text{ years } (t \text{ in years}) \\ F_{3,\text{original}} + 500\Delta F & \text{if } t > 500 \text{ years} \end{cases} \qquad (3.66)$$

The freshwater flux in the southern box (box 1) is increased at $\frac{3}{10}$ of the rate of increase in the northern box. The results of this are shown in Figures 3.8, 3.9, 3.10, and 3.11. The Figures 3.9, and 3.11 show the effects of this same increase over the first 500 years followed by 1000 years of that increased flux, and then followed by 500 years of the flux reducing by the same rate back to the original values. For the second graph, the flux in the high-latitude box changes according to:

$$F_{3,\text{current}} = \begin{cases} F_{3,\text{original}} + t\Delta F & \text{if } t \leq 500 \text{ years } (t \text{ in years}) \\ F_{3,\text{original}} + 500\Delta F & \text{if } 500 < t \leq 1500 \\ F_{3,\text{original}} + (2000 - t)\Delta F & \text{if } 1500 < t \leq 2000 \\ F_{3,\text{original}} & \text{if } t > 2000 \end{cases} \qquad (3.67)$$

Again, the freshwater flux in the southern box (box 1) is increased at $\frac{3}{10}$ of the rate of increase in the northern box. The second value of ΔF , shown in Figures 3.10 and 3.11 are where $\Delta F = 2.01$ so that the total freshwater flux in the northern box

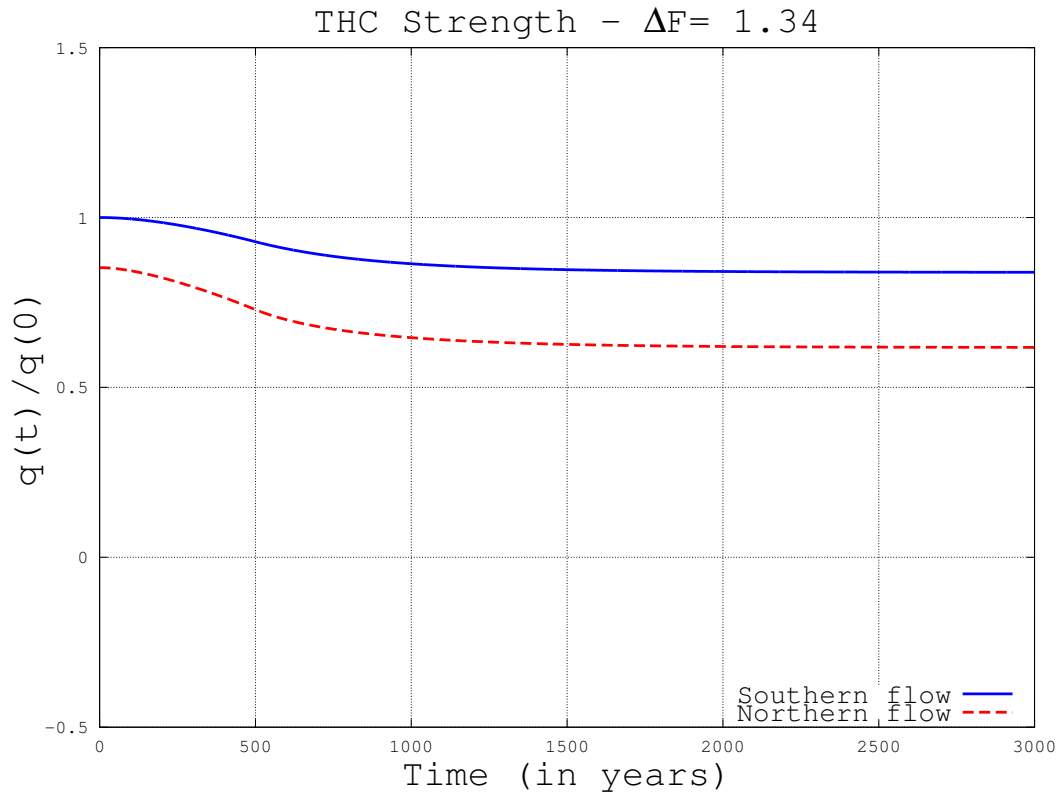


Figure 3.8. Welander model with a 134% increase in the freshwater flux. The northern flux of freshwater is increased by 134%. The flows reach a new equilibrium without reversing directions.

increased by 201%. In this set of graphs, the flows between the boxes change to a new set of equilibrium values and the northern flow reverses direction. The graphs in Figure 3.11 show that this model does not always exhibit hysteresis, that with the same parameters, the model can reach a different equilibrium point.

Also, these four graphs show another facet of the Welander 3-box model. The initial equilibrium state has sea water up-welling in the equatorial box with surface flows proceeding from the equatorial box to both of the high-latitude boxes. However, in Figure 3.11, the surface flow eventually changes so that both surface flows go from North to South. That is, the value of q_3 switches from a positive value to a negative value. These directions for the flows are the opposite of today's flows in the Atlantic Ocean. In this model, the precipitation in the high-latitude boxes must increase by more than 160% for this state change to happen. While the Welander 3-box model is a simple extension of Stommel's 2-box model, it does not match the current conditions

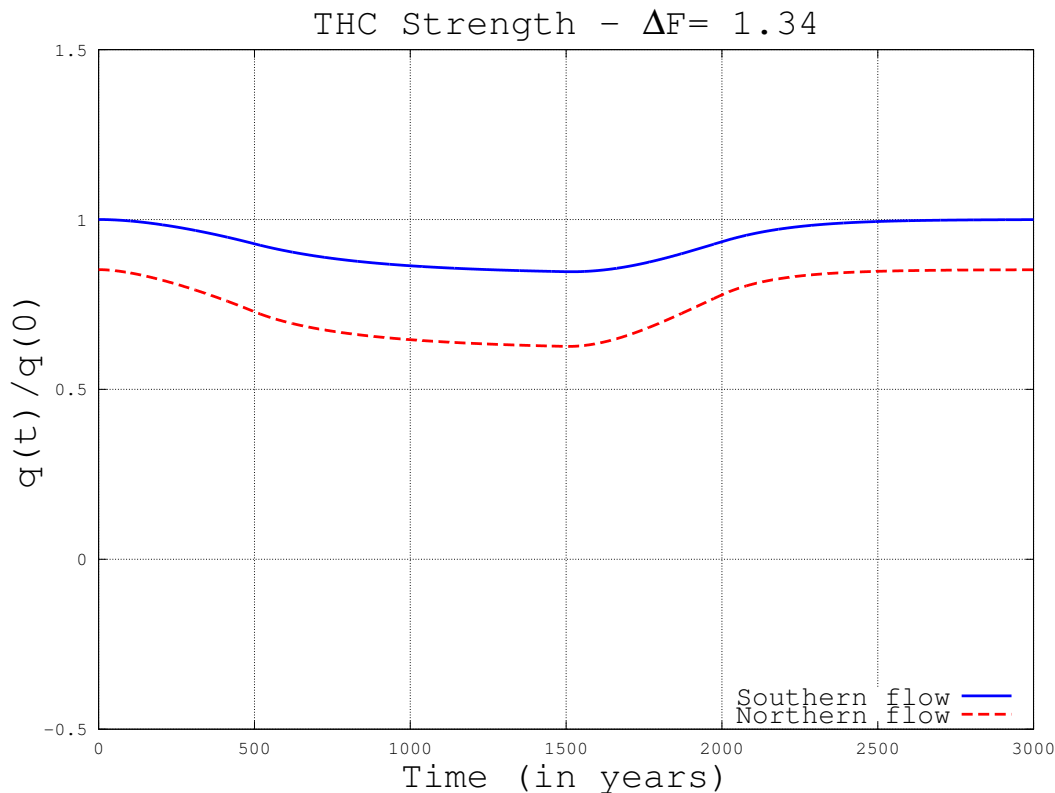


Figure 3.9. Welander model with a short-term 134% increase in the freshwater flux. The freshwater flux is increased the northern flux 134% and then reduced to the original flux value. The flows return to their original values.

of the Atlantic Ocean very accurately.

3.2.2 Rooth's 3-Box Model

The Rooth 3-box model is another model of the Atlantic Ocean. Figure 3.12 shows how the components of this model interact with each other. This model is closer to the actual flows in the Atlantic Ocean, that is, there is a deep flow of colder sea water which does not mix to any extent with the warmer sea water in the equatorial region.

3.2.2.1 Equations for Rooth's 3-Box Model

The deep flow is the key flow for this model. It is driven by the density differences between the two high-latitude boxes. Note that because these are both high-latitude boxes, their temperatures and densities are very similar so the hydraulic constant k is much larger than for the 2-box model. The other two flows have the same magnitude as the deep flow, but flow in the opposite of the direction of the deep flow. The

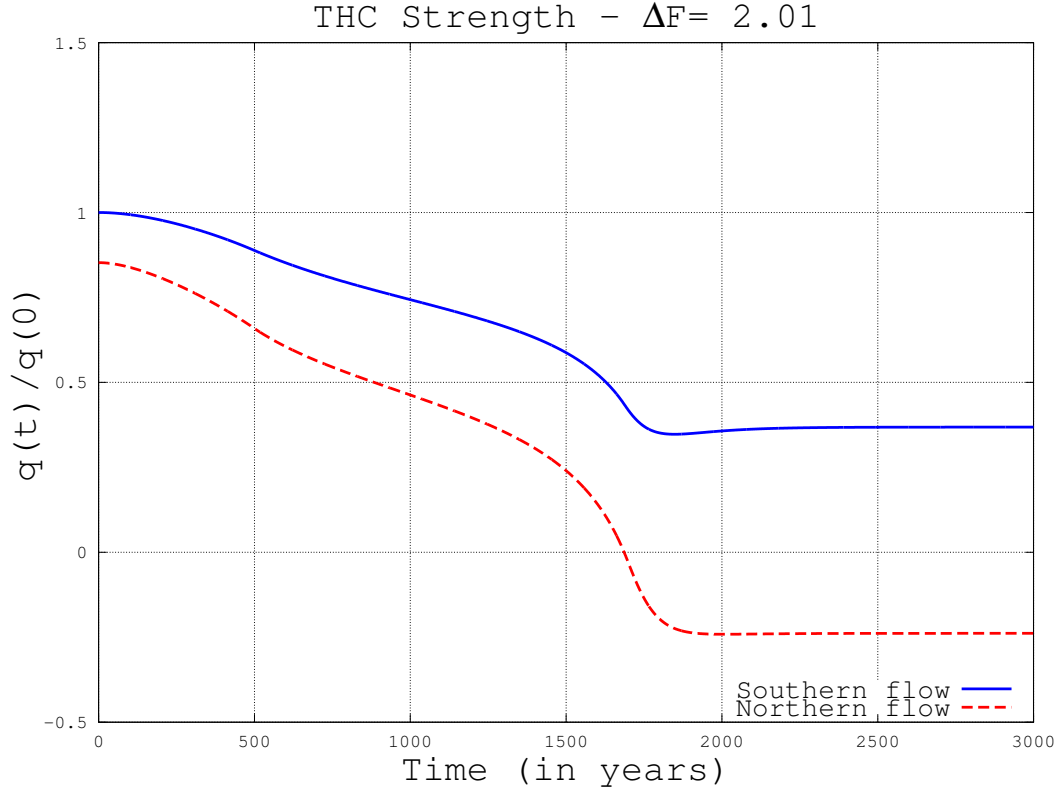


Figure 3.10. Welander model with a 201% increase in the freshwater flux. The northern flux of freshwater is increased by 201%. The flows reach a new equilibrium with the northern flow reversing direction.

direction of the flow determines which box supplies the sea water flowing into each of the boxes in the model. That is, the box upstream from a particular box provides the new contents for that box. Also, a positive flow value is a flow where the surface flows travel from South to North, or from box 1 (southern) to box 2 (equatorial) and then to box 3 (northern). The equations for this model are:

$$q = k(\alpha(T_1 - T_3) - \beta(S_1 - S_3)) \quad \text{Strength and direction of the flow} \quad (3.68)$$

$$\frac{dT_1}{dt} = \begin{cases} q(T_1 - T_2) + \lambda(\tau_1 - T_1) = q(T_1 - T_2) + H_1 & \text{if } q < 0 \\ q(T_3 - T_1) + \lambda(\tau_1 - T_1) = q(T_3 - T_1) + H_1 & \text{if } q \geq 0 \end{cases} \quad (3.69)$$

$$\frac{dT_2}{dt} = \begin{cases} \frac{q}{V}(T_2 - T_3) + \lambda(\tau_2 - T_2) = \frac{q}{V}(T_2 - T_3) + H_2 & \text{if } q < 0 \\ \frac{q}{V}(T_1 - T_2) + \lambda(\tau_2 - T_2) = \frac{q}{V}(T_1 - T_2) + H_2 & \text{if } q \geq 0 \end{cases} \quad (3.70)$$

$$\frac{dT_3}{dt} = \begin{cases} q(T_3 - T_1) + \lambda(\tau_3 - T_3) = q(T_3 - T_1) + H_3 & \text{if } q < 0 \\ q(T_2 - T_3) + \lambda(\tau_3 - T_3) = q(T_2 - T_3) + H_3 & \text{if } q \geq 0 \end{cases} \quad (3.71)$$

$$\frac{dS_1}{dt} = \begin{cases} q(S_1 - S_2) - F_1 & \text{if } q < 0 \\ q(S_3 - S_1) - F_1 & \text{if } q \geq 0 \end{cases} \quad (3.72)$$

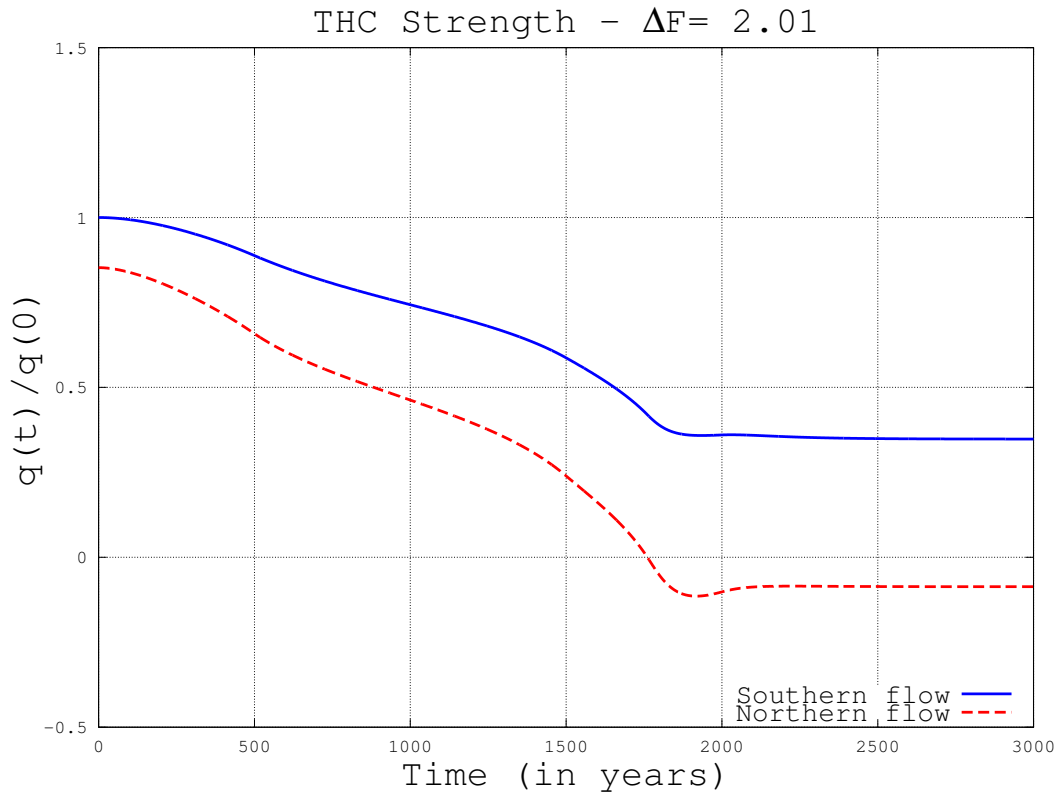


Figure 3.11. Welander model with a short-term 201% increase in the freshwater flux. The freshwater flux in the high-latitudes is increased. The freshwater flux in the northern box is increased to 201% of its original value and then reduced to the original flux value. The flows do not return to their original values, but reach a new equilibrium with the northern flow in a reverse direction.

$$\frac{dS_2}{dt} = \begin{cases} \frac{q}{V}(S_2 - S_3) - F_2 & \text{if } q < 0 \\ \frac{q}{V}(S_1 - S_2) - F_2 & \text{if } q \geq 0 \end{cases} \quad (3.73)$$

$$\frac{dS_3}{dt} = \begin{cases} q(S_3 - S_1) - F_3 & \text{if } q < 0 \\ q(S_2 - S_3) - F_3 & \text{if } q \geq 0 \end{cases} \quad (3.74)$$

Again, the variable λ is not the same as the temperature restoring coefficient given in Table 3.1. The second version of the differential equations for temperature compress these terms into a single variable, H_i , where i is the box number the value corresponds to.

Because the total salt content of the sea water is held constant in this model, then $F_2 = -\frac{1}{V}(F_1 + F_3)$. So the amount of water in the system also remains constant meaning that evaporation in the equatorial box is balanced by precipitation in the high-latitude boxes.

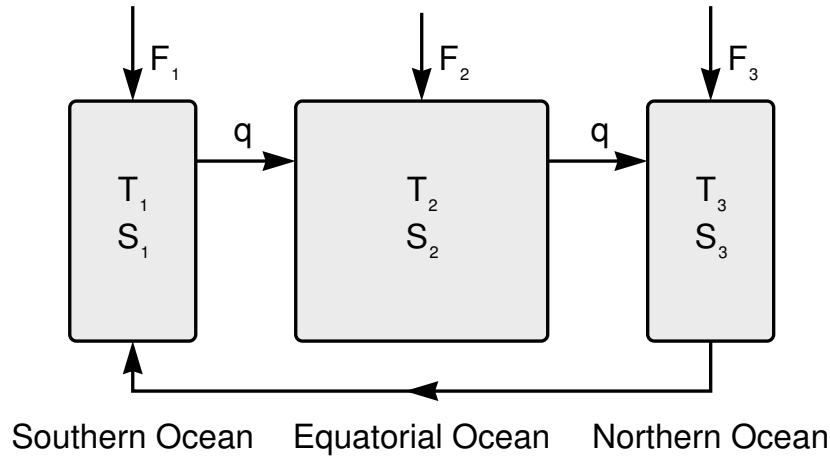


Figure 3.12. Rooth's 3-box model of thermohaline circulation. The northern and southern boxes are connected with a deep current that does not flow into the equatorial box.

To find equilibrium values of q when $q < 0$, set the equations for $\frac{dT_3}{dt}$ (3.71) and $\frac{dS_3}{dt}$ (3.74) equal to zero as they would be for equilibrium and then form the sum:

$$0 = -\alpha \frac{dT_1}{dt} + \beta \frac{dS_1}{dt} = -\alpha(q(T_3 - T_1) + H_3) + \beta(q(S_3 - S_1) - F_3) \quad (3.75)$$

$$= q(\alpha(T_1 - T_3) - \beta(S_1 - S_3)) - \alpha H_3 - \beta F_3 \quad (3.76)$$

$$= \frac{1}{k} q^2 - \alpha H_3 - \beta F_3 \quad (3.77)$$

$$q = -\sqrt{k(\alpha H_3 + \beta F_3)} \quad (3.78)$$

Similarly, if $q \geq 0$ then using equations (3.69) and (3.72) in the same manner results in:

$$q = \sqrt{k(\alpha H_1 + \beta F_1)} \quad (3.79)$$

From these equations, the equilibrium value of the strength of the flow depends on the equilibrium values of the heat and freshwater fluxes in the box that has an up-welling of water.

3.2.2.2 Equilibrium Points

To find equilibrium points for this model, again assume that the temperatures come to equilibrium values more quickly than the salinities. This means that the

differences between the three temperatures can be taken as constant values. Here, the values of $\Delta T_1 = T_2 - T_1$ and $\Delta T_3 = T_2 - T_3$ will become constant values. Taking this further, the value of $\Delta T_1 - \Delta T_3 = \Delta T$ will also be constant. With temperatures at equilibrium, the derivatives of each of the three temperatures will be zero. Adding the three differential equations for temperature shows that the sum of the products of the equilibrium temperatures and the mass of water in each box is equal to the sum of the products of the target temperatures and the mass of water in each box. That is, $T_1 + VT_2 + T_3 = \tau_1 + V\tau_2 + \tau_3$ when the temperatures are at an equilibrium point. The three remaining differential equations for salinity are:

$$q = k(\alpha(\Delta T_3 - \Delta T_1) - \beta(S_1 - S_3)) \quad \text{The equilibrium flow} \quad (3.80)$$

$$= -k(\alpha\Delta T + \beta(S_1 - S_3)) \quad (3.81)$$

$$\frac{dS_1}{dt} = \begin{cases} q(S_1 - S_3) - F_1 & \text{if } q < 0 \\ q(S_2 - S_1) - F_1 & \text{if } q \geq 0 \end{cases} \quad (3.82)$$

$$\frac{dS_2}{dt} = \begin{cases} \frac{q}{V}(S_2 - S_1) - F_2 & \text{if } q < 0 \\ \frac{q}{V}(S_3 - S_2) - F_2 & \text{if } q \geq 0 \end{cases} \quad (3.83)$$

$$\frac{dS_3}{dt} = \begin{cases} q(S_3 - S_2) - F_3 & \text{if } q < 0 \\ q(S_1 - S_3) - F_3 & \text{if } q \geq 0 \end{cases} \quad (3.84)$$

Using the fact that the salinities of the three boxes must be such that the total average salinity is a constant, or that $S_1 + VS_2 + S_3 = S_0$ is a constant, these three differential equations can be reduced to two equations. To do this, let $\Delta S_1 = S_2 - S_1$ and $\Delta S_3 = S_2 - S_3$ and make use of the identity $F_1 + VF_2 + F_3 = 0$ or $F_2 = -\frac{1}{V}(F_1 + F_3)$. This system of differential equations can be reduced to two differential equations:

$$\frac{d\Delta S_1}{dt} = \frac{dS_2}{dt} - \frac{dS_1}{dt} = \begin{cases} \frac{q}{V}(S_2 - S_3) - F_2 - q(S_1 - S_2) + F_1 & \text{if } q < 0 \\ \frac{q}{V}(S_1 - S_2) - F_2 - q(S_3 - S_1) + F_1 & \text{if } q \geq 0 \end{cases} \quad (3.85)$$

$$= \begin{cases} \frac{q}{V}\Delta S_3 + \frac{F_1 + F_3}{V} + q\Delta S_1 + F_1 & \text{if } q < 0 \\ -\frac{q}{V}\Delta S_1 + \frac{F_1 + F_3}{V} + q(\Delta S_3 - \Delta S_1) + F_1 & \text{if } q \geq 0 \end{cases} \quad (3.86)$$

$$= \begin{cases} q\Delta S_1 + \frac{1}{V}q\Delta S_3 + \frac{V+1}{V}F_1 + \frac{1}{V}F_3 & \text{if } q < 0 \\ -\frac{V+1}{V}q\Delta S_1 + q\Delta S_3 + \frac{V+1}{V}F_1 + \frac{1}{V}F_3 & \text{if } q \geq 0 \end{cases} \quad (3.87)$$

$$\frac{d\Delta S_3}{dt} = \frac{dS_2}{dt} - \frac{dS_3}{dt} = \begin{cases} \frac{q}{V}(S_2 - S_3) - F_2 - q(S_3 - S_1) + F_3 & \text{if } q < 0 \\ \frac{q}{V}(S_1 - S_2) - F_2 - q(S_2 - S_3) + F_3 & \text{if } q \geq 0 \end{cases} \quad (3.88)$$

$$= \begin{cases} \frac{q}{V}\Delta S_3 + \frac{F_1 + F_3}{V} + q(\Delta S_3 - \Delta S_1) + F_3 & \text{if } q < 0 \\ -\frac{q}{V}\Delta S_1 + \frac{F_1 + F_3}{V} - q\Delta S_3 + F_3 & \text{if } q \geq 0 \end{cases} \quad (3.89)$$

$$= \begin{cases} -q\Delta S_1 + \frac{V+1}{V}q\Delta S_3 + \frac{1}{V}F_1 + \frac{V+1}{V}F_3 & \text{if } q < 0 \\ -\frac{1}{V}q\Delta S_1 - q\Delta S_3 + \frac{1}{V}F_1 + \frac{V+1}{V}F_3 & \text{if } q \geq 0 \end{cases} \quad (3.90)$$

Small perturbations near the equilibrium points of these equations can be used to investigate the stability of the equilibrium points. For a small perturbation, let $\Delta\bar{S}_1$ and $\Delta\bar{S}_3$ be equilibrium values for the variables ΔS_1 and ΔS_3 . Then let x be a small perturbation of $\Delta\bar{S}_1$ and y be a small perturbation of $\Delta\bar{S}_3$. With these changes of the variables in place, assume that the temperatures of the boxes remain essentially constant so that the value of ΔT does not change. Also, the value of the flow q becomes the sum of the equilibrium flow \bar{q} and a change to the flow q^* . Using these perturbations in equations (3.87) and (3.90) gives new differential equations in the variables x and y . This model is symmetric, meaning that box 1 can be interchanged with box 3 without changing the equations. This analysis of equilibrium points does not need to consider the changes in the equations which come about when the direction of the flow reverses or when q changes to a negative value:

$$\bar{q} + q^* = -k(\alpha\Delta T + \beta(\Delta\bar{S}_3 + y - \Delta\bar{S}_1 - x)) \quad (3.91)$$

$$= -k(\alpha\Delta T + \beta(\Delta\bar{S}_3 - \Delta\bar{S}_1)) + k\beta(x - y) \quad (3.92)$$

$$\begin{aligned} \frac{d\Delta\bar{S}_1}{dt} + \frac{dx}{dt} &= -\frac{V+1}{V}(\bar{q} + q^*)(\Delta\bar{S}_1 + x) + (\bar{q} + q^*)(\Delta\bar{S}_3 + y) \\ &\quad + \frac{V+1}{V}F_1 + \frac{1}{V}F_3 \end{aligned} \quad (3.93)$$

$$\begin{aligned} \frac{d\Delta\bar{S}_3}{dt} + \frac{dy}{dt} &= -\frac{1}{V}(\bar{q} + q^*)(\Delta\bar{S}_1 + x) - (\bar{q} + q^*)(\Delta\bar{S}_3 + y) \\ &\quad + \frac{1}{V}F_1 + \frac{V+1}{V}F_3 \end{aligned} \quad (3.94)$$

These equations can be simplified by removing expressions which are equal to zero because of the equilibrium at $\Delta S_1 = \Delta\bar{S}_1$ and $\Delta S_3 = \Delta\bar{S}_3$. These equations become a system of differential equations in the variables for the perturbations:

$$\frac{dx}{dt} = \bar{q} \left(-\frac{V+1}{V}x + y \right) + q^* \left(-\frac{V+1}{V}(\Delta\bar{S}_1 + x) + (\Delta\bar{S}_3 + y) \right) \quad (3.95)$$

$$\frac{dy}{dt} = -\bar{q} \left(\frac{1}{V}x + y \right) + q^* \left(-\frac{1}{V}(\Delta\bar{S}_1 + x) - (\Delta\bar{S}_3 + y) \right) \quad (3.96)$$

To analyze this system of equations, note that they have an equilibrium point at the origin $(x, y) = (0, 0)$, because $q^* = 0$ at the origin. Then calculate the Jacobian of this system. For $q \geq 0$ and $(x, y) = (0, 0)$ the components of the Jacobian are:

$$\frac{\partial}{\partial x} \left(\frac{dx}{dt} \right) \Bigg|_{(0,0)} = \left[-\frac{V+1}{V}\bar{q} + k\beta \left(-\frac{V+1}{V}(\Delta\bar{S}_1 + x) + (\Delta\bar{S}_3 + y) \right) \right]$$

$$\left. -\frac{V+1}{V}q^* \right]_{(0,0)} \quad (3.97)$$

$$= -\frac{V+1}{V}\bar{q} + k\beta \left(-\frac{V+1}{V}\Delta\bar{S}_1 + \Delta\bar{S}_3 \right) \quad (3.98)$$

$$= \frac{V+1}{V}k\alpha\Delta T + k\beta \left(-2\frac{V+1}{V}\Delta\bar{S}_1 + \frac{2V+1}{V}\Delta\bar{S}_3 \right) \quad (3.99)$$

$$\left. \frac{\partial}{\partial y} \left(\frac{dx}{dt} \right) \right|_{(0,0)} = \left[\bar{q} - k\beta \left(-\frac{V+1}{V}(\Delta\bar{S}_1 + x) + (\Delta\bar{S}_3 + y) \right) + q^* \right]_{(0,0)} \quad (3.100)$$

$$= \bar{q} - k\beta \left(-\frac{V+1}{V}\Delta\bar{S}_1 + \Delta\bar{S}_3 \right) \quad (3.101)$$

$$= -k\alpha\Delta T + k\beta \left(\frac{2V+1}{V}\Delta\bar{S}_1 - 2\Delta\bar{S}_3 \right) \quad (3.102)$$

$$\left. \frac{\partial}{\partial x} \left(\frac{dy}{dt} \right) \right|_{(0,0)} = \left[-\frac{1}{V}\bar{q} + k\beta \left(-\frac{1}{V}(\Delta\bar{S}_1 + x) - (\Delta\bar{S}_3 + y) \right) - \frac{1}{V}q^* \right]_{(0,0)} \quad (3.103)$$

$$= -\frac{1}{V}\bar{q} + k\beta \left(-\frac{1}{V}\Delta\bar{S}_1 - \Delta\bar{S}_3 \right) \quad (3.104)$$

$$= \frac{1}{V}k\alpha\Delta T + k\beta \left(-\frac{2}{V}\Delta\bar{S}_1 - \frac{V-1}{V}\Delta\bar{S}_3 \right) \quad (3.105)$$

$$\left. \frac{\partial}{\partial y} \left(\frac{dy}{dt} \right) \right|_{(0,0)} = \left[-\bar{q} - k\beta \left(-\frac{1}{V}(\Delta\bar{S}_1 + x) - (\Delta\bar{S}_3 + y) \right) - q^* \right]_{(0,0)} \quad (3.106)$$

$$= -\bar{q} - k\beta \left(-\frac{1}{V}\Delta\bar{S}_1 - \Delta\bar{S}_3 \right) \quad (3.107)$$

$$= k\alpha\Delta T + k\beta \left(-\frac{V-1}{V}\Delta\bar{S}_1 + 2\Delta\bar{S}_3 \right) \quad (3.108)$$

To determine the stability of this system, the eigenvalues of the appropriate Jacobian need to be calculated. If both eigenvalues have a real part less than zero then the equilibrium point is stable. The eigenvalues have a value of $\frac{1}{2}(T \pm \sqrt{T^2 - 4\delta})$ where T is the trace of the Jacobian and δ is the determinant of the Jacobian. These values can be calculated, but are very complicated expressions. One quick approximation of the eigenvalues is to assume that the value of $\Delta T = 0$ so that the temperatures of both high-latitude boxes is the same. This assumption does not make physical sense for this model because the sea water flowing into one of the high-latitude boxes comes from the equatorial box and is warmer than the sea water which flows into the

other high-latitude box from the first high-latitude box. The temperature between the two high-latitude boxes should be different, however, these two temperatures can be close to each other so the assumption does work as an approximation. Making this assumption simplifies the values of the Jacobian and makes calculations of the eigenvalues much easier. Making these changes to the Jacobian for $q \geq 0$, which is the case for the current Atlantic Ocean gives:

$$J_+ = \begin{bmatrix} k\beta \left(-2\frac{V+1}{V}\Delta\bar{S}_1 + \frac{2V+1}{V}\Delta\bar{S}_3\right) & k\beta \left(\frac{2V+1}{V}\Delta\bar{S}_1 - 2\Delta S_3\right) \\ k\beta \left(-\frac{2}{V}\Delta\bar{S}_1 - \frac{V-1}{V}\Delta\bar{S}_3\right) & k\beta \left(-\frac{V-1}{V}\Delta\bar{S}_1 + 2\Delta\bar{S}_3\right) \end{bmatrix} \quad (3.109)$$

For the eigenvalues of this Jacobian to have negative real parts, two things must occur. First, the trace of the Jacobian must be negative. Second, the value of the determinant of the Jacobian δ must be positive. In this way, both eigenvalues will either be negative real numbers or complex numbers with negative real parts. The determinant of this Jacobian is:

$$\begin{aligned} \delta &= k\beta \left(-2\frac{V+1}{V}\Delta\bar{S}_1 + \frac{2V+1}{V}\Delta\bar{S}_3\right) \cdot k\beta \left(-\frac{V-1}{V}\Delta\bar{S}_1 + 2\Delta\bar{S}_3\right) \\ &\quad - k\beta \left(\frac{2V+1}{V}\Delta\bar{S}_1 - 2\Delta S_3\right) \cdot k\beta \left(-\frac{2}{V}\Delta\bar{S}_1 - \frac{V-1}{V}\Delta\bar{S}_3\right) \end{aligned} \quad (3.110)$$

$$\begin{aligned} &= \frac{k^2\beta^2}{V^2} \left[(-2(V+1)\Delta\bar{S}_1 + (2V+1)\Delta\bar{S}_3) (- (V-1)\Delta\bar{S}_1 + 2V\Delta\bar{S}_3) \right. \\ &\quad \left. - ((2V+1)\Delta\bar{S}_1 - 2V\Delta S_3) (-2\Delta\bar{S}_1 - (V-1)\Delta\bar{S}_3) \right] \end{aligned} \quad (3.111)$$

$$= \frac{k^2\beta^2}{V^2} (2V^2 + 4V)(\Delta\bar{S}_1 + \Delta\bar{S}_3)^2 \quad (3.112)$$

From this, the determinant of the Jacobian is always positive because $V > 0$. To determine when the trace of the Jacobian is less than zero, solve this inequality for $\frac{\Delta\bar{S}_3}{\Delta\bar{S}_1}$:

$$0 \geq k\beta \left(-2\frac{V+1}{V}\Delta\bar{S}_1 + \frac{2V+1}{V}\Delta\bar{S}_3\right) + k\beta \left(-\frac{V-1}{V}\Delta\bar{S}_1 + 2\Delta\bar{S}_3\right) \quad (3.113)$$

$$\frac{\Delta\bar{S}_3}{\Delta\bar{S}_1} \leq \frac{4V+1}{3V+1} \quad (3.114)$$

This expression can be changed from an expression involving $\Delta\bar{S}_1$ and $\Delta\bar{S}_3$ into one involving F_1 and F_3 . Then, using equations (3.82) and (3.83) for $q \geq 0$, the values of $\Delta\bar{S}_1 = \frac{1}{q}(F_1 + F_3)$ and $\Delta\bar{S}_3 = \frac{1}{q}F_1$. From this, the ratio $\frac{\Delta\bar{S}_3}{\Delta\bar{S}_1} = \frac{F_1}{F_1 + F_3}$. Then

the ratio $\frac{F_1}{F_3}$ can be calculated as $\frac{F_1}{F_3} = \frac{\Delta\bar{S}_3}{\Delta\bar{S}_1} - 1$. Then the inequality for this real part of the eigenvalues being less than zero can be solved for the ratio of $\frac{F_1}{F_3}$:

$$\frac{F_1}{F_3} < \frac{4V + 1}{3V + 1} - 1 = \frac{V}{3V + 1} \quad (3.115)$$

By equation (3.115), if the ratio between the freshwater fluxes in the high-latitude boxes is such that the ratio is less than an amount that depends on the value of V , then the equilibrium point is stable. This is for the nonphysical case where the sea water temperatures in the two high-latitude boxes are equal, but it is a close approximation for the physical cases where these temperatures are not equal but within two or three Kelvins of each other. The full ratio of F_1 to F_3 for stability is calculated in Scott et al. [14] and is:

$$\frac{F_1}{F_3} < \frac{k\beta F_1}{k\alpha(\bar{T}_3 - \bar{T}_1)\left(1 + \frac{1}{2}V\right)\left[k\alpha(\bar{T}_3 - \bar{T}_1) + \sqrt{k^2\alpha^2(\bar{T}_3 - \bar{T}_1)^2 + 4k\beta F_1}\right] + k\beta F_1\left(3 + \frac{1}{V}\right)} \quad (3.116)$$

This expression simplifies to equation (3.115) if $\bar{T}_3 = \bar{T}_1$ or $\Delta T = 0$. This illustrates the fact that the model has stable equilibrium points when F_1 is smaller than F_3 by some factor. Note that when this system has unstable equilibrium points, the instability will move the model to a state where the value of the flow q will change sign and the model will change state to a stable equilibrium point with the flow being reversed.

3.2.2.3 Numerical Modeling

A numerical model in which the freshwater fluxes can be varied slowly can be used to illustrate the lack of hysteresis in this system. A GNU Octave (Matlab compatible) script was used for the model. The basic parameters used in the model are from the study performed by Lucarini and Stone [7]. What will be varied from that study are the amounts of freshwater flux in the high-latitude boxes of the model with corresponding adjustments to the equatorial freshwater flux. The freshwater flux in the southern high-latitude box will be kept at approximately $\frac{3}{10}$ of the freshwater flux in the northern high-latitude box, this is in keeping with the actual freshwater flux amounts in the today's Atlantic Ocean. The equilibrium temperatures in the boxes

will be determined by allowing the model to run, beginning with initial conditions near the estimated values for equilibrium and then using the temperatures of the boxes after several thousand years of model time.

The variations in the freshwater flux in this model are similar to the variations in the 2-box model. The Figures 3.13, and 3.14 show what happens to the model when the freshwater fluxes are changed over time. For Figure 3.13, the flux in the high-latitude boxes increases in each of the first 500 years with the flux in the equatorial box decreasing by a similar amount in order to maintain the total average salinity at a constant value. For Figure 3.14, the flux changes are reversed between years 1,500 and 2,000 after the start of the modeling time. For the northern high-latitude box the freshwater flux changes according to:

$$F_{3,\text{current}} = \begin{cases} F_{3,\text{original}} + \frac{\Delta F_3 t}{500} & \text{if } t < 500 \text{ years} \\ F_{3,\text{original}} + \Delta F_3 & \text{if } t \geq 500 \text{ years} \end{cases} \quad (3.117)$$

The change in the freshwater flux for the southern high-latitude box will be kept to $\frac{3}{10}$ of the change in the northern high-latitude box so that $\Delta F_1 = \frac{3}{10} \Delta F_3$. The difference in the changes in the flux represents the fact the northern high-latitude box receives more precipitation than the southern high-latitude box. This change in the freshwater flux is one possible effect of global climate change.

The northerly surface flow becomes stronger for lower levels increases in the freshwater flux. This is because while the salinity difference between the two high-latitude boxes becomes slightly larger, so does the difference in temperature. This is due to the fact that the sea water flowing into the northern high-latitude box comes from the warmer and saltier equatorial box. The change in the difference in salinity has a larger effect on the strength of the flow than does the change in the temperatures.

For a high enough increase in the freshwater flux, the surface flow in the Atlantic Ocean will change direction according to this model. This is because the freshwater flux in the northern high-latitude box becomes enough to offset the gain in salinity in that box which is from the incoming flow from the equatorial box. That is, even though the salinity of the southern box decreases, the salinity of the northern box decreases much more quickly. The change in the salinity is enough to reverse the direction of the flow of the system because the salinity of the equatorial box must

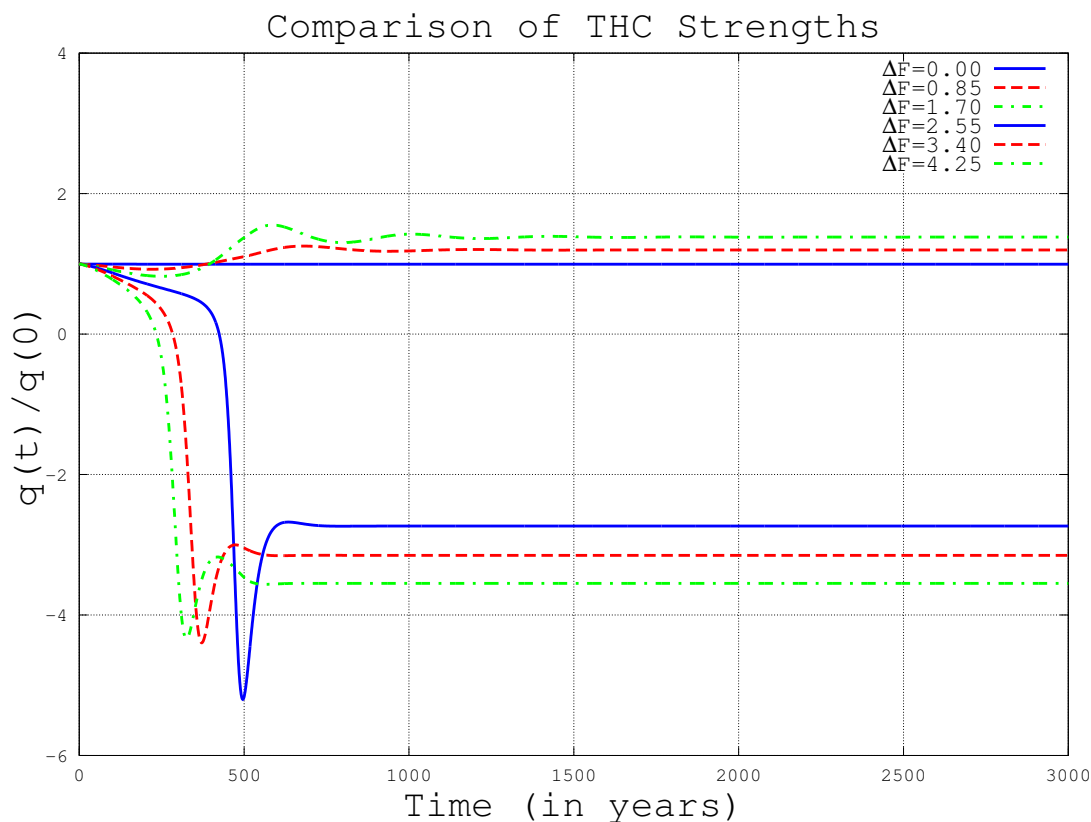


Figure 3.13. Rooth’s 3-box model with changes to the freshwater flux. The THC strengths when the freshwater flux is increased in the high-latitudes, the equilibrium for the system has a smaller difference in temperatures. For a high enough change in the freshwater flux, the system changes from T-mode to S-mode stability.

increase which means that the system changes to the analog of *S-mode*.

Also, for the scenarios where the flow of the system is reversed, the flow magnitude oscillates to some extent about the final equilibrium value for the system. This shows that the Jacobian for the system has complex eigenvalues as the system moves through these states.

To show the lack of hysteresis, the same changes to the freshwater flux were applied as were applied to the other box models. That is, the freshwater flux is increased for 500 years, remains fixed at the higher values for 1000 years, is reduced to the original value over the next 500 years, and then remains at the original values. For the higher increases in the freshwater flux, the system comes to a new equilibrium state even when the freshwater fluxes are lowered back to their original values. The value of the freshwater flux in the northern high-latitude box is this piecewise linear function:

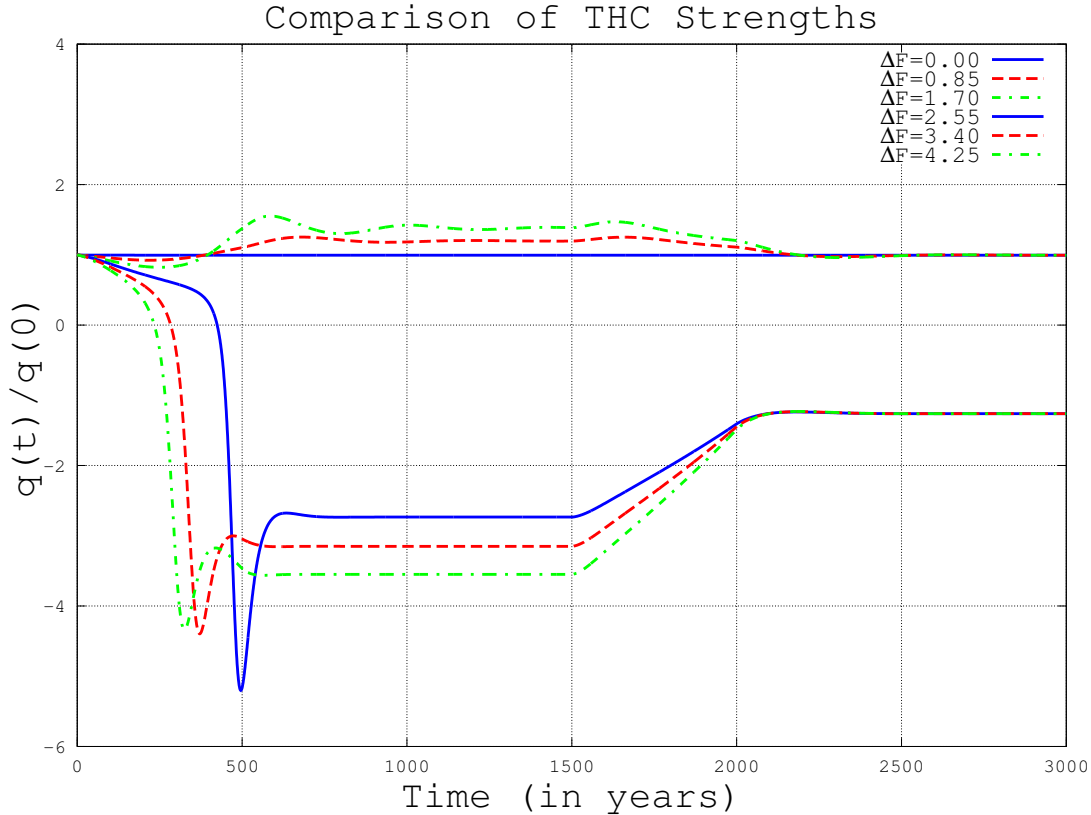


Figure 3.14. Rooth's 3-box model with short-term changes to the freshwater flux. The changes to the freshwater flux are that the high-latitude fluxes increase for the first 500 years, remain at that higher level for 1000 years, and then decrease back to the original amounts in the third 500 year period. For a high enough change in the freshwater flux, the system changes from *T-mode* to *S-mode* stability and the direction of the surface flow remains changed even when the fluxes return to their original values.

$$F_{3,\text{current}} = \begin{cases} F_{3,\text{original}} + t\Delta F & \text{if } t \leq 500 \text{ years } (t \text{ in years}) \\ F_{3,\text{original}} + 500\Delta F & \text{if } 500 < t \leq 1500 \\ F_{3,\text{original}} + (2000 - t)\Delta F & \text{if } 1500 < t \leq 2000 \\ F_{3,\text{original}} & \text{if } t > 2000 \end{cases} \quad (3.118)$$

From the graph in Figure 3.14, the initial changes in the freshwater flux cause the system to come to a different equilibrium state that what had been the original equilibrium. Then changing the freshwater fluxes back to their original value causes the system to either return to its original equilibrium state state, or to come to a new equilibrium state. In the new equilibrium state, the directions of the surface and deep-water flows are reversed. This means that, given a large enough change in the parameters of the system, eventually returning the parameters to their original values

may not return the system to its original state.

3.3 Models with More Boxes

There are other box models of thermohaline circulation of the oceans. These are models with additional boxes added in ways to make the model better fit the actual physical operation of the circulation. As box models show new and unexpected results, additional updates are made to help in the understanding of the stability of the thermohaline circulation. The equations for each of these models becomes more complicated as additional variables are added to the system of differential equations.

One of the models that is often used is a 4-box model which is an extension of Rooth's 3-box model. See Figure 3.15 for this model. The new box is a box containing deep water in the equatorial Atlantic Ocean. Variations on this model include adding a flow between the surface and deep equatorial boxes. If that flow is added, then the model resembles the Welander 3-box model. Without that flow the model is similar to the Rooth 3-box model. The equations for those two models are very much like the corresponding 3-box model.

Figure 3.16 shows another model which is used to model circulation between the Atlantic and Pacific Oceans. These models include differing sizes of freshwater fluxes between the two oceans. That is, the amount of precipitation can vary between the corresponding regions of the Atlantic and Pacific Oceans. Depending on how the boxes are connected with flows, this model can resemble a series of 2-box models or two connected Rooth 3-box models.

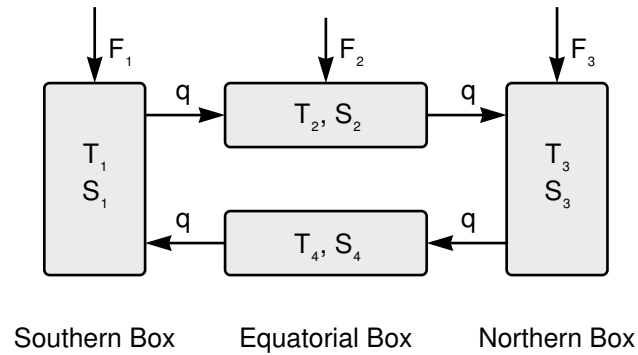


Figure 3.15. A 4-box model of thermohaline circulation. Some models add an additional flow between the two equatorial boxes.

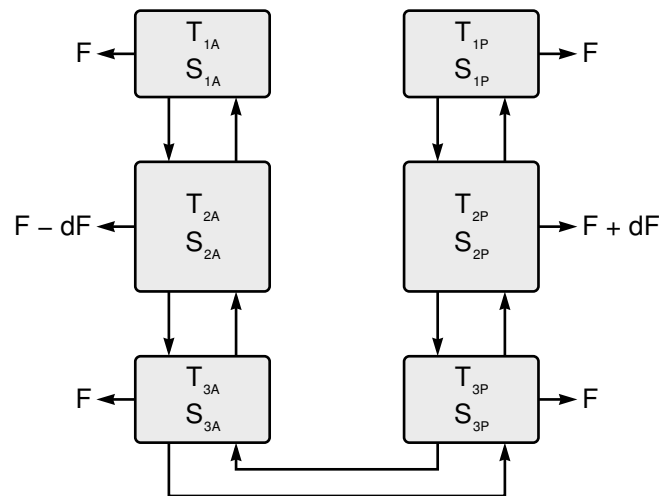


Figure 3.16. A 6-box model of thermohaline circulation. Each side of this model represents one of the Atlantic or Pacific Oceans. The two oceans are connected with flows either in the Strait of Magellan below South America or with flows through the East Indies and Indian Ocean. The differences in the fresh water flux values in the equatorial boxes reflects the fact that the rate of evaporation and precipitation in the equatorial regions of the Atlantic and Pacific Oceans differ.

APPENDIX

SALT WATER DENSITY

A.1 Salt Water Density

The density of salt water varies with the temperature, salinity, and pressure of the water. In the box models used for oceanic circulation, the variation of the density is modeled as a linear function of the temperature and density. The currently accepted formulas for the density of sea water are published in a manual prepared by the Intergovernmental Oceanographic Commission, a part of the United Nations [4]. A simplified description of the formulas is given by Gill [3], and Millero and Poission [8]. The density of sea water at a temperature of $T^\circ\text{C}$, S salinity (in psu's), and at one atmosphere (1013.25 hPa) of pressure is given by these formulas:

$$A = 8.24493 \times 10^{-1} - 4.0899 \times 10^{-3} T + 7.6438 \times 10^{-5} T^2 - 8.2467 \times 10^{-7} T^3 + 5.3875 \times 10^{-9} T^4 \quad (\text{A.1})$$

$$B = -5.72466 \times 10^{-3} + 1.0227 \times 10^{-4} T - 1.6546 \times 10^{-6} T^2 \quad (\text{A.2})$$

$$C = 4.8314 \times 10^{-4} \quad (\text{A.3})$$

$$\rho = AS + BS^{3/2} + CS^2 + \rho_0 \quad (\text{A.4})$$

The reference density ρ_0 is given by:

$$\rho_0 = 999.842594 + 6.793952 \times 10^{-2} T - 9.095290 \times 10^{-3} T^2 + 1.001685 \times 10^{-4} T^3 - 1.120083 \times 10^{-6} T^4 + 6.536332 \times 10^{-9} T^5 \quad (\text{A.5})$$

Further manipulations are required to get the density of sea water when it is under a pressure higher than one atmosphere. However, the effects of high pressure on the density of sea water is minimal as sea water is largely incompressible. The average surface density of sea water is approximately 1027 kg m^{-3} while the average density used for sea water in global box models is approximately 1035 kg m^{-3} . This difference

comes from the increase in density due to the higher pressures encountered at depth for sea water throughout an ocean.

The graph in Figure A.1 shows how the density of sea water varies with temperature and salinity at one atmosphere of pressure. Each of the lines in the graph represents a particular density. As the temperature increases, the density of water at the same salinity decreases. As the salinity increases, the density of water at the same temperature increases. While this is not a linear relationship between density, the density of salt water is only needed for salinities between 33 psu and 37 psu for the box models of oceanic circulation.

The graph in Figure A.2 shows how the approximation of density used in the box models compares to the density as calculated by the equations in this appendix for the range of salinities between 33 and 37 psu's. The calculated densities appear to have a higher slope than in Figure A.1 because the graph has been stretched in the vertical direction. The dashed red (light-gray) lines in the graph show the slope of the linear

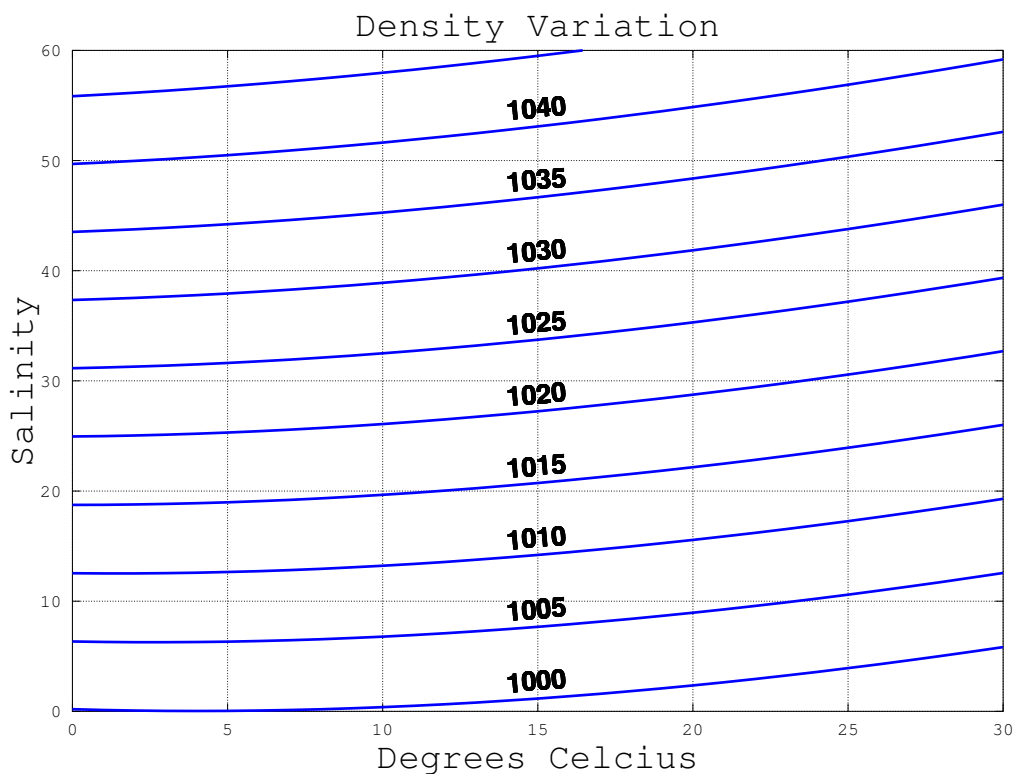


Figure A.1. The density of salt water. This is the density of salt water as calculated for a range of temperatures and salinities.

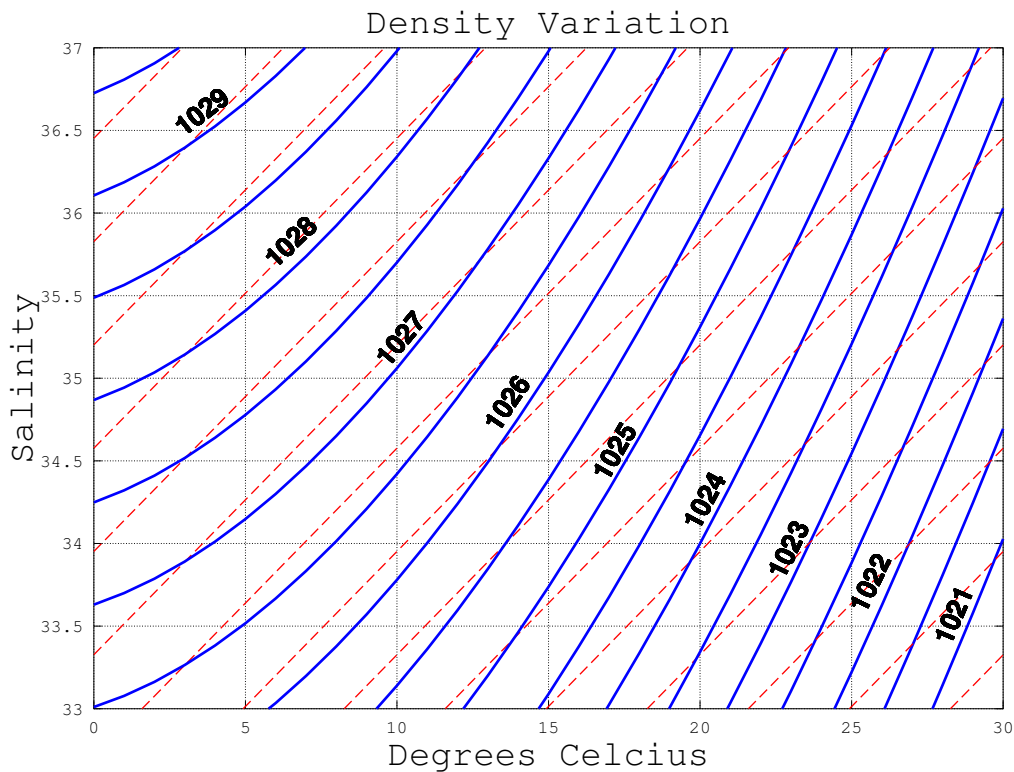


Figure A.2. The density of salt water for selected temperatures and salinities. This is the density of salt water as calculated for the range of temperatures and salinities found in the oceans of the Earth. The dashed red (light gray) lines show the slope of the linear approximation used in the box models.

approximation for density used in the box models. While the approximation is not as close as could be desired, it is close enough. Using a linear approximation for density makes the differential equations used in the box models of thermohaline circulation easier to work with. Using the linear approximation for density makes the functions in the differential equations no more complicated than second order polynomials in the variables involved. This makes the analysis of the resulting equations much easier, although possibly not as accurate as they could be.

REFERENCES

- [1] A. ARAKAWA AND C. S. KONOR, *Unification of the anelastic and quasi-hydrostatic systems of equations*, Monthly Weather Review, 137 (2009), pp. 710–736.
- [2] A. ARAKAWA AND V. R. LAMB, *Computational design of the basic dynamical processes of the ucla general circulation model*, Methods of Computational Physics, 17 (1977), pp. 173–265.
- [3] A. E. GILL, *Atmosphere-Ocean Dynamics*, Academic Press, Inc, New York, 1982.
- [4] IOC, SCOR, AND IAPSO, *The international thermodynamic equation of seawater 2010: Calculation and use of thermodynamic properties*, Intergovernmental Oceanographic Commission, Manuals and Guides No. 56, UNESCO (English), New York, 2010.
- [5] M. Z. JACOBSON, *Fundamentals of Atmospheric Modeling 2nd Edition*, Cambridge University Press, United Kingdom, 2005.
- [6] H. KAPER AND H. ENGLER, *Mathematics and Climate*, Siam, Philadelphia, 2013.
- [7] V. LUCARINI AND P. H. STONE, *Thermohaline circulation stability: A box model study. Part I: Uncoupled model*, Journal of Climate, 18 (2004), pp. 501–513.
- [8] F. J. MILLERO AND A. POISSON, *International one-atmosphere equation of state for seawater*, Deep Sea Research, 28 (1981), pp. 625–629.
- [9] Y. OGURA AND N. A. PHILLIPS, *Scale analysis of deep and shallow convection in the atmosphere*, Journal of Atmospheric Science, 19 (1962), pp. 173–179.
- [10] J. P. PEIXOTO AND A. H. OORT, *Physics of Climate*, American Institute of Physics, New York, 1992.
- [11] D. A. RANDALL, *General Circulation Model Development*, Academic Press, San Diego, 2000.
- [12] D. ROEMMICH AND C. WUNSCH, *Is the north atlantic in sverdrup balance*, Journal of Physical Oceanography, 15 (1985), pp. 1876–1880.
- [13] M. SATOH, *Atmospheric Circulation Dynamics and General Circulation Models*, Praxis Publishing Ltd., Chichester, UK, 2004.

- [14] J. R. SCOTT, J. MAROTZKE, AND P. H. STONE, *Interhemispheric thermohaline circulation in a coupled box model*, Journal of Physical Oceanography, 29 (1999), pp. 351–365.
- [15] H. STOMMEL, *Thermohaline convection with two stable regimes of flow*, Tellus, 13 (1961), pp. 224–230.
- [16] K. E. TRENBERTH, *Climate System Modeling*, Butler and Tanner, London, 1992.
- [17] J. ZHANG, *Box and low-order models of the thermohaline circulation*, Master's thesis, University of Bremen, September 2007. Downloaded from http://www.iup.uni-bremen.de/PEP_master_thesis/thesis_2007/thesis_zang.pdf.